

**CANISTER DESIGN FOR DEEP BOREHOLE DISPOSAL
OF NUCLEAR WASTE**

By
CHRISTOPHER IAN HOAG
B.S. Naval Architecture, United States Naval Academy, 1998

Submitted to the
DEPARTMENT OF NUCLEAR SCIENCE AND ENGINEERING

For the Degree of
MASTER OF SCIENCE IN NUCLEAR SCIENCE AND ENGINEERING

At the
MASSACHUSETTS INSTITUTE OF TECHNOLOGY
May, 2006

© 2005 Christopher Ian Hoag. All rights reserved

The author hereby grants to MIT permission to reproduce and to distribute publicly
paper and electronic copies of this thesis document in whole or in part in any medium now
known or hereafter created

Signature of Author:

Department of Nuclear Science and Engineering
May 2006

Certified by:

Professor Emeritus Michael J. Driscoll
Department of Nuclear Science and Engineering
Thesis Supervisor

Certified by:

Professor Richard K. Lester
Department of Nuclear Science and Engineering
Thesis Reader

Accepted by:

Associate Professor Jefferey A. Coderre
Department of Nuclear Science and Engineering
Chairman, Committee for Graduate Students

Report Documentation Page			Form Approved OMB No. 0704-0188		
Public reporting burden for the collection of information is estimated to average 1 hour per response, including the time for reviewing instructions, searching existing data sources, gathering and maintaining the data needed, and completing and reviewing the collection of information. Send comments regarding this burden estimate or any other aspect of this collection of information, including suggestions for reducing this burden, to Washington Headquarters Services, Directorate for Information Operations and Reports, 1215 Jefferson Davis Highway, Suite 1204, Arlington VA 22202-4302. Respondents should be aware that notwithstanding any other provision of law, no person shall be subject to a penalty for failing to comply with a collection of information if it does not display a currently valid OMB control number.					
1. REPORT DATE 01 MAY 2006		2. REPORT TYPE N/A		3. DATES COVERED -	
4. TITLE AND SUBTITLE Canister Design for Deep Borehole Disposal of Nuclear Waste				5a. CONTRACT NUMBER	
				5b. GRANT NUMBER	
				5c. PROGRAM ELEMENT NUMBER	
6. AUTHOR(S)				5d. PROJECT NUMBER	
				5e. TASK NUMBER	
				5f. WORK UNIT NUMBER	
7. PERFORMING ORGANIZATION NAME(S) AND ADDRESS(ES) Massachusetts Institute of Technology				8. PERFORMING ORGANIZATION REPORT NUMBER	
9. SPONSORING/MONITORING AGENCY NAME(S) AND ADDRESS(ES)				10. SPONSOR/MONITOR'S ACRONYM(S)	
				11. SPONSOR/MONITOR'S REPORT NUMBER(S)	
12. DISTRIBUTION/AVAILABILITY STATEMENT Approved for public release, distribution unlimited					
13. SUPPLEMENTARY NOTES See also ADM002021., The original document contains color images.					
14. ABSTRACT					
15. SUBJECT TERMS					
16. SECURITY CLASSIFICATION OF:			17. LIMITATION OF ABSTRACT UU	18. NUMBER OF PAGES 125	19a. NAME OF RESPONSIBLE PERSON
a. REPORT unclassified	b. ABSTRACT unclassified	c. THIS PAGE unclassified			

CANISTER DESIGN FOR DEEP BOREHOLE DISPOSAL OF NUCLEAR WASTE

By Christopher Ian Hoag

Submitted to the Department of Nuclear Engineering on May 12th, 2006 in partial fulfillment of the requirements for the degree of Master of Science in Nuclear Science and Engineering

Abstract

The objective of this thesis was to design a canister for the disposal of spent nuclear fuel and other high-level waste in deep borehole repositories using currently available and proven oil, gas, and geothermal drilling technology. The canister is suitable for disposal of various waste forms, such as fuel assemblies and vitrified waste. The design addresses real and perceived hazards of transporting and placing high-level waste, in the form of spent reactor fuel, into a deep igneous rock environment with particular emphasis on thermal performance.

The proposed boreholes are 3 to 5 km deep, in igneous rock such as granite. The rock must be in a geologically stable area from a volcanic and tectonic standpoint, and it should have low permeability, as shown in recent data taken from a Russian deep borehole. Although deep granite should remain dry, water in flooded boreholes is expected to be reducing, but potentially corrosive to steel. However, the granite and plug are the containment barrier, not the canister itself.

The canisters use standard oil drilling casings. The inner diameter is 315.32mm in order to accommodate a PWR assembly with a width of 214mm. At five meters tall, each canister holds one PWR assembly. The canister thickness is 12.19mm, with an outer diameter of 339.7mm. A liner can extend to the bottom of the emplacement zone to aid in retrievability. The liner has an outer diameter of 406.4mm and a thickness of 9.52mm. The standard drill bit used with a liner of this size has an outer diameter of 444.5mm.

Sample calculations were performed for a two kilometer deep emplacement zone in a four kilometer deep hole for the conservative case of PWR fuel having a burnup of 60,000 MWd/kg, cooled ten years before emplacement. Tensile and buckling stresses were calculated, and found to be tolerable for a high grade of steel used in the drilling industry. In the thermal analysis, a maximum borehole wall temperature of 240°C is computed from available correlations and used to calculate a maximum canister centerline temperature of 337°C, or 319°C if the hole floods with water. Borehole repository construction costs were calculated to be on the rate of 50 \$/kg spent fuel, which is competitive with Yucca Mountain construction costs. Recommendations for future work on the very deep borehole concept are suggested in the areas of thermal analysis, plugging, corrosion of the steel canisters, site selection, and repository economics.

Acknowledgements

Thank you, Professor Driscoll for your vigorous interest in this topic, countless hours, and volumes of articles and references. Great thanks are also in order for Professor Lester who introduced me to the very deep borehole concept.

This would not have been possible without the United States Navy affording me the opportunity to study at MIT, and providing funding for tuition while maintaining my standard Navy benefits.

Professor Tester and Chad Augustine shared their on-going work and valuable time to provide the most recent information on drilling costs. For this I am very grateful.

To my wife, I dedicate this work for the future of our children. Her love and support have been a great help to me throughout this time.

I am most grateful for my parents, who raised me to strive for challenging goals, and taught me to exceed even my own expectations.

I would also like to thank my office mates, Craig Gerardi, Chris Handwerk, and Sung Joong Kim for their friendship.

The staff and faculty of Nuclear Science and Engineering Department have also contributed making this work enjoyable,

Thank you all!

Table of Contents

TITLE PAGE	1
ABSTRACT.....	2
ACKNOWLEDGEMENTS.....	3
TABLE OF CONTENTS.....	4
LIST OF FIGURES	7
LIST OF TABLES	8
1 INTRODUCTION	9
1.1 OBJECTIVE OF THE THESIS	9
1.2 OVERVIEW OF THE DEEP BOREHOLE CONCEPT.....	9
1.3 LITERATURE REVIEW.....	17
1.4 SCOPE OF THE PROBLEM.....	17
1.4.1 Disposal Canister Production	18
1.4.2 Transportation / Accidents	18
1.4.3 Terrorist Attack	23
1.4.4 Emplacement Process.....	23
1.4.5 Short & Long Term Environment of the Borehole.....	30
1.4.6 Retrievability	31
1.5 ARRANGEMENT OF THE THESIS.....	32
1.5.1 Canister Reference Design	33
1.5.2 Stress Analysis	33
1.5.3 Thermal Analysis	34
1.5.4 Economic Analysis.....	34
2 REFERENCE DESIGN SELECTION	35
2.1 INTRODUCTION	35
2.2 INITIAL CONSIDERATIONS.....	35
2.2.1 Waste Forms.....	35
2.2.2 Design Basis	37
2.2.3 Depth	41
2.2.4 Required Diameter	41
2.2.5 Canister Height.....	42
2.2.6 Borehole Casing	42
2.2.7 Tensile and Compressive Stress	43

2.3	SUMMARY	43
3	STRESS ANALYSIS	45
3.1	INTRODUCTION	45
3.2	TENSILE STRESS	45
3.2.1	Waste String Casing Mass	46
3.2.2	Mass of the Waste	47
3.2.3	Mass of the Packing Material	48
3.2.4	Total Mass and Tensile Stress	49
3.3	COMPRESSIVE STRESS	49
3.4	THERMAL STRESS	50
3.5	SUMMARY	50
4	THERMAL ANALYSIS	52
4.1	INTRODUCTION	52
4.2	FUEL ASSEMBLY HOMOGENIZATION	52
4.3	CALCULATION OF THE CANISTER CENTERLINE TEMPERATURE	54
4.3.1	Heat Transfer Between the Liner and Granite	55
4.3.1.1	Maximum Granite Temperature	55
4.3.1.2	Convection and Conduction.....	56
4.3.1.3	Thermal Radiation	58
4.3.2	Heat Transfer Through the Liner.....	59
4.3.3	Heat Transfer Between the Liner and Canister.....	60
4.3.4	Heat Transfer Through the Canister	60
4.3.5	Heat Transfer Through the Packing Material and Waste.....	60
4.3.6	Temperature Profile Inside the Borehole.....	62
4.4	PARAMETRIC STUDY OF TEMPERATURES IN THE BOREHOLE SYSTEM	65
4.5	SUMMARY	69
5	ECONOMICS.....	71
5.1	INTRODUCTION	71
5.2	DAILY RIG COSTS	72
5.3	TOTAL DRILLING OPERATION COST FOR A SINGLE HOLE.....	72
5.4	ESTIMATION OF CURRENT COSTS FOR DRILLING	73
5.5	COMPARISON TO YUCCA MOUNTAIN COSTS.....	74
5.6	SUMMARY	75
6	CONCLUSIONS.....	77
6.1	THESIS SUMMARY	77

6.1.1	Canister Reference Design	78
6.1.2	Stress Analysis	79
6.1.3	Thermal Analysis	79
6.1.4	Economic Analysis.....	80
6.2	FUTURE WORK	81
6.2.1	Thermal Analysis	81
6.2.2	Plugging	82
6.2.3	Corrosion of Steel Canisters.....	83
6.2.4	Site Selection.....	83
6.2.5	Repository Economics.....	84
7	APPENDICES	85
7.1	APPENDIX A: REFERENCE FUEL DATA	85
7.2	APPENDIX B: STRESS AND THERMAL CALCULATIONS	94
7.2.1	Thermal Calculations in Air	94
7.2.2	Thermal Calculations in Water.....	108
7.3	APPENDIX C: SENSITIVITY ANALYSIS OF THERMAL CALCULATIONS	113
7.4	APPENDIX D: PROPERTIES OF AIR ⁴⁰	119
	REFERENCES.....	122

List of Figures

Figure 1-1 Tectonic Map of Eastern North America and Northern South America ⁵	13
Figure 1-2 Fault Lines in North America ⁵	14
Figure 1-3 Sites of Measured Granite-Forming Events Over a Billion Years Old ⁵	15
Figure 1-4 Precambrian Mineral Date Provinces of North America ⁵	16
Figure 1-5. Typical Spent Fuel Transportation Casks.....	22
Figure 1-6 Layout of Emplacement Facility ⁶	25
Figure 1-7 Schematic of Waste Emplacement Rig ⁶	26
Figure 1-8 Transfer of a Transport Cask from Truck to Rail ⁶	27
Figure 1-9 Alignment of Waste Canister for Lowering into the Hole ⁶	28
Figure 1-10 Emplacement Rig Basement ⁶	29
Figure 2-1 Decay Power of a 17X17 Pin Fuel Assembly	36
Figure 2-2. High Level Waste Borehole	38
Figure 2-3. Individual Canister	39
Figure 2-4. TPS Casing Buttress Thread Coupling Connection to API Spec. 5CT & 5B ²⁷	40
Figure 4-1 Flow Diagram for Calculation of the Canister Centerline Temperature, T_{CL}	62
Figure 4-2 Expected Temperature Profile Inside the Borehole, using the homogenized interior approximation for #16 SiC grit.....	64
Figure 4-3 Center Line Temperature, T_{CL} , as a function of linear power, q' , and ambient granite temperature, T_{amb}	66
Figure 4-4 Borehole Temperature Difference between Center Line, T_{CL} , and Borehole Wall, T_{rock} as a function of linear power, q' , and ambient granite temperature, T_{amb}	67
Figure 4-5 Effect of Packing Material Conductivity on Centerline Temperature, T_{CL} , and the "Delta T" of the Canister, ΔT_{can}	68
Figure 6-1 Center Line Temperature, T_{CL} , as a function of linear power, q' , and ambient granite temperature, T_{amb}	80

List of Tables

Table 1-1. Department of Transportation Regulations for Nuclear Waste.....	19
Table 1-2. Nuclear Regulatory Commission Regulations for Nuclear Waste.....	20
Table 1-3. Environmental Protection Agency Regulations for Nuclear Waste.....	20
Table 1-4. Representative Properties of Granite	30
Table 2-1 Casing Parameters For A 2km Emplacement Zone ²⁶	44
Table 3-1 API Steel Specifications	46
Table 3-2 Waste Specifications.....	48
Table 3-3 Packing Material Data	49
Table 5-1 Applicable Rig Costs and Overhead Factors	72
Table 5-2 Drilling Operations Cost Analog per Hole	73
Table 5-3 Monitored Geologic Repository Costs by Phase (in Millions of 2000\$).....	75
Table 6-1 Casing Parameters For A 2km Emplacement Zone ²⁶	78
Table 6-2 API Steel Specifications ²⁹	78
Table 6-3 Summary of Data for Stress Calculations	79

1 INTRODUCTION

1.1 *Objective of the Thesis*

The objective of this thesis is to design a canister for the disposal of spent nuclear fuel and other high-level waste in deep borehole repositories. The canister is suitable for disposal of various waste forms, such as fuel assemblies and vitrified waste. The design addresses real and perceived hazards of transporting and placing high-level waste, in the form of spent reactor fuel, into a deep igneous rock environment. The thermal performance of the design is emphasized.

To provide an option for second generation repositories at a competitive cost, the canister reference design is based on standard oil drilling technology. Calculations are conducted to assess stresses in the waste string and granite, temperatures and thermal gradients, sensitivity of thermal calculations to variables, and cost. Recommendations are made for future work.

1.2 *Overview of the Deep Borehole Concept*

Nuclear power has the potential to make a dramatic improvement in the earth's environment by providing large amounts of energy without producing CO₂ or other harmful gases. But one of the greatest challenges to the nuclear industry is how to dispose of the nuclear waste. Isotopes in the decay chain of uranium and plutonium, and several long lived fission products, can potentially be harmful for over a million years. The current repository design at Yucca Mountain relies principally on manmade barriers to prevent those radioisotopes from reaching water supplies, crops, and air. These manmade barriers, combined with the natural barriers of Yucca Mountain, must assure protection for over 100,000 years,

based on models having a high degree of uncertainty, including the potential for volcanic activity (Yucca Mountain is in fact in a volcanically active region). The very deep borehole concept relies on the ability of the granite to contain the waste, as evidence from a Russian deep borehole shows.¹

Even if Yucca Mountain is built, it is legislatively limited to 70,000 metric tons of heavy metal (MTHM). If existing reactors operate for the extent of their licenses, there will be over 80,000 MTHM of waste, which means it is already oversubscribed.² Furthermore, the Bush administration is pushing to expand the nuclear power industry in order to mitigate some of the effects of greenhouse gases on global warming, which will significantly increase the need for repository capacity.

Due to continuing advances in the oil and gas drilling industry, the idea of placing nuclear waste in three to five kilometer deep boreholes in igneous rock shows great promise for a final repository. Drilling companies are becoming more proficient at drilling deep (over 10km), drilling through hard rock, and drilling larger diameter holes. With more experience also comes more knowledge of the geologic environment at depth. These recent developments provide the base of information necessary to develop a preliminary canister design.

Drilling through granite is already being done for geothermal energy. The rock desired for geothermal wells is very similar to that desired for a nuclear waste repository, with one exception. Geothermal wells require fractured granite to allow water to pass from one hole to another as it is heated. In a waste repository, fractures are undesirable because they allow the migration of radionuclides. A five kilometer deep geothermal well has been drilled in Soultz, France, proving the necessary drilling capability exists.³

A deep borehole for disposal of nuclear waste will be very similar to an oil well or geothermal well, with multiple layers of casing near the surface where the ground is unstable and likely to cave in. At depth, in a solid block of granite, the borehole could be either lined or unlined. The waste canisters can be lowered by cable, or as part of a drill pipe. Once the canisters are in place, the casings near the surface can be left in place or removed, but the hole needs to be plugged, to close the direct pathway between the decaying waste and the atmosphere. The hole can be plugged immediately with a temporary plug, to ease recovery of the waste in case a better use for it is found, or in case a different disposal method is desired; however, a permanent plug should eventually be emplaced, due to the length of time during which the waste will be hazardous.

However, before drilling can start a site must be selected. An ideal site would have an unfractured granite shelf extending in depth from within one kilometer of the earth's surface down to at least four kilometers deep. A site with granite within one kilometer of the surface is not an exact requirement, but allows a four kilometer deep hole to have two kilometers of waste emplacement and one kilometer of plugging within the granite. Unfractured granite in a geologically stable zone provides a natural barrier to migration of radionuclides which is potentially far superior to any man-made barriers. *Structural and Tectonic Principles* by Peter C. Bradley⁴ contains some useful maps of the granite lithology of North America. Figure 1-1 is a tectonic map covering most of North America. Note that there is an area in the vicinity of North Dakota (93°W 43°N) labeled "stable shelf." Figure 1-2 is a map of fault lines in North America. Notice the lack of fault lines in North Dakota and South Dakota. Figure 1-3 shows that the granite formation in North Dakota occurred about two billion years ago. Figure 1-4 combines the data from Figure 1-2 and Figure 1-3 and labels the stable precambrian shelf

below North Dakota as “Superior Province.” The various shaded areas of Figure 1-4 indicate the age of the Precambrian basement in billions of years, matching the age measurements of Figure 1-3. These maps illustrate a possible site for a very deep borehole repository. Upon more detailed inspection, sites other than North Dakota may also be found. Even though North Dakota appears suitable from a geologic standpoint, it is difficult politically to obtain approval for construction of a nuclear waste repository in any state.

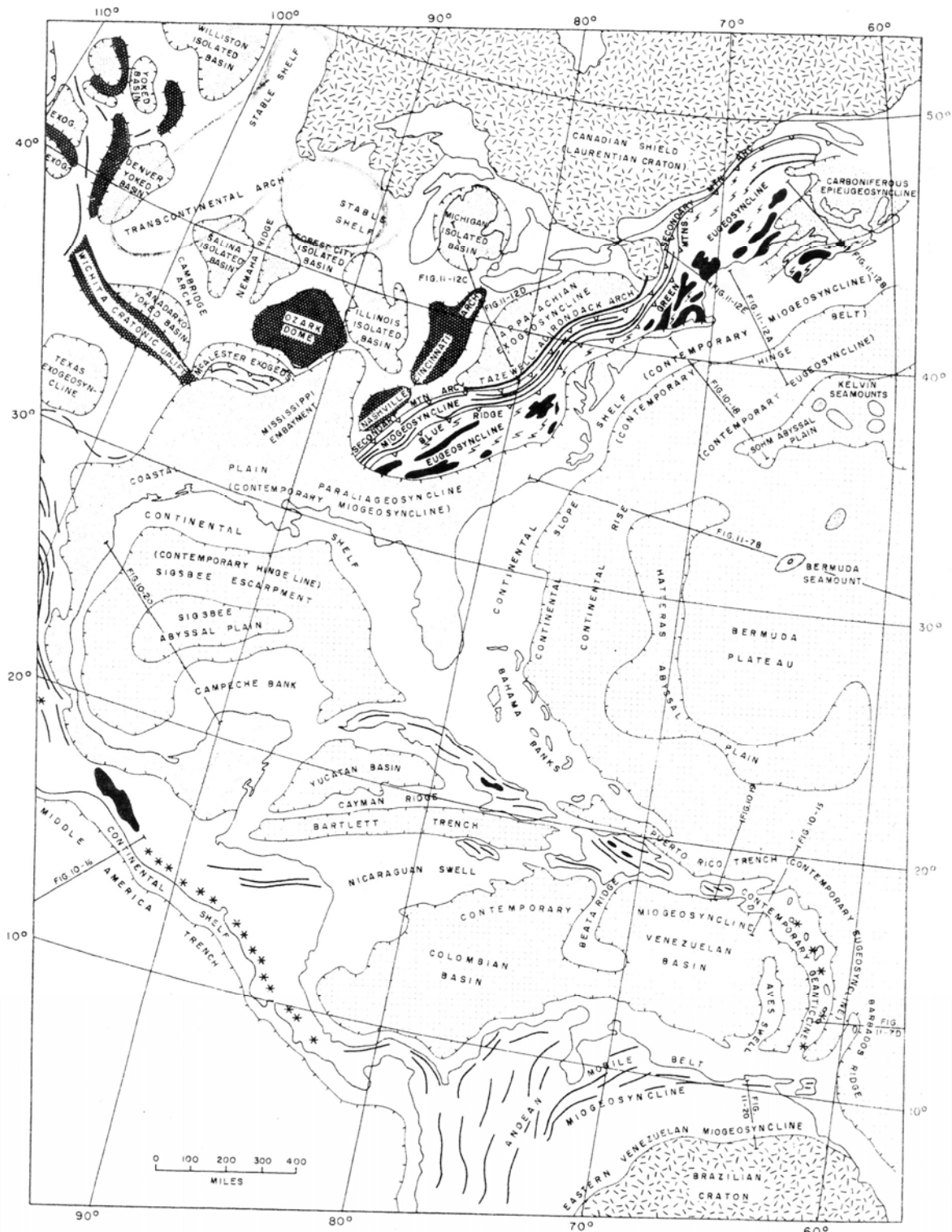


Figure 1-1 Tectonic Map of Eastern North America and Northern South America⁴

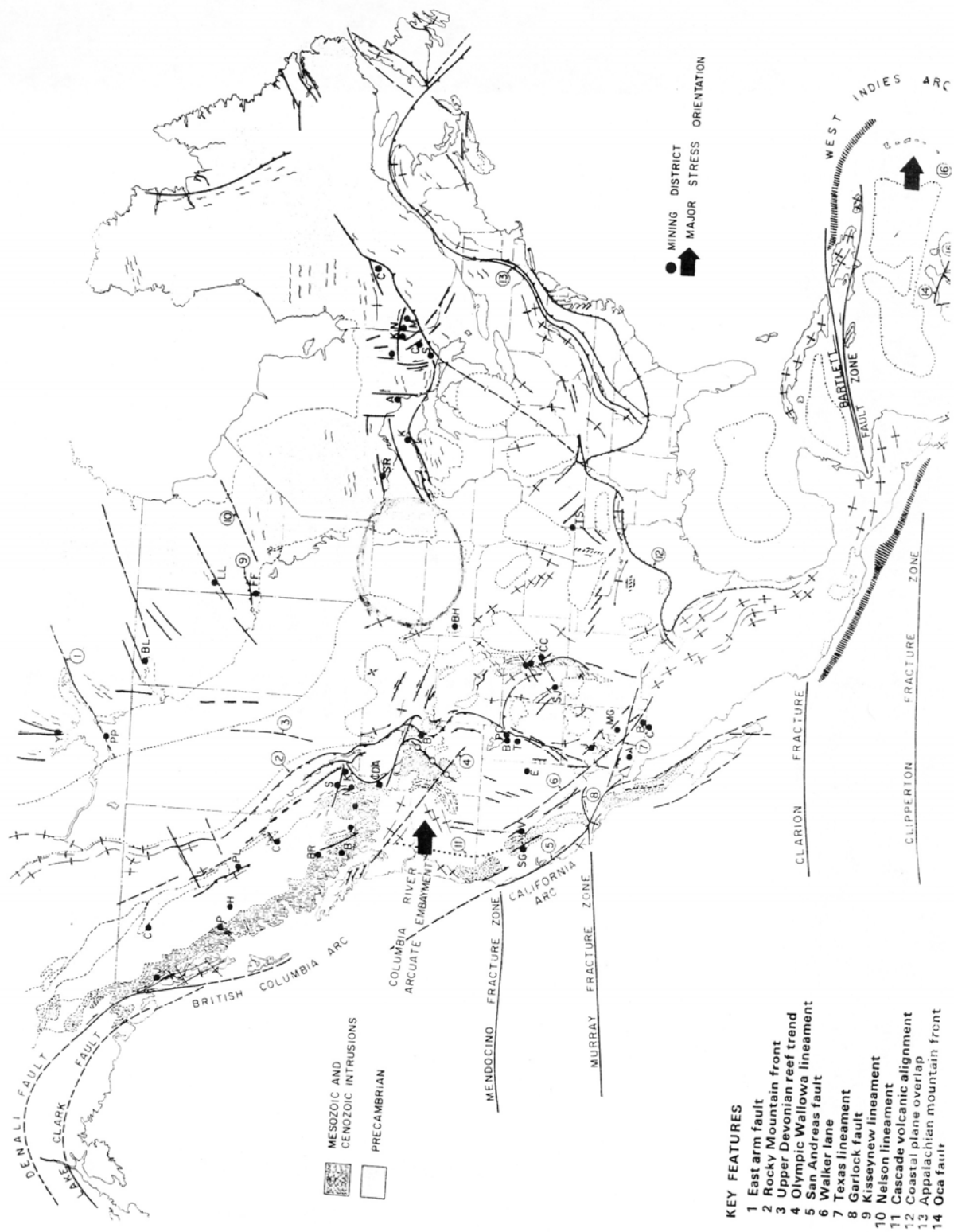


Figure 1-2 Fault Lines in North America⁴

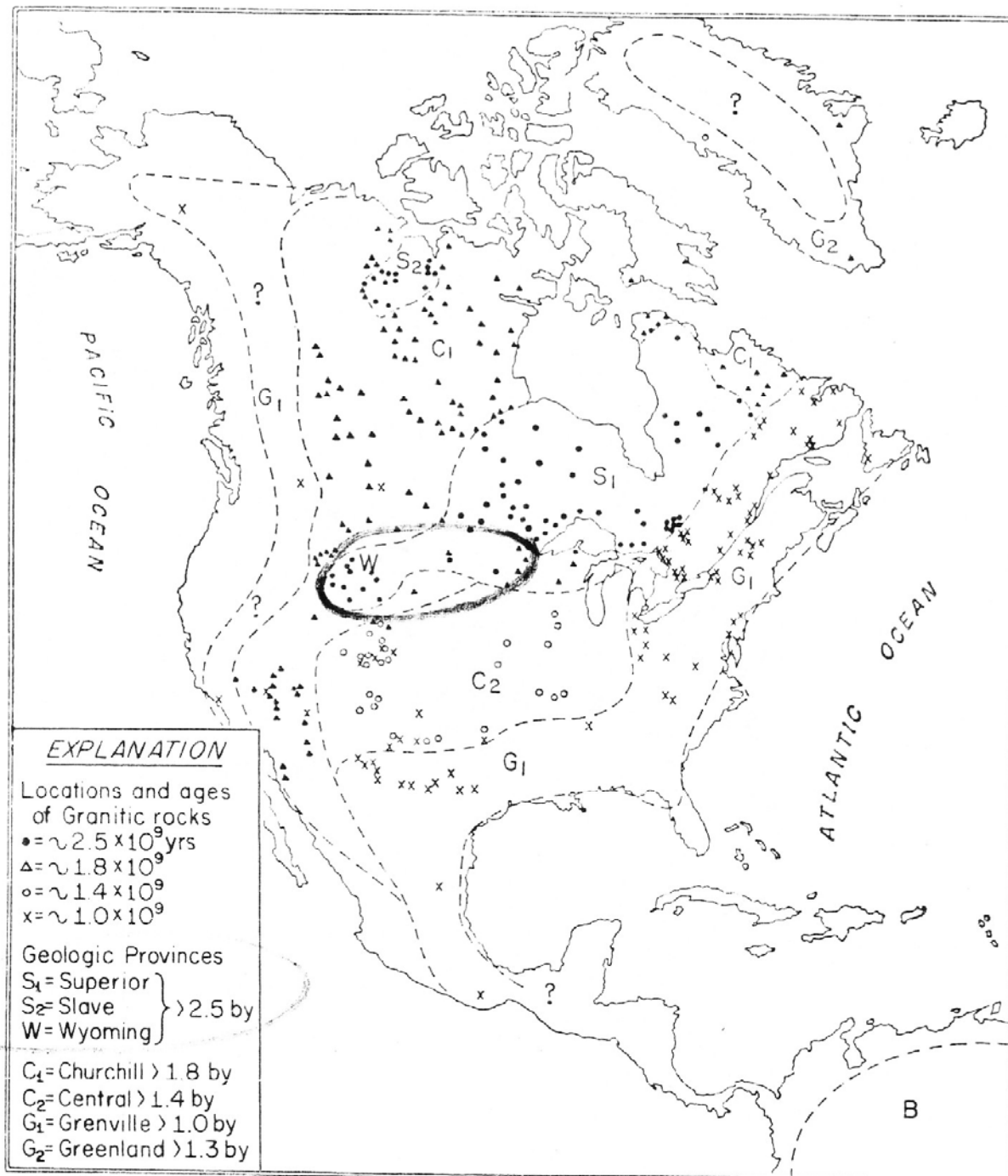


Figure 1-3 Sites of Measured Granite-Forming Events Over a Billion Years Old⁴

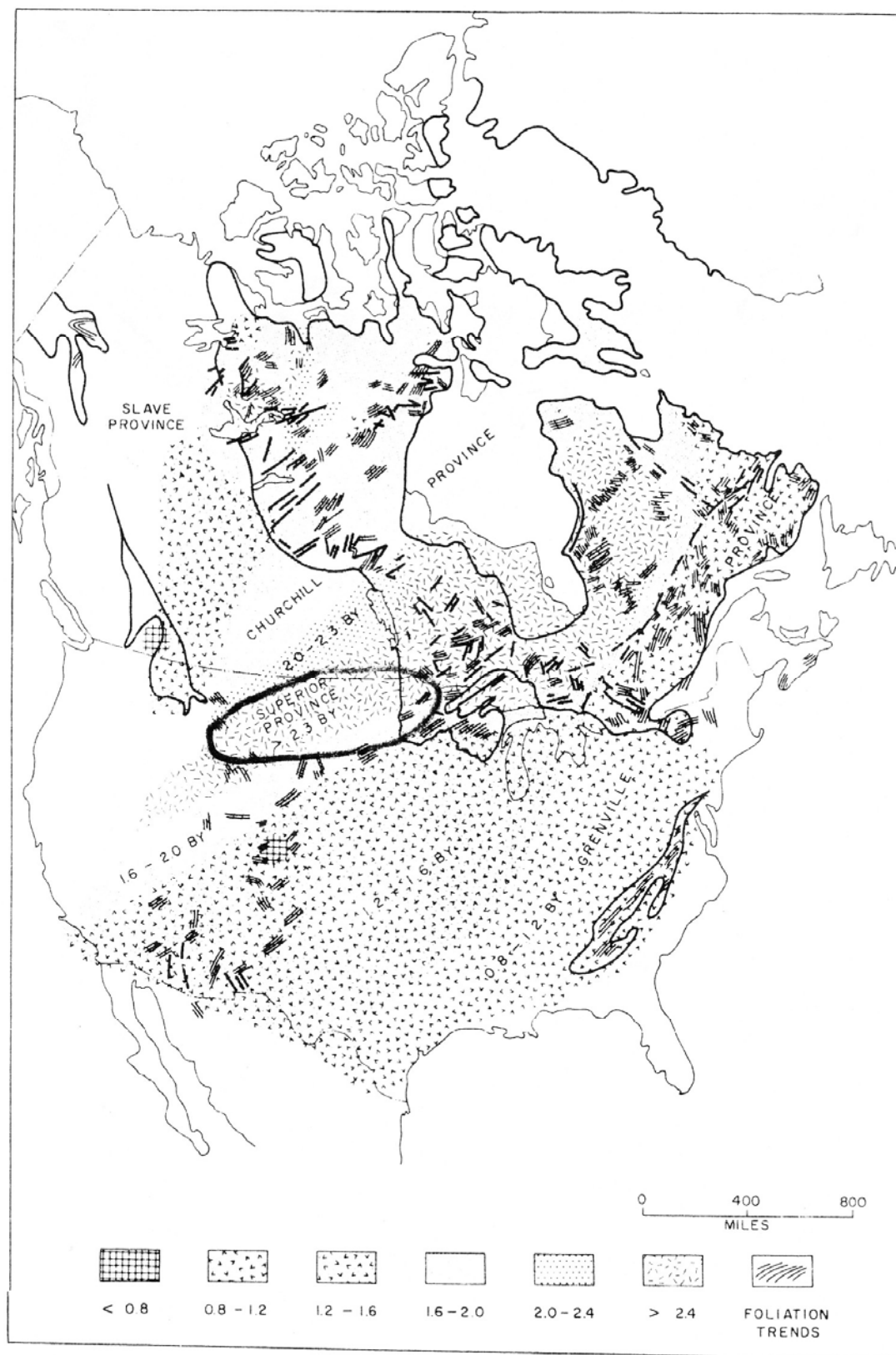


Figure 1-4 Precambrian Mineral Date Provinces of North America⁴

1.3 Literature Review

In December of 1983, a thorough technical report, Very Deep Hole Systems Engineering Studies, was published by Woodward-Clyde Consultants for the Office of Nuclear Waste Isolation⁵. This report first described the concept, and analyzed the thermal impacts, containment and isolation, site qualification, a waste package system, the repository system, depth criteria, surface facilities, borehole design, emplacement facilities, plugs, monitoring, costs, and an engineering program plan. As thorough as this report is, it does not have a thermal analysis of the waste packages.

Over a decade ago, Weng-Sheng Kuo wrote a thesis on the feasibility of deep borehole disposal, and found the concept to be promising based on data prior to 1992.⁶ Advances since then have the potential to make it even more economical. For example, the ability to steer drilling and to drill multiple holes from one rig could greatly reduce drilling costs as well as reduce the number of potential pathways for radionuclides to return to the surface.

Victoria Anderson wrote a relevant thesis in 2002 on the deep borehole chemical environment.⁷ Professors Driscoll, Lester, and others in the Nuclear Science and Engineering Department at the Massachusetts Institute of Technology (MIT), researchers at US national laboratories, and Professor Gibb⁸ in the UK continue to carry out research in support of the deep borehole disposal concept.

1.4 Scope of the Problem

The following sections discuss aspects which should be considered in the design process.

1.4.1 Disposal Canister Production

Canister production refers to the process of placing the waste inside the canister. The canister transitions from a cool non-irradiated state to a warm irradiated state. The canister may expand and change the way the waste is seated in the canister.

Also, in the case of spent fuel assemblies the waste is very fragile, and needs a smooth and gentle transition into the canister. In a shielded area, automated or remotely operated machinery will remove the fuel assemblies from the shipping casks and place them into the canister casings. End caps will be welded to the end of the casings using automated resistance or e-beam welding to ensure a high quality weld.

Canister production should be revisited after a design and materials are chosen. Depending on the metals used there may be some aspects of fabrication which will have an effect on the performance of the canister.

1.4.2 Transportation / Accidents

Ohio State University has the following information available on its website.⁹ There are three federal agencies which have published regulations governing the transport of nuclear waste in the United States: the Department of Transportation (DOT), the Nuclear Regulatory Commission (NRC), and the Environmental Protection Agency (EPA).

DOT regulations specify requirements for hazardous materials. The following are applicable DOT regulations for the shipment of radioactive waste:

Table 1-1. Department of Transportation Regulations for Nuclear Waste	
49 CFR 171	General information, regulations, and definitions
49 CFR 172	Hazardous materials table, special provisions, hazardous materials communications requirements, and emergency response information requirements
49 CFR 173	General requirements for shipment and packaging
49 CFR 174 to 179	Requirements for shipments by various means (truck, rail, ship, etc.)

The NRC has established licensing requirements for radioactive waste facilities and for the packaging and shipping of radioactive waste. The NRC also sets limits on the annual radiation exposure allowed at the boundary of radioactive waste disposal facilities. NRC regulations also state that exposure to radiation should always be kept as low as reasonably possible. The following is a list of NRC regulations applicable to transport of radioactive waste to a radioactive waste disposal facility:

Table 1-2. Nuclear Regulatory Commission Regulations for Nuclear Waste	
10 CFR 19	Requirements for training of radiation workers and inspections of licensed facilities
10 CFR 20	Limits on radiation doses and concentrations of radioactive materials
10 CFR 51	Environmental protection regulations applicable to facilities licensed by the Nuclear Regulatory Commission
10 CFR 61	Requirements for low-level radioactive waste disposal facilities
10 CFR 71	Requirements for packaging and transportation of radioactive materials; standards for Nuclear Regulatory Commission approval of packaging and shipping procedures

The EPA regulations set limits on radiation doses allowed for members of the public and the amount of radioactive material introduced by nuclear facilities into the environment. The following are the EPA regulations:

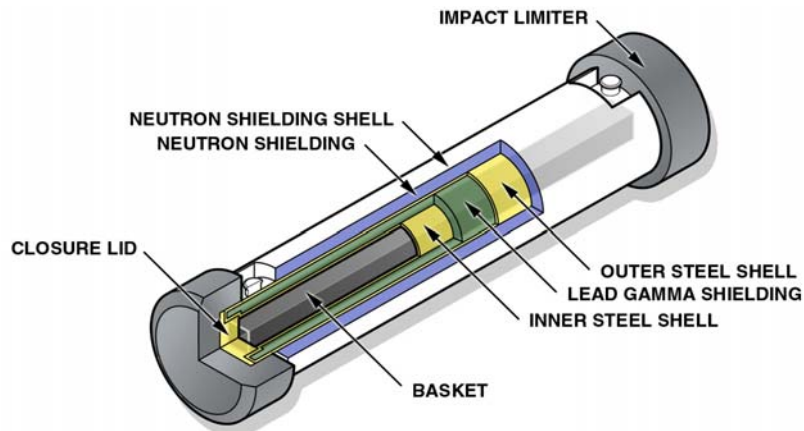
Table 1-3. Environmental Protection Agency Regulations for Nuclear Waste	
40 CFR 190	Limits on radiation doses to the public
40 CFR 193	Radiation protection standards for low-level radioactive waste disposal (not yet released)

Fortunately, transportation casks for spent fuel have already been approved, built, and used as shown in Figure 1-5. The remaining question is whether to transport the assemblies prior to placing them in the permanent disposal canisters, which would allow use of the current designs for transportation casks; or, place the fuel assemblies into the final disposal canisters

prior to transport. Placing the assemblies into the disposal canisters prior to transport would require a redesign of the basket in the transportation casks, and would result in less efficient use of the limited volume in the transportation casks. In addition to the information, tables, and diagrams found on the Ohio State University Website, a specific centerline temperature for transportation and storage of fuel is provided in a paper by Manteufel.¹⁰ That maximum centerline temperature is 380°C.

The decision about whether to place the fuel assemblies in disposal canisters prior to shipment is a current issue at the Department of Energy. Nucleonics Week recently reported that a new DOE plan “shifts the canister loading onus to the utilities.”¹¹ Since either approach could be employed for the very deep borehole concept, this analysis will not attempt to down-select either option.

Another possible advantage to disposing of nuclear waste in deep boreholes is that for some waste, transport may not be necessary. If the rock below a power plant is suitable for a nuclear waste borehole, the hole could be drilled on site. However, licensing of individual holes at multiple locations would drive up the cost of disposal per ton, making this unlikely option less favorable. Thus, the present work focuses on a centralized repository.



Generic Truck Cask for Spent Fuel

Typical Specifications

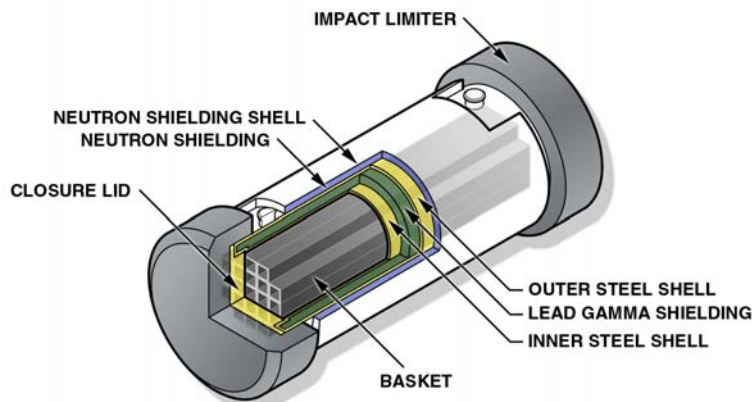
Gross Weight (including fuel): 50,000 pounds (25 tons)

Cask Diameter: 4 feet

Overall Diameter (including Impact Limiters): 6 feet

Overall Length (including Impact Limiters): 20 feet

Capacity: Up to 4 PWR or 9 BWR fuel assemblies



Generic Rail Cask for Spent Fuel

Typical Specifications

Gross Weight (including fuel): 250,000 pounds (125 tons)

Cask Diameter: 8 feet

Overall Diameter (including Impact Limiters): 11 feet

Overall Length (including Impact Limiters): 25 feet

Capacity: Up to 26 PWR or 61 BWR fuel assemblies

Figure 1-5. Typical Spent Fuel Transportation Casks

1.4.3 Terrorist Attack

Terrorist attacks are a serious concern in today's world. Many fear that explosives applied to a nuclear waste canister could spread radioactive material over a significant area causing localized panic and civil unrest in addition to the trauma and fatalities due to the explosion itself. Immediate death from radiation, however, is not likely. Transportation of nuclear materials already occurs on a regular basis. Precautions are taken to ensure safe transportation, as outlined in the Code of Federal Regulations.

Burying waste deep underground makes access to the waste much more difficult for those who intend to use the material unlawfully. In a mined repository, should the criminals breach the security, they might be able to drive a vehicle into the mine where they could work on retrieving the waste while out of sight. In order to retrieve waste from a borehole, however, criminals would need months to construct a drilling platform and they would have to do this in plain sight.

1.4.4 Emplacement Process

As the waste string is lowered into the borehole, each section of casing will have to be attached remotely, in a shielded area. At the emplacement stage, the borehole has already been drilled. With a final casing extending to the bottom of the hole, the waste string should move smoothly into the borehole. Should the waste string become stuck, then a retrieval process would begin.

The Woodward-Clyde technical report⁵ provides some illustrations of a proposed emplacement process for very deep boreholes. Figure 1-6 shows a proposed layout for an emplacement facility at a deep borehole. This facility can serve multiple holes along a single

rail line, or even multiple rail lines running to an array of boreholes. Figure 1-7 shows more detail of the A-frame style emplacement rig. Under the derrick is a special rail car designed for transporting the waste from a truck, and positioning it above the borehole. Figure 1-8 shows a transport truck transferring a cask to the rail car. Figure 1-9 shows the waste canister positioned for lowering into a borehole, with shielding and cameras for aligning the canister remotely. Figure 1-10 shows more detail of the emplacement rig basement.

The emplacement process shown here requires a special transport cask with doors at each end. Transport casks like those shown in Figure 1-5 may only have an opening at one end, and they certainly do not have the sliding doors shown in the following figures; however, with some modification to the emplacement equipment, currently licensed transport casks could be used. While the design or redesign of the emplacement process is beyond the scope of this thesis, it is important to understand the complexities of the process, as emplacement operations account for a large portion of the cost of a repository.

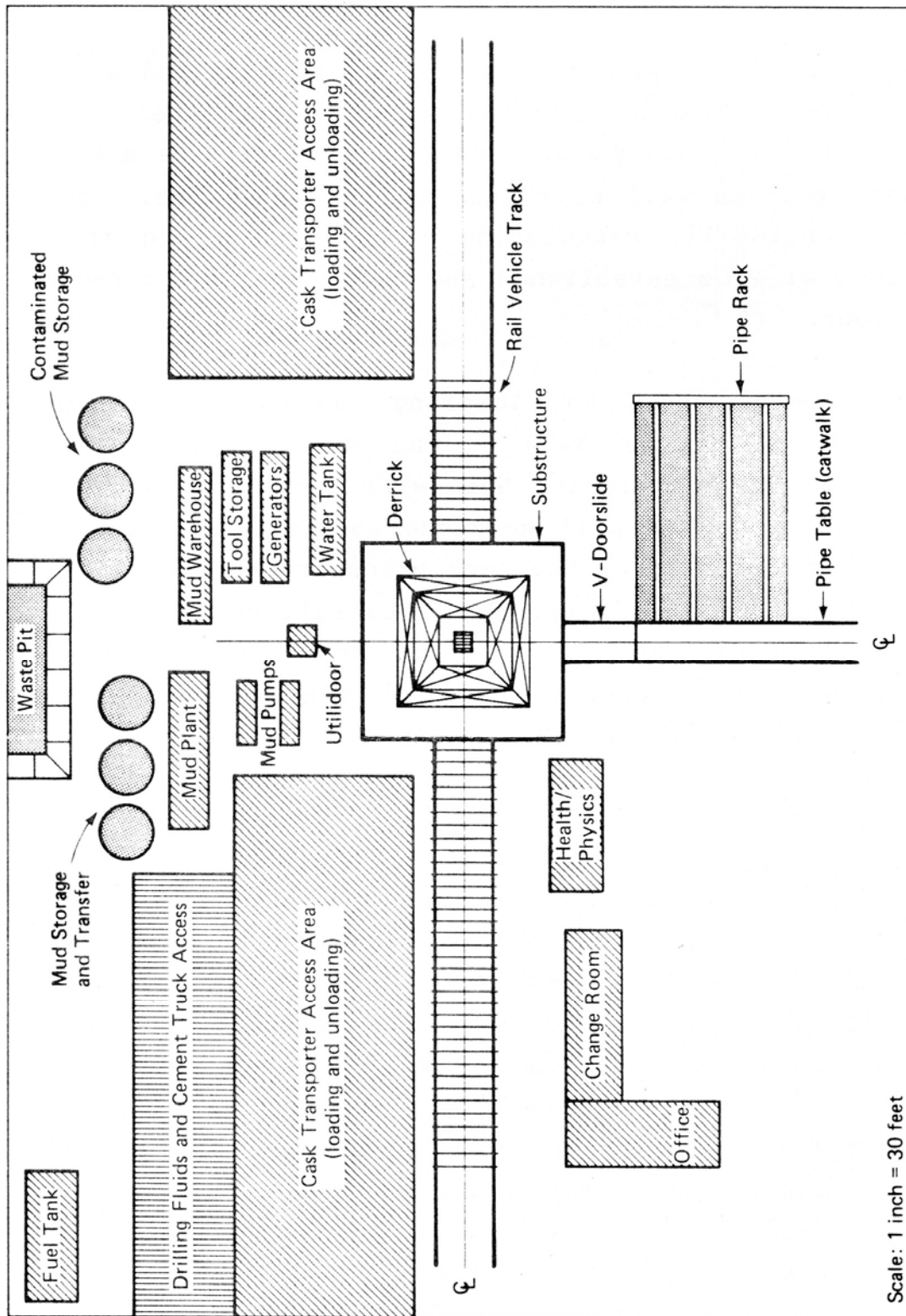


Figure 1-6 Layout of Emplacement Facility⁵

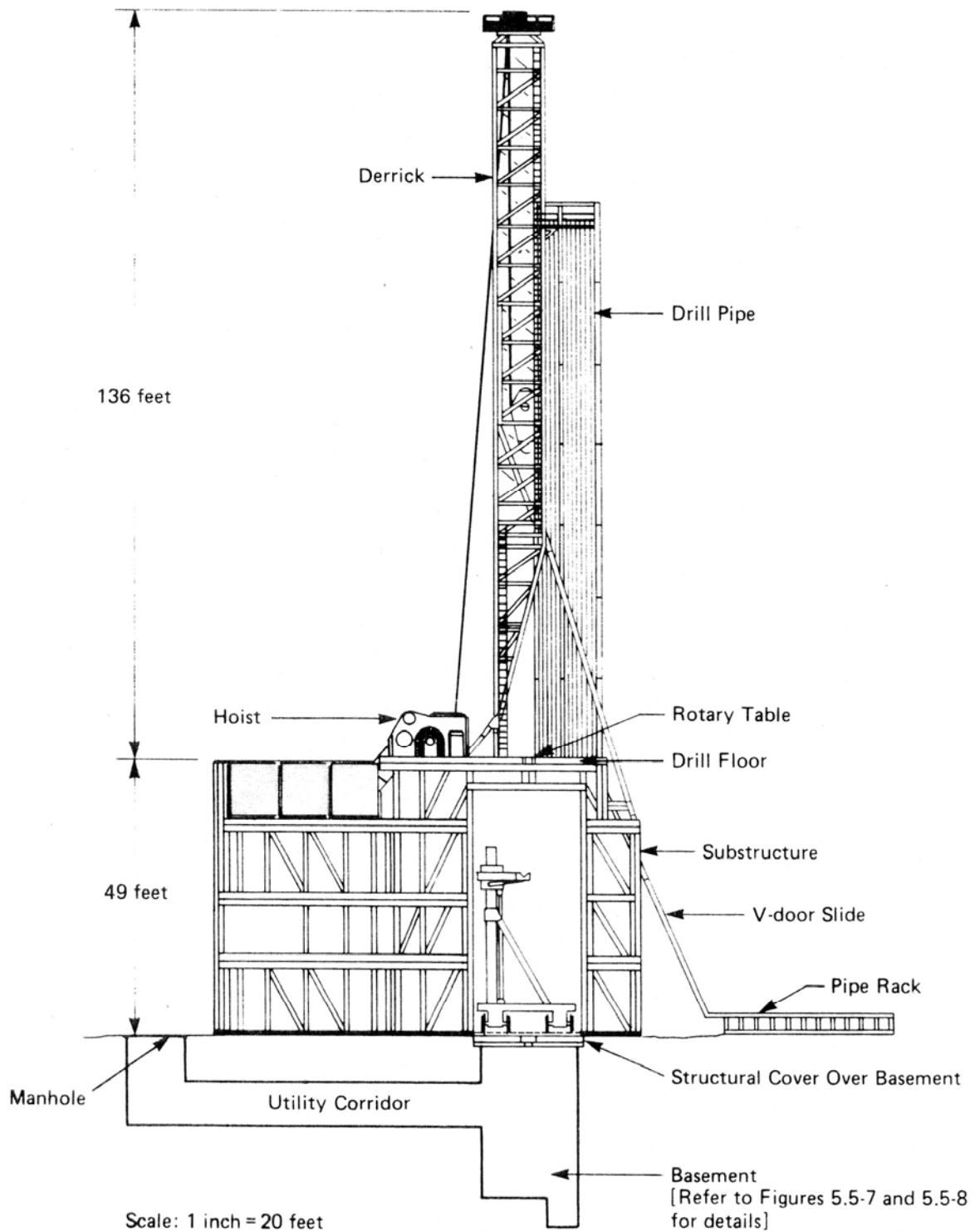
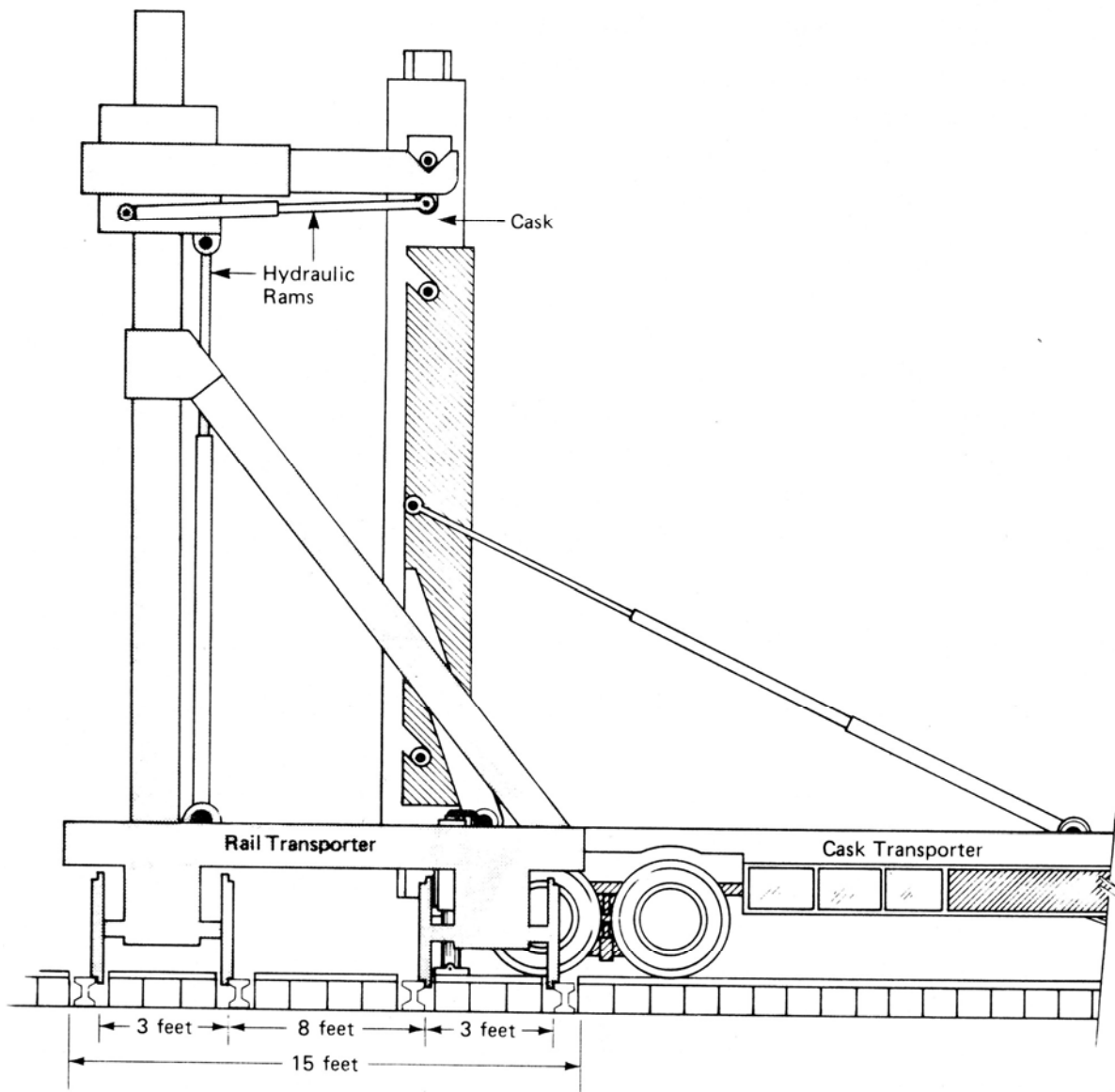


Figure 1-7 Schematic of Waste Emplacement Rig⁵



Approximate Scale: 1 inch = 5 feet

Figure 1-8 Transfer of a Transport Cask from Truck to Rail⁵

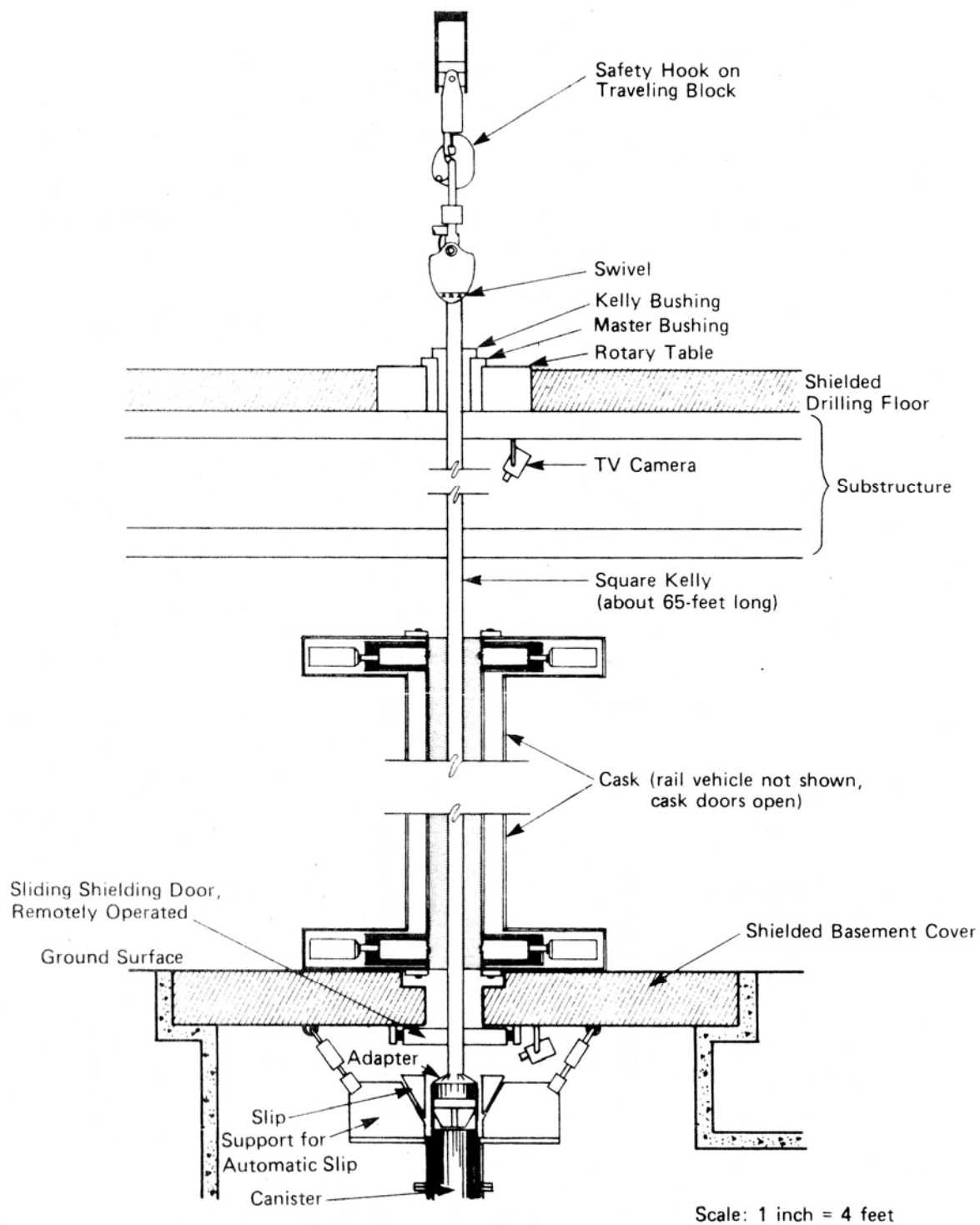


Figure 1-9 Alignment of Waste Canister for Lowering into the Hole⁵

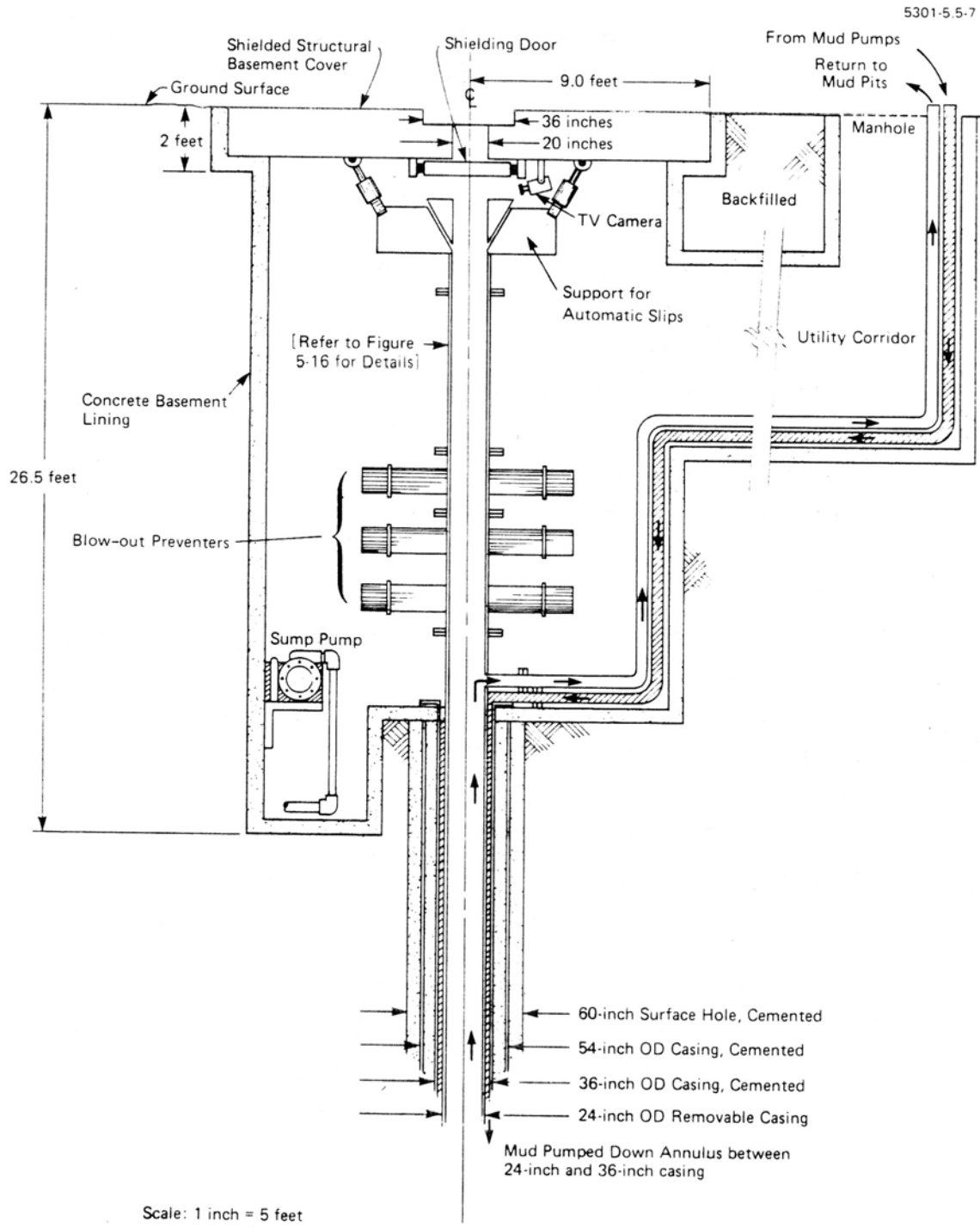


Figure 1-10 Emplacement Rig Basement⁵

1.4.5 Short & Long Term Environment of the Borehole

The ideal environment for a disposal borehole would have dry unfractured granite within one kilometer of the Earth's surface, and remaining unfractured to a depth of at least four kilometers. The following is a list of properties for granite (type of granite in parentheses):

Table 1-4. Representative Properties of Granite		
Composition (by wt%): 74.1 SiO ₂ , 0.43 TiO ₂ , 11.9 Al ₂ O ₃ , 1.63 Fe ₂ O ₃ , 1.80 FeO, 0.16 MnO, 0.27 MgO, 0.39 CaO, 4.76 Na ₂ O, 4.57 K ₂ O, 0.03 P ₂ O ¹²		
Property	Value	(Type of Granite)
Density, ρ :	2.7 to 2.8 g / cm ³	(Various) ¹³
Porosity, Φ :	0.2 to 4%	(Various) ¹²
Specific heat, C_p :	~790 J / kg °K	(Various) ¹⁴
Thermal conductivity, k :	2.4 to 3.8 W / m °K	(Various) ¹⁵
Thermal diffusivity, κ :	0.00741 to 0.011 cm ² / sec	(Various)
Poisson's ratio, ν :	0.10	(Barre) ¹⁶
Young's modulus, E :	3.04 x 10 ¹⁰ Pa	(Barre) ¹⁶
Shear modulus, μ :	1.38 x 10 ¹⁰ Pa	(Barre) ¹⁶
Bulk modulus, K :	1.26 x 10 ¹⁰ Pa	(Barre) ¹⁶
Compression strength, C_0 :	60 to 180 MPa	(Various) ¹⁷
Laboratory measured permeability, K_p :	10 ^{-4.1} to 10 ⁻⁹ darcy	(Various) ¹⁸
Melting temperature, T_m :	650° to 1100°C	(Various) ¹⁹
Emissivity, ϵ :	0.45	(Unknown) ²⁰

Anderson's thesis⁷ describes, in detail, the chemistry of water in deep granite as being reducing, with a pH of 8.5 to 9, and a likely Eh of -0.3 volts. While many pure metals show resistance to corrosion in these conditions, iron does not. Some steels would also be susceptible to environmentally induced corrosion cracking. Although the waste canisters could

be plated with copper (the most promising metal for corrosion resistance), this is not necessary, since granite has been shown by, natural analogs²¹, to prevent migration of metallic nuclides.

Research at Sweden's Aspo Hard Rock Laboratory²² has found microbial life in deep rocks. Some of the bacteria may accelerate corrosion by producing sulfides. Other bacteria may greatly reduce the corrosion rate by removing oxygen from the environment. A third function the microbes may perform, after the canisters and fuel cladding corrode through, is to slow the migration of metallic nuclides by binding the metal particles to the rock.

The down-hole environment is most likely to be dry due to the low permeability of granite. The ambient temperature of the rock at the bottom of the hole should be above the boiling point of water at atmospheric pressure. Upon emplacement of the waste, the temperature will quickly rise high enough to evaporate moisture in the entire emplacement zone; however, if the hole is completely flooded, the hydrostatic pressure is enough to prevent boiling. Once the hole is permanently plugged, it could maintain lithostatic pressure, which is far greater than hydrostatic pressure. Thus, any water leaking in at lithostatic pressure would remain in the liquid phase, so both dry and wet environments are possible.

In the long term, the environment should remain unchanged, except for the temperature. The site should be selected in an area that has a million year history of no tectonic or volcanic activity capable of fracturing the granite.

1.4.6 Retrievability

Current law requires radioactive waste be retrievable for at least 50 years after first emplacement at Yucca Mountain, and the waste must be retrievable until closure, which may be more than 300 years after first emplacement.²³ However, retrievability is not well defined.

Deep boreholes provide a good balance of retrievability and irretrievability. Retrievability provides the assurance that waste can be relocated if a better use or disposal method is discovered or required. Irretrievability provides security that the radioactive material will stay out of the hands of those who would use it for undesirable purposes.

There are various options to provide different levels of retrievability from deep boreholes. For the highest level of retrievability, a “final casing” can be placed in the hole, extending to the bottom. This final casing will act as a liner to prevent the “waste string” (the drill pipe containing the waste) from becoming stuck in the hole. The top part of the hole could remain unplugged for the first century after emplacement. However, leaving the hole unplugged may increase the corrosion rate on the waste string. This thesis will explore a design with a final casing extending to the full depth of the hole.

Should retrieval be necessary and the waste string is stuck, the hole can be over-drilled or a parallel retrieval hole could be drilled using well-developed oil field technology. In any case, retrievability will always be possible, although it may cost more than retrieval from a mined repository like Yucca Mountain.

1.5 *Arrangement of the Thesis*

The problem of disposing of nuclear waste is not simple. Approving and building a repository is challenging both politically and scientifically. The permanent repository must prevent hazardous levels of radiation from reaching the biosphere for up to a million years. At the time of emplacement the waste is so hazardous that it must be handled remotely. The waste must be transported in casks capable of surviving catastrophic highway and rail accidents. Special drilling derricks must be constructed to allow positioning of the waste, and

remote handling. After emplacement the environment surrounding the waste may change over the required decay time. An originally dry hole may partially or completely flood. Despite the technically complex process of emplacing the waste and the possibility of a changing environment, the best quality of the very deep borehole concept is that it relies on the proven capability of the host granite to maintain stability and prevent migration of nuclides for over a million years. And, should retrieval be necessary, it is possible, yet difficult enough to make it unlikely that the waste will fall into the hands of those who would use it against society.

1.5.1 Canister Reference Design

Before analyzing the canister design, the details of the design must be specified. Chapter 2 discusses the initial considerations and resulting reference design to be analyzed throughout the thesis. The initial considerations address: waste forms, design basis, depth of the borehole, required diameter, canister height, borehole casing, and tensile and compressive stress.

1.5.2 Stress Analysis

Chapter 3 is a detailed analysis of the tensile and compressive stresses of the waste string during the emplacement process, and thermal stress on the borehole wall. The stress analysis must be performed prior to the thermal analysis since strength requirements for the waste string affect the thickness of the canisters. However, packing material requirements are driven by the thermal calculations and the density of the packing material affects the mass and stress of the waste string.

1.5.3 Thermal Analysis

The main focus of this thesis is on the thermal analysis of the interior of the borehole. Chapter 4 describes the iterative calculations required to perform accurate thermal calculations using physical laws and correlations. Calculation of the canister center line temperature is broken down into steps corresponding to the layers of material in the borehole: an outer air gap, a liner casing, an inner air gap, the canister casing, and the homogenized canister contents. After establishing a method for calculating the temperatures in the canister, a parametric analysis is performed on key variables that affect the temperatures in the canister.

1.5.4 Economic Analysis

For the very deep borehole concept to be considered a viable option, an economic analysis must show that it is economically competitive with other options. Chapter 5 combines a previous cost analog with a recently developed depth-dependent drilling cost index to estimate the cost of a single borehole. The single borehole cost is multiplied by the number of boreholes for a conservative estimate of a repository construction cost. The very deep borehole repository construction cost estimate is compared to the construction cost estimate for Yucca Mountain.

2 REFERENCE DESIGN SELECTION

2.1 *Introduction*

In 1983, the Battelle Memorial Institute released a report defining a reference “deep drillhole” (DH) concept.⁵ This report evaluated the feasibility of the DH system and the estimated cost at that time. The Battelle report is summarized in Kuo’s thesis⁶, and provides a good reference design for beginning the canister design. A reference borehole design was also proposed by I. S. Roxburgh in a book published in 1987, called *Geology of High-Level Nuclear Waste Disposal: An Introduction*.²⁴ Both of these designs appear to be based on geothermal wells which use larger than standard diameter casings. Furthermore, the inner diameter of the canisters is larger than necessary for a PWR assembly.

2.2 *Initial Considerations*

2.2.1 Waste Forms

While several waste forms exist, such as various types and sizes of assemblies, and vitrified glass or synthetic rock, this thesis focuses mainly on existing US PWR assemblies. (For the case of vitrified glass and Synroc, Calvin Sizer is concurrently writing a thesis at MIT on the loading limits for these waste forms for disposal in a very deep borehole repository.) For the present study, the Westinghouse 17X17 pin fuel assembly was chosen. See Appendix A for details on the Westinghouse PWR assemblies. Figure 2-1 shows the decay power of one metric ton initial heavy metal from a 5% enrichment 17X17 pin fuel assembly with 60,000 MWday/MTU burnup over three power cycles at 85% operation at 80% power and ten years of cooling, calculated using the SCALE5 and OrigenArp code. These numbers are not representative of a typical assembly currently in storage, but are intended to produce

conservatively high power values for design purposes; however, the basic geometric properties of the assembly cover most commercial PWR assembly designs.²⁵ Decay heat in watts is approximately proportional to fuel burnup, and cooling time in years is to the -0.75 power. PWR fuel assemblies in the United States, which are about four meters tall, have average burnups between 18 and 40 GWd/MTU for assemblies with at least ten years of cooling.²⁶ Thus all assemblies with at least ten years of cooling have linear powers less than 250 W/m.

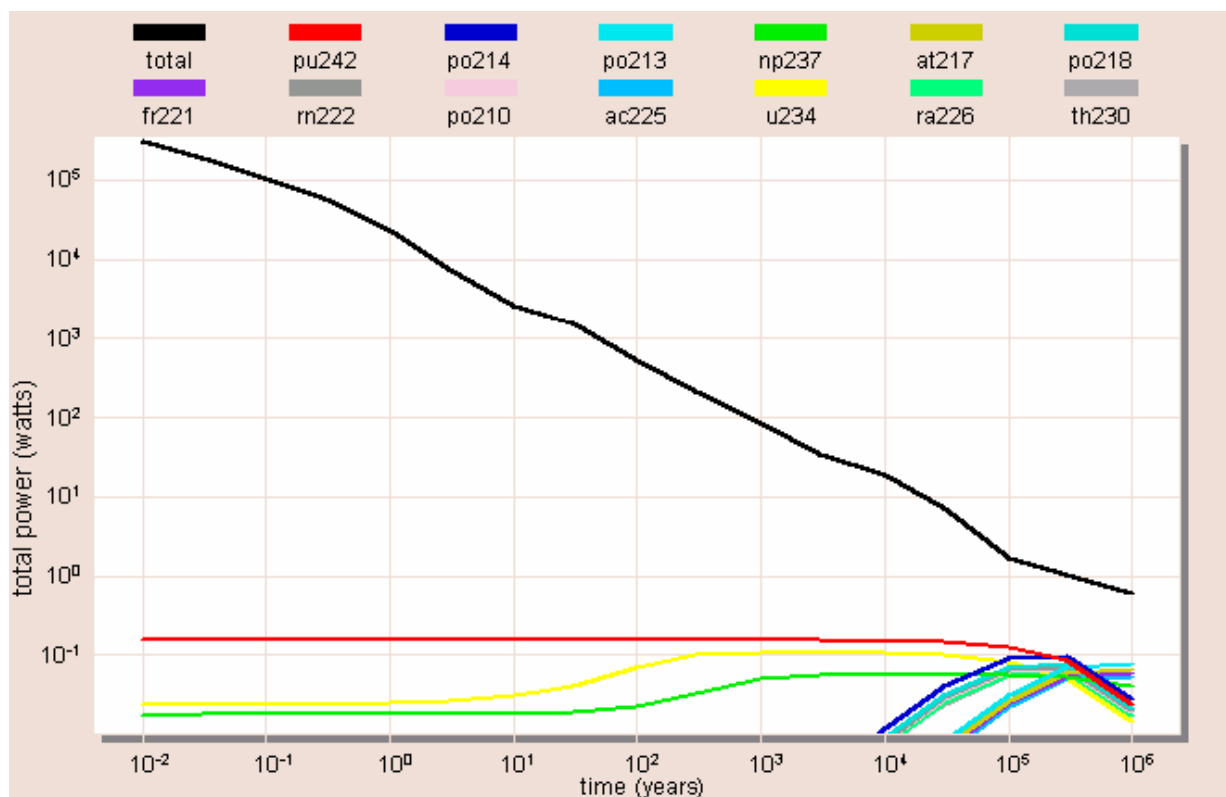


Figure 2-1 Decay Power of a 17X17 Pin Fuel Assembly

At ten years cooling, the total power for one metric ton of uranium is about 2,000 watts. Since a PWR assembly has about half a metric ton of uranium, the power per assembly is about a kilowatt, and the linear power is about 250 W/m for a four meter tall assembly. This value is rounded up to 300 W/m for an added degree of conservatism in the reference calculations.

2.2.2 Design Basis

The baseline design in this thesis is similar, but not exactly the same as the Battelle or Roxburgh designs. It uses standard oil drilling casing sizes, and proposes using an oil-type drill string for the actual canisters. By using standard drilling technology, research and development costs can be cut significantly. The American Petroleum Institute (API) sets drillpipe specifications. The API specifications can be found in Berger and Anderson's book *Modern Petroleum*,²⁷ and on the TPS website²⁸. Figure 2-2 shows a top down view and a side cutaway of the proposed borehole design. Figure 2-3 shows a side cutaway of a single canister containing a PWR assembly. The canisters are connected with external buttress thread coupling tubing as shown in Figure 2-4.

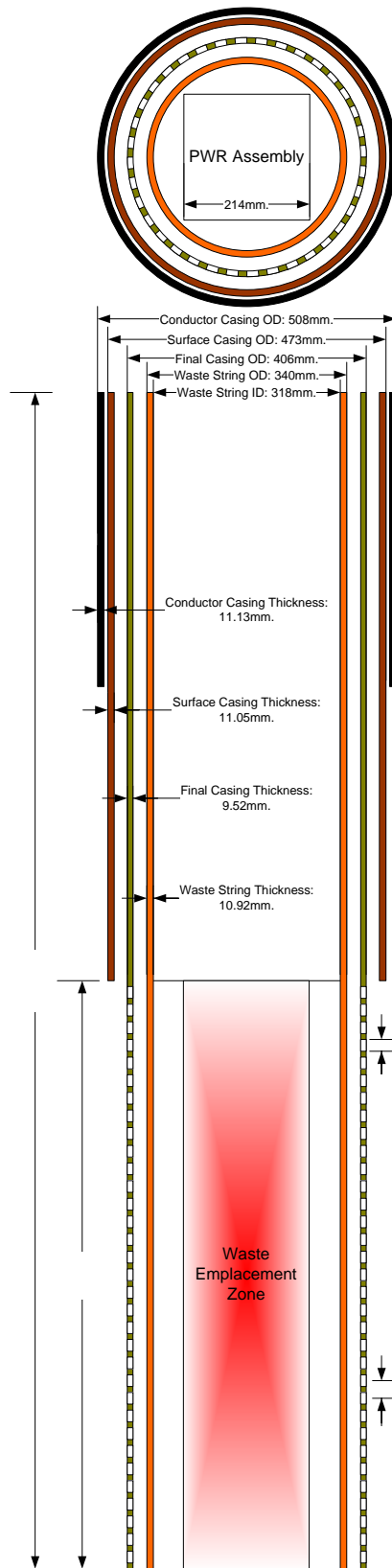


Figure 2-2. High Level Waste Borehole

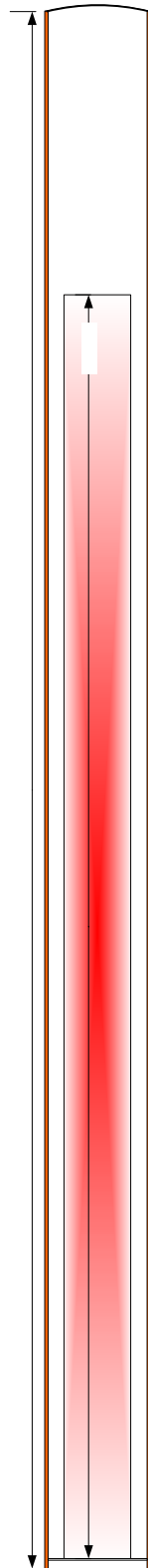


Figure 2-3. Individual Canister

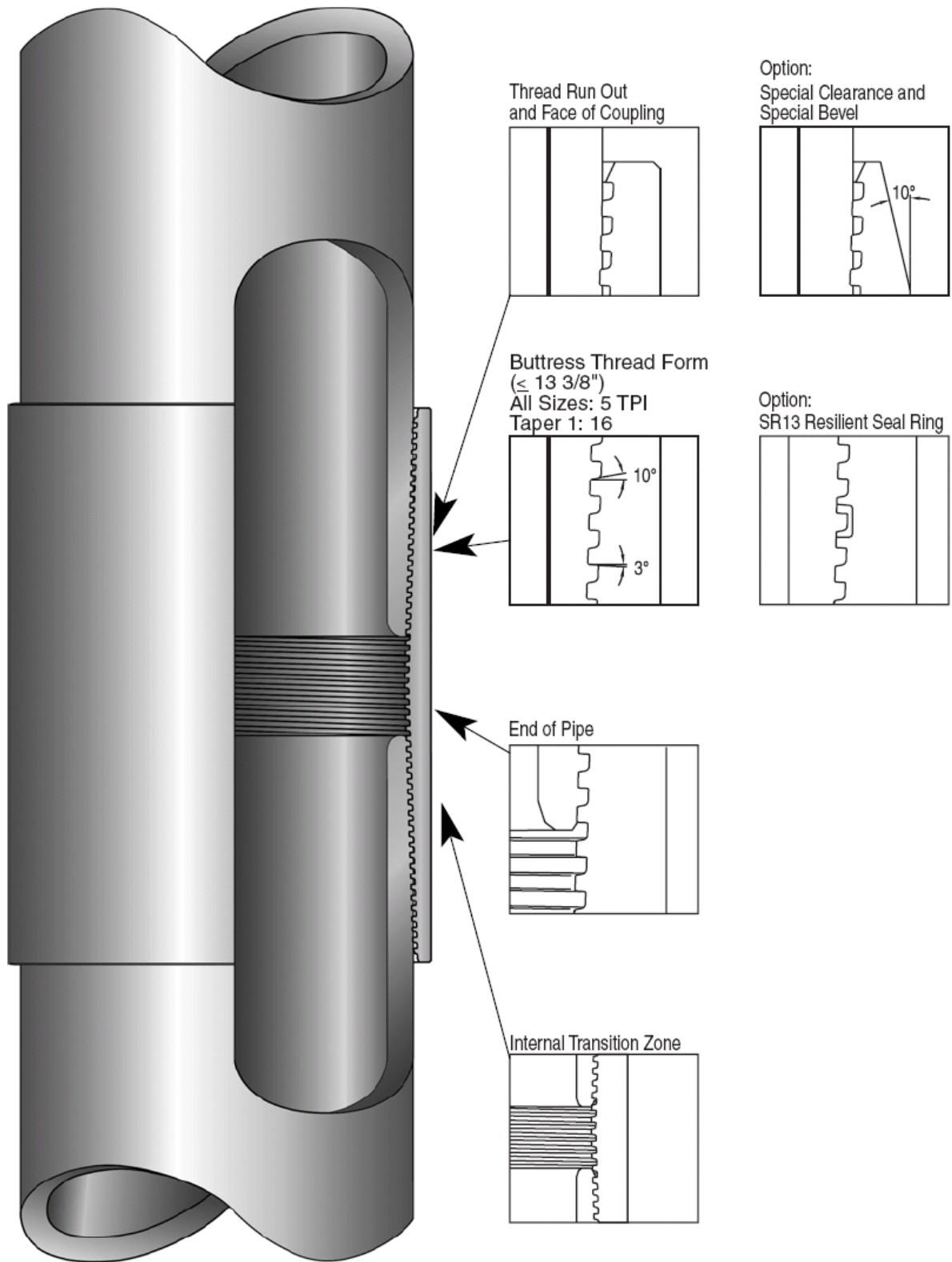


Figure 2-4. TPS Casing Buttress Thread Coupling Connection to API Spec. 5CT & 5B²⁸

2.2.3 Depth

Prior analysis by Woodward-Clyde Consultants⁵, Kuo⁶, and Anderson⁷ has been for a one kilometer emplacement zone in a four kilometer deep hole. The average depth of the upper surface of granite lithostructures is at about two kilometers. Based on the assumption that the granite formation begins at a depth of two kilometers, and the bottom kilometer of the hole is filled with waste, there is one kilometer of granite above the waste in which to employ plugging materials. However, this thesis assumes that a suitable granite formation can be found within one kilometer of the surface, allowing for a two kilometer emplacement zone in a four kilometer deep hole. The change in size of the emplacement zone does not require any recalculation of previous work, since previous calculations modeled the borehole as an infinite line source.

2.2.4 Required Diameter

The design starts with the requirement to place inside the canister a 17 X 17 pin PWR fuel assembly, 214mm in width and 4058mm long. The diagonal width of the PWR fuel assembly is 303mm. The smallest standard casing capable of encasing this PWR fuel assembly has an outer diameter of 340mm and an inner diameter of 318mm. This casing can hold almost every type of fuel assembly listed in Nuclear Engineering International, September 2005.²⁹ The exceptions are the Westinghouse Sweden & European Fuel Group Performance+ 18x18 assembly, which has a width of 229.6mm. Custom casings could be easily manufactured for these assemblies. A custom casing could also be manufactured to hold 3 BWR assemblies without changing any other casing sizes.

2.2.5 Canister Height

In Figure 2-3, a five meter canister is shown with a PWR assembly inside. Standard casing is normally 10m long, so 5m sections could easily be made by cutting standard casing in half. The floor of the canister is slightly raised to prevent corrosion of the floor if the canisters become partially or fully submerged in water while awaiting emplacement. The top of the canister is cambered to cause any dripping water to roll off, thus reducing corrosion. By sealing each assembly separately, the release rate of radioactive nuclides due to canister failure will be spread out.

2.2.6 Borehole Casing

Working outward, and leaving room for coupling, the “final” casing, which also acts as a liner string, has an outer diameter of 406mm. For improved heat transfer from the canister to the rock wall of the hole by radiation and convection, circular openings can be drilled in the final casing. However, calculations presented later in the thesis show that this step is not necessary for disposal of single intact PWR assemblies; however, if the assembly is disassembled, the fuel pins could be packed in a tight hexagonal array, increasing the linear power of the waste, and thus requiring improved heat transfer. The small openings shown in the drawing are sized to prevent pieces of rock from falling or protruding through the liner and damaging the waste canisters, or jamming them in the hole, should retrieval be required. With a 20mm diameter, the openings are only big enough for a small piece of rock to pass through. These small pieces of rock would then fall down through the 33mm gap between the canister and the liner.

The surface casing should meet the same requirements as in oil drilling, for example: protection of freshwater sands from contamination. During drilling operations, carefully controlled chemical mixtures, called “mud,” are used to lubricate and flush debris out of the hole. However, after the waste has been placed in the hole and the hole is ready to be permanently closed, the surface casing and conductor casing could be removed and recycled. The upper part of the waste string, which does not contain any waste, can also be reused.

Conductor casing normally extends only about 10 to 20 meters into the ground. The conductor casing shown in the diagram has an outer diameter of 508 mm and leaves little space for coupling, requiring “extreme-line” coupling. However, a larger conductor casing could be used as shown in the Battelle report⁵.

2.2.7 Tensile and Compressive Stress

Weight and stress calculations were performed using MathCad to determine the tensile stress on the waste string as it is lowered into the hole. Sample calculations discussed in Chapter 3 are shown in Appendix B. Based on these calculations, T95 or C95 steel is required to support a two kilometer emplacement zone in a four kilometer deep hole; however, a one kilometer emplacement zone could be deployed using H40 steel. The two kilometer emplacement zone would also require buttress thread coupling, as shown in Figure 2-4.

2.3 Summary

Table 2-1 lists the specifications required for each layer of casing in the borehole. In the case of the waste string, the thickness listed is not the minimum standard thickness available, but results from the stress calculations discussed in Chapter 3. The types of steel and associated thread options listed for the waste string are those available for the thickness listed.

Table 2-1 Casing Parameters For A 2km Emplacement Zone²⁷						
	<u>Conductor Casing:</u>		<u>Surface Casing:</u>		<u>Final Casing:</u>	<u>Waste String:</u>
OD (mm)	508.00		473.10		406.40	339.70
ID (mm)	485.74		451.00		387.36	315.32
t (mm)	11.13		11.05		9.52	12.19
NW (kg/m)	139.89		130.21		96.73	101.20
Steel	H40	J55, K55	H40	J55, K55	H40	J55- P110
Threads	P,S,L	P,S,L,B	P,S	P,S,B	P,S	P,S,B
Bit size (mm)					508.00	444.50

OD = Outer Diameter, ID = Inner Diameter, t = thickness, NW = Nominal Weight.

Thread options: P = plain, S = short round, L = long round, B = buttress.

3 STRESS ANALYSIS

3.1 *Introduction*

As the waste string, containing tons of waste material, is lowered into the borehole the tensile stress on the pipe at the surface increases. The waste string casing and the couplings must be able to hold this weight. There are a few controllable variables which will determine how the stress is handled. Obviously, less waste can be placed in a string by simply limiting the length of the emplacement zone. Another option for reducing stress is to use supports to transfer some of the weight to the liner. Also, boreholes can be drilled horizontally, in which case the length of the emplacement zone is limited only by the size of the rock formation and the drilling capability. Different grades of steel can be used to accommodate more stress. And, different size casing (diameter or thickness) can be used.

Sample calculations were performed as shown in Appendix B. The sample calculations assume a two kilometer emplacement zone at the bottom of a four kilometer deep hole, and determine the required grade of steel and casing thickness.

3.2 *Tensile Stress*

In the calculation of tensile stress at the top of the waste string as it is being lowered into the hole, there are three categories of mass to take into account: 1) waste string casing, 2) waste, and 3) packing material. Once the mass of the waste string is determined, it is divided by the cross sectional area of the casing, and the stress is compared to the maximum tensile stress ratings for casing steel. The American Petroleum Institute (API) sets tensile strength

limits for the available grades of steel at 80% of the average test strength. Some applicable API steel specifications are listed in Table 3-1.

Table 3-1 API Steel Specifications ³⁰									
<u>Grade</u>	<u>Heat Treatment</u>	<u>Min. Yield Strength</u>	<u>Min. Tensile Strength</u>	<u>Chemical Analysis Maximum Concentrations</u>					
		<i>N/mm²</i>	<i>N/mm²</i>	<i>C</i>	<i>Si</i>	<i>Mn</i>	<i>P</i>	<i>S</i>	<i>Other</i>
H40		276	414						
J55	Normalized	380	520				0.03	0.03	
K55	Normalized	380	655				0.03	0.03	
N80	Heat treated, full length after upsetting	550	690				0.03	0.03	
L80	Quenched and Tempered	550	655	0.43	0.45	1.9	0.03	0.03	Ni 0.25 Cu 0.35
C90		620	690	0.35		1.0	0.02	0.01	Mo 0.75 Ni 0.99 Cr 1.2
T95		655	725	0.45	0.45	1.9	0.03	0.03	
P110		760	860				0.03	0.03	
Emissivity of steel with a rough oxide layer ³¹ :									0.8

3.2.1 Waste String Casing Mass

Identifying the optimum casing for the waste string is an iterative process. The most cost effective solution to the problem would be casing with the minimum standard inner diameter (a PWR assembly with a width of 214mm has a diagonal dimension of 303mm), minimum thickness, and cheapest grade of steel, so these assumptions were used as the starting point for the calculations. However, a four kilometer deep hole, with a two kilometer emplacement zone, requires a higher grade steel than H40. The standard thickness for the higher grade casing is thicker than the minimum standard casing available. The thicker casing,

increases the mass of the waste string casing, but also increases the cross sectional area which reduces the stress.

The weight of the waste string is calculated from the nominal weight listed in Table 2-1. The sample calculations shown in Appendix B use the same nominal weight for the entire waste string; however, thinner and lower grade steel could be used for lower parts of the waste string if it can withstand the compressive stress after the waste string is released at the surface. The mass of the waste string calculated for the reference design is just under 405 MT.

3.2.2 Mass of the Waste

Table 3-2 lists representative values for the waste, using a PWR fuel assembly for the reference case. This table lists information for the stress calculations as well as for the thermal analysis. Those numbers pertaining to the thermal analysis will be discussed in Chapter 4. At 700 kg, the mass of a fuel assembly listed here is one of the higher masses found in the literature, but is not the highest. In any given waste string, some assemblies will be heavier than others, so by using a high value for the mass of a single assembly, the total mass of the waste will be conservatively high. Of course, in an actual repository, the mass of each waste string and its associated stress will have to be verified in advance of actual operations.

Table 3-2 Waste Specifications (Assembly data for a typical PWR assembly)			
Length of Emplacement Zone	2 km		
Height of an Assembly ³³	4058 mm	Mass of a Fuel Assembly ³²	700 kg
Width of a Fuel Assembly ³³	214 mm	Number of Fuel Pins ³³	17X17
Fuel Pin Diameter ³³	9.5 mm	Pitch ³³	12.6 mm
Cladding Thickness ³³	0.57 mm	Fuel Pellet Diameter ³³	8.2 mm
Cladding thermal conductivity ³³	13 W/m*°K	Cracked UO ₂ Thermal Conductivity Estimate ³³	2.0 W/m*°K
Fuel pin effective thermal conductivity	1.87 W/m*°K	Homogenized assembly thermal conductivity	0.63 W/m*°K
Initial Uranium Enrichment	4%	Burn-up	60,000 MWd/MTU
Effective diameter of homogenized assembly			241.7 mm

For the reference case, the total mass of all the assemblies in each borehole was calculated to be 280 MT, based on an estimated mass for a spent fuel assembly of 700kg. This is based on placing an assembly at every five meters of the two kilometer emplacement zone, for a total of 400 assemblies per hole.

3.2.3 Mass of the Packing Material

By filling the canisters with a packing material, the canisters will be more resistant to crushing under the enormous lithostatic pressure (over 100 MPa) which could be encountered at four kilometers deep in granite. Therefore, the packing material must have a high compressive strength. It must also exhibit good thermal conductivity, since it will block radiative and convective heat transfer between the spent fuel and the canister. Two good candidates for packing material are graphite, silicon carbide, or perhaps boron carbide particle beds. Table 3-3 lists some useful properties of silicon carbide, graphite, and boron carbide.

Table 3-3 Packing Material Data			
	Graphite ³⁴	Silicon Carbide ⁶	Boron Carbide ³⁵
Density (gm/cc)	1.3 to 1.95	3.1	2.45 to 2.52
Compressive Strength (MPa)	20 to 200	3900	1400 to 3400
Thermal Conductivity (W/m*°K)	160 ³⁶	120	30 to 42
Coefficient of Thermal Expansion (10 ⁻⁶ °K ⁻¹)	1.2 to 8.2	4	5.6
Specific Heat (J/kg*°K)	710 to 830	750	950
Thermal Conductivity of #16 Grit (W/m*°K)		0.33	

The reference design uses #16 silicon carbide grit. The total mass of the reference packing material is calculated to be 236 MT. By decreasing the canister length to fit the fuel assembly more closely, and maintaining the number of canisters per hole, the depth of the hole could be decreased, thus significantly decreasing the mass of the waste string casing and packing material. This improvement would decrease the total mass of the waste string by 14%.

3.2.4 Total Mass and Tensile Stress

The total mass of a reference design waste string is just under 921 MT. The cross section area of the waste string casing is 12,542 mm², resulting in a tensile stress of 720 MPa. As mentioned in Chapter 0, this tensile stress requires the use of T95 or C95 steel.

3.3 **Compressive Stress**

Since the waste string is confined within the borehole, column buckling is unlikely; however, localized buckling must be considered. Roark³⁷ provides Equation 3-1 for localized buckling in a pipe:

$$s' := \frac{E}{\sqrt{3} \cdot \sqrt{1 - \nu^2}} \cdot \frac{t_{wvs}}{R_{ws}}$$

Where: s' is the critical stress for buckling to occur, E is Young's modulus (~190,000 MPa for steel), ν is the Poisson ratio (0.26 for steel), t_{wvs} is the thickness of the waste string wall, and R_{ws} is the mean radius of the annulus (the average of the inner radius and outer radius). Equation 3-1 results in a critical stress of 8.46 GPa. The actual stress, 721 MPa, is far less than the stress required to cause localized buckling.

3.4 Thermal Stress

Ranade³⁸ calculated the thermal stress in granite for a peak temperature change of 61.2°C at the borehole wall to be 4,226 psi. This thermal stress is considerably less than the lithostatic compressive stress at a depth of 4 km, which is about 100 MPa or 15,000 psi. The tolerable limit of thermal stress in granite was found to be 26,200 psi. It is clear that the temperature change caused by the waste will not cause spalling on the borehole wall, unless there are pre-existing weaknesses. It is unlikely that there would be a problem due to small pieces of granite breaking off into the hole. Future work would be required to determine what pre-existing weaknesses are likely, and how extensive the weaknesses would need to be to pose a problem in the unfractured granite desired for disposal of nuclear waste.

3.5 Summary

Calculations in this chapter were performed for a two kilometer emplacement zone in a four kilometer deep hole. The waste string will not fail in tensile or compressive stress. The tensile stress in this case is close to the limits for some of the lower grades of steel. Maximum waste mass was not calculated for the various types of steel, since there are many variables

(types of waste, length of emplacement zone, and thickness of the waste string) which may vary for each hole, requiring that stress calculations for each hole be verified.

4 THERMAL ANALYSIS

4.1 Introduction

A common concern regarding any nuclear waste material is: how hot will it be? Will it get hot enough to melt the host rock or perhaps just cause the host rock to crack? Fortunately, as will be shown, the deep borehole is capable of keeping the fuel centerline temperature below acceptable limits for storage and transportation of high level waste. Although the current storage and transportation limit, quoted by Manteufel¹⁰, is not necessarily the ultimate limit for permanent disposal, it is a reasonable and achievable goal.

The first step in the thermal analysis is to homogenize the fuel assembly and packing material as a cylinder so that the temperature change calculations can be done in cylindrical coordinates. The temperature calculations are then performed from the rock surface to the centerline, starting with a maximum wall temperature based on the ambient temperature of the rock and the peak rise in temperature caused by the fuel.

4.2 Fuel Assembly Homogenization

The fuel assembly homogenization is performed using Selengut's Relation³⁹ shown in Equation 4-1:

$$k_{\text{hom}} = \frac{(1 + n \cdot v) \cdot k_0 + n(1 - v) \cdot k_1}{(1 - v) \cdot k_0 + (n + v) \cdot k_1} \cdot k_1$$

4-1

where: k_{hom} is the homogenized conductivity, n represents the number of dimensions (0 for one dimensional problems, 1 for two dimensional problems such as this one, 2 for three

dimensional problems), v is the volume fraction calculated using 4-2, k_1 is the thermal conductivity of the primary conductor, and k_0 is the thermal conductivity of the filler (or packing) material.

$$v = \frac{\pi \cdot d^2}{4 \cdot p^2}$$

4-2

where: d is the diameter of the fuel pin, and p is the pitch between fuel pins (distance from the center of one fuel pin to another).

In order to use Selengut's Relation, the effective thermal conductivity of a fuel pin must be calculated. Todreas and Kazimi³³ provide the following heat transfer equation for a cylindrical fuel pin:

$$\Delta T = q' \cdot \left(\frac{1}{4 \cdot \pi k_f} + \frac{1}{2 \cdot \pi \cdot R_g \cdot h_g} + \frac{1}{2 \cdot \pi \cdot k_c} \cdot \ln \left(\frac{R_{co}}{R_{ci}} \right) \right)$$

4-3

Where: ΔT is the temperature difference between the centerline of the fuel pin and the outer surface of the fuel pin, q' is the linear heat rate of the fuel pin, k_f is thermal conductivity of the fuel, R_g is the radius to the center of the gap between the fuel and the cladding, h_g is the conduction coefficient for the gas in the gap, k_c is the thermal conductivity of the cladding, R_{co} is the radius to the outer surface of the cladding, and R_{ci} is the radius to the inner surface of the cladding.

An effective thermal conductivity, k_{eff} , can be found by setting the thermal resistance

terms equal to a single thermal resistance term:

$$\frac{1}{4 \cdot \pi k_{\text{eff}}} = \frac{1}{4 \cdot \pi k_f} + \frac{1}{2 \cdot \pi \cdot R_{g1} \cdot h_g} + \frac{1}{2 \cdot \pi \cdot k_c} \cdot \ln \left(\frac{R_{co}}{R_{ci}} \right)$$

4-4

Solving for k_{eff} results in the following formula:

$$k_{\text{eff}} = \frac{k_{\text{UO}_2} \cdot R_{g1} \cdot h_{g1} \cdot k_{\text{clad}}}{R_{g1} \cdot h_{g1} \cdot k_{\text{clad}} + 2k_{\text{UO}_2} k_{\text{clad}} + 2 \ln \left(\frac{R_{co}}{R_{ci}} \right) \cdot k_{\text{UO}_2} \cdot R_{g1} \cdot h_{g1}}$$

4-5

where: for syntax purposes in Mathcad, k_f has been replaced with k_{UO_2} , R_g has been replaced with R_{g1} , h_g has been replaced with h_{g1} , and k_c has been replaced with k_{clad} .

An equivalent diameter is also calculated such that the circle defined by the equivalent diameter has the same area as the cross section of the fuel assembly. The space between the equivalent diameter of the fuel assembly and the inner diameter of the waste canister is treated as an annulus of packing material.

4.3 Calculation of the Canister Centerline Temperature

Calculation of the centerline temperature is performed in a series of five steps corresponding to the different physical layers of the borehole and canister: 1) the gap between the granite and the liner, 2) the liner, 3) the gap between the liner and the canister, 4) the canister wall, 4) the packing material, and 5) the homogenized fuel assembly.

4.3.1 Heat Transfer Between the Liner and Granite

In the following calculations the subscript 1 is used to indicate values for the first gap. There is a second gap between the liner and the canister.

The temperature at the outer surface of the liner is calculated using Equation 4-6; however, k_{g1} depends on the temperature of the liner outer surface (T_1), so this becomes an iterative calculation.

$$T_{1\text{new}} = T_{\text{rock}} + q' \cdot \frac{\ln\left(\frac{OD_f + 2 \cdot \delta_1}{OD_f}\right)}{2\pi \cdot k_{g1}}$$

4-6

Where: $T_{1\text{new}}$ is the liner outer surface temperature, q' is the linear heat rate produced by the waste, OD_f is the outer diameter of the fuel, δ_1 is the gap thickness (distance between the liner and the granite), and k_{g1} is the combined thermal conductivity due to conduction, convection, and radiation across the gap.

$$k_{g1} = k_{eq1} + k_{rad1}$$

4-7

Where: k_{eq1} is the combined thermal conductivity due to conduction and convection, and k_{rad1} is the thermal conductivity due to radiation. Both k_{eq1} and k_{rad1} depend on T_1 .

4.3.1.1 *Maximum Granite Temperature*

Although the vertical temperature gradient in granite is likely to be 20°C/km, the granite temperature is conservatively approximated using a temperature gradient of 40°C/km,

and the ~60°C peak radial temperature change at the borehole wall, as calculated by Ranade³⁸. All assumptions made by Ranade are consistent with this thesis. The resulting estimated maximum wall temperature is 240°C and occurs about three years after emplacement. This estimated maximum wall temperature is used for the reference case calculations. A sensitivity analysis to the wall temperature is performed in Section 4.4.

4.3.1.2 Convection and Conduction

A very general correlation for the combined effect of convection and conduction in air is found in Fundamentals of Heat Transfer by M. Mikheyev⁴⁰. Data shows that the correlation works well for varying geometries.

$$k_{eq1} = k_{air} \cdot 0.18 Ra^{0.25} \quad (Ra > 10^3)$$

4-8

Where: k is thermal conductivity, and Ra is the Rayleigh number. The Rayleigh number is the product of the Grashof number and Prandtl number. The Grashof number is:

$$Gr := \frac{g \cdot (T_1 - T_{rock}) \cdot \delta_1^3}{T_{avg} \cdot \nu^2}$$

4-9

Where: g is the acceleration of gravity, T_1 is the temperature at the outer surface of the liner, T_{rock} is the rock temperature, δ_1 is the gap thickness (distance between the liner and the rock), T_{avg} is the average of T_1 and T_{rock} , and ν is the kinematic viscosity. Kinematic viscosity is:

$$\nu = \frac{\mu}{\rho}$$

4-10

Where: μ is the dynamic viscosity, and ρ is density calculated using the ideal gas law at one atmosphere. Using a pressure of one atmosphere is a safe approximation, since thermal convection increases with density. The dynamic viscosity is found using an empirical formula: the Sutherland Equation⁴¹. The coefficients in Equation 4-11 have been calculated for air, based on measured values.

$$\mu = \frac{1.464 \times 10^{-6} \cdot T_{\text{avg}}^{1.5}}{T_{\text{avg}} + 113.29\text{K}} \cdot \frac{\text{Pa} \cdot \text{s}}{\sqrt{\text{K}}}$$

4-11

Where: T_{avg} is the same as in 4-9, and K is °K.

The Prandtl number is:

$$\text{Pr} = \frac{C_p \cdot \nu \cdot \rho}{k_{\text{air}}}$$

4-12

Where: C_p is the constant pressure specific heat, ν is the kinematic viscosity, ρ is density, and k_{air} is the thermal conductivity of air.

The specific heat of air is found using a quadratic equation as an approximation based on data between 100 and 300 degrees Celsius⁴².

$$C_p = \left[0.0005 \left(\frac{T_{\text{avg}}}{\text{K}} - 273 \right)^2 - 0.3 \left(\frac{T_{\text{avg}}}{\text{K}} - 273 \right) + 1010 \right] \frac{\text{kJ}}{\text{kg} \cdot \text{K}}$$

4-13

Combining Equations 4-8 through 4-12 results in the following equation for the equivalent gap conductivity due to conduction and convection in air:

$$k_{eq1} = 5.175 \left[\frac{g \cdot C_p \cdot \rho^2 \cdot k_{air}^3 \cdot \delta_1^3 \cdot (T_1 - T_{rock})}{\frac{T_{avg}^{2.5}}{T_{avg} + 113.299K} \cdot \frac{Pa \cdot s}{\sqrt{K}}} \right]^{0.25}$$

4-14

The thermal conductivity due to conduction and convection, k_{eq1} , can now be used in Equation 4-7, but the thermal conductivity due to radiation, k_{rad1} , is still required.

4.3.1.3 Thermal Radiation

The following equation for gap conductance due to radiation and conduction between parallel slabs is found in Nuclear Systems 1³³.

$$h = \frac{k}{\delta} + \frac{\sigma}{\frac{1}{\varepsilon_1} + \frac{1}{\varepsilon_2} - 1} \cdot \left(\frac{T_1^4 - T_2^4}{T_1 - T_2} \right)$$

4-15

Where: k is thermal conductivity due to conduction, δ is the thickness of the gap, σ is the Stephan-Boltzmann constant ($5.67 \times 10^{-12} \text{ W/cm}^2 \cdot \text{K}^4$), ε is emissivity, and T is temperature.

Since, the conductivity has already been accounted for in 4-8, the k/δ term must be removed.

Also, accounting for the annular shape according to Eqn. 12-53 in of the text Basic Heat Transfer, by M. Necati Ozisik⁴³, the resulting equation for radiative heat transfer is:

$$h_{rad1} = \frac{\sigma}{\frac{1}{\varepsilon_1} + \left(\frac{OD_f}{OD_f + 2 \cdot \delta_1} \right) \cdot \left(\frac{1}{\varepsilon_2} - 1 \right)} \cdot \left(\frac{T_1^4 - T_{rock}^4}{T_1 - T_{rock}} \right)$$

4-16

Where: ε_1 is the emissivity of the liner outer surface, ε_2 is the emissivity of granite, and all other variables are as previously defined.

To convert the conductance, h_{rad1} , to conductivity, k_{rad1} , the following equation is used, which also accounts for the annular shape:

$$k_{rad1} = h_{rad1} \cdot \frac{OD_f}{2} \cdot \ln \left(\frac{OD_f + 2 \cdot \delta_1}{OD_f} \right)$$

4-17

Where all the variables are as previously defined. The thermal conductivity due to radiation, k_{rad1} , can be used in Equation 4-7, and T_{1new} can be calculated using Equation 4-6. If T_{1new} differed from T_1 by more than $0.1^\circ K$, T_1 was adjusted, and the calculations were repeated until T_{1new} and T_1 were within $0.1^\circ K$ of each other.

4.3.2 Heat Transfer Through the Liner

Thermal conductivity through the steel liner (or final casing) is dominated by conduction; therefore, only one equation is required:

$$T_{ID.f} = T_{OD.f} + \frac{q' \cdot \ln \left(\frac{OD_f}{ID_f} \right)}{2 \cdot \pi \cdot k_{steel}}$$

4-18

Where: $T_{ID.f}$ is the temperature at the inner diameter of the final casing, $T_{OD.f}$ is the temperature at the outer diameter of the final casing (equal to T_1 from above), OD_f is the outer diameter of the final casing, ID_f is the inner diameter of the final casing, q' is the linear heat rate of the waste, and k_{steel} is the thermal conductivity of steel.

4.3.3 Heat Transfer Between the Liner and Canister

The calculation of heat transfer across the second gap, between the liner and canister, is performed using the same equations as those used for the first gap (except that all subscript 1's are changed to subscript 2's).

4.3.4 Heat Transfer Through the Canister

The calculation of heat transfer through the canister (or waste string) is performed using the same equations as those used for liner (except that subscript f is changed to subscript ws).

4.3.5 Heat Transfer Through the Packing Material and Waste

The waste and packing material are treated in a manner similar to that used by Manteufel and Todreas¹⁰. The contents of the canister are divided into two sections: the Interior and the Edge regions. The Interior region consists of the homogenized fuel assembly in a silicon carbide particle bed. The Edge region consists only of the silicon carbide particle bed. These regions are separated by an imaginary line at the effective diameter of the homogenized cylindrical Interior region, as calculated in the homogenization section.

The equation used for the Edge region is similar to that used for the liner and canister, since conduction is the dominant mode of heat transfer through the particle bed.

$$T_e = T_{ID.ws} + \frac{q' \cdot \ln\left(\frac{ID_{ws}}{d_{int}}\right)}{2 \cdot \pi \cdot k_{SiC.bed}}$$

4-19

Where: T_e is the temperature at the effective diameter of the Interior region, d_{int} is the effective diameter of the Interior region, $k_{SiC.bed}$ is the thermal conductivity of the silicon carbide particle bed, and all other variables are as previously defined.

Finally, the homogenized Interior region is also dominated by conduction, but has a cylindrical shape, rather than an annulus, so the equation for the centerline temperature is:

$$T_{CL} = T_e + \frac{q'}{4 \cdot \pi \cdot k_{hom}}$$

4-20

Where: k_{hom} is the homogenized thermal conductivity calculated using Equation 4-1, and all other variables are as previously defined.

Figure 4-1 is a flow diagram for the calculation of the centerline temperature, TCL, using the equations and process described in Sections 4.2 and 4.3.

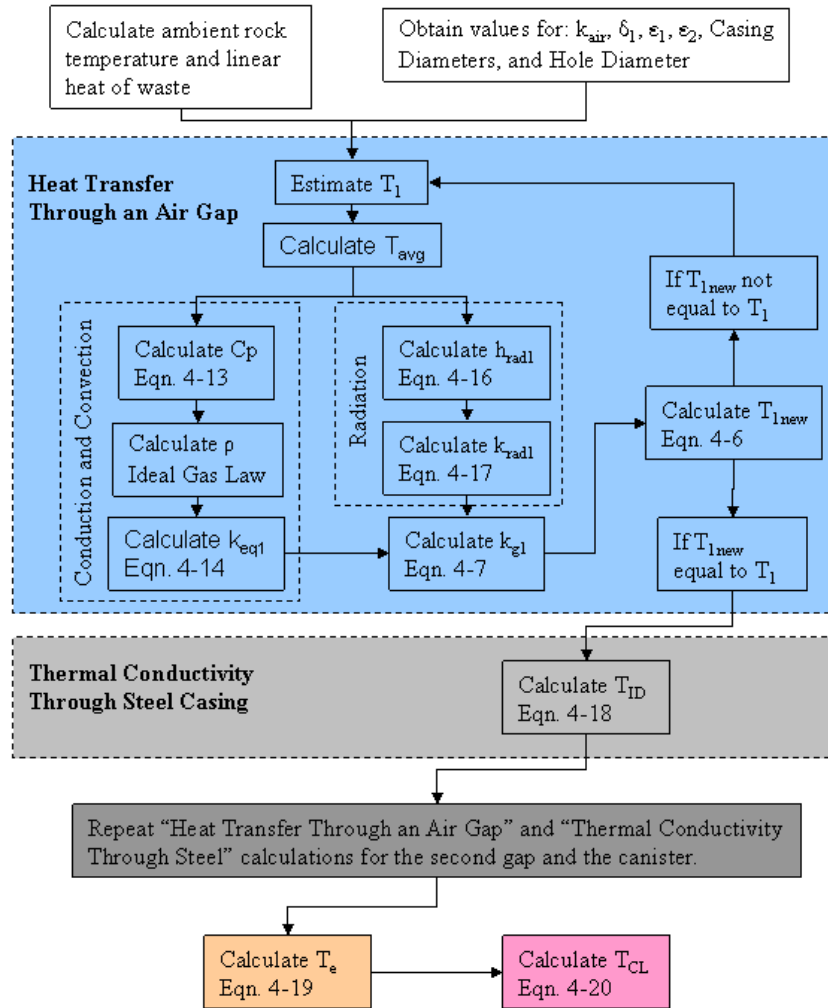


Figure 4-1 Flow Diagram for Calculation of the Canister Centerline Temperature, T_{CL}

4.3.6 Temperature Profile Inside the Borehole

Figure 4-2 shows a cross section of the borehole in the emplacement zone. The square in the middle represents a PWR assembly, and the dashed circle represents the equivalent diameter for the homogenized interior region. Below the cross section of the borehole is the expected temperature profile for the reference case. ΔT_1 is the temperature difference between the borehole wall and the liner. ΔT_2 is the temperature difference between the borehole wall

and the canister wall. ΔT_{hole} is the temperature difference between the borehole wall and the canister centerline. Since the temperature change through the liner and the change through the canister wall are so small, those temperature changes are not specified in Figure 4-2; however they are listed in Appendix C.

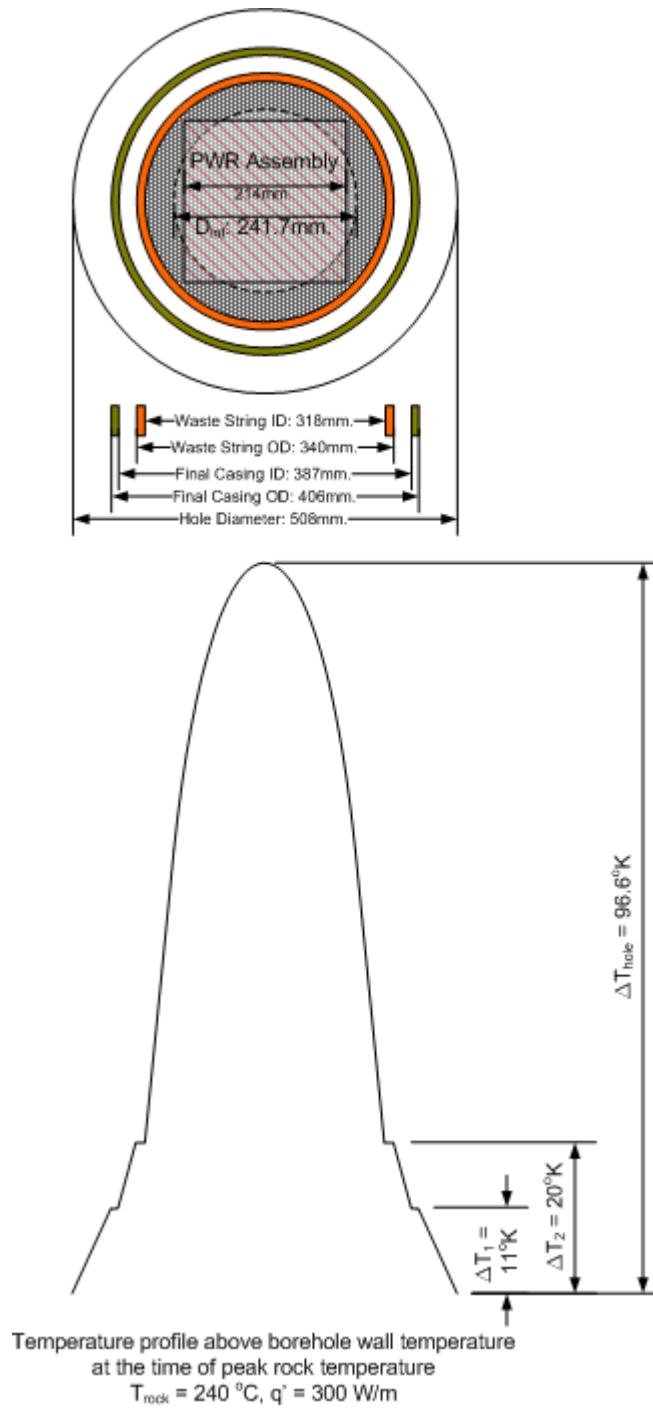


Figure 4-2 Expected Temperature Profile Inside the Borehole, using the homogenized interior approximation for #16 SiC grit

4.4 Parametric Study of Temperatures in the Borehole System

The Mathcad code was run for an array of 110 combinations of ambient granite temperature and linear power. Microsoft Excel was used to calculate trendline formulas for the two variables (ambient granite temperature and linear power of the waste). Using the trendlines, a correlation was derived to approximate the center line temperature of the waste based on the ambient granite temperature and linear power of the waste:

$$T_{CL} := T_{amb} + \frac{G \cdot q'}{4 \cdot \pi \cdot k_{granite}} + \left(7 \cdot 10^{-8} \cdot T_{amb} - 5.25 \cdot 10^{-5} \right) \cdot q'^2 + \left(3.5 \cdot 10^{-9} \cdot T_{amb}^3 - 1.4 \cdot 10^{-6} \cdot T_{amb}^2 - 8 \cdot 10^{-5} \cdot T_{amb} + 0.3742 \right) \cdot q'$$

4-21

Where: T_{amb} is the ambient granite temperature prior to waste emplacement in °C, q' is the linear power of the waste in W/m, and $k_{granite}$ is the thermal conductivity of granite in W/m°C.

The second term representing the peak temperature change at the borehole wall (ΔT_{rock}),

$$\Delta T_{rock} = \frac{G \cdot q'}{4 \cdot \pi \cdot k_{granite}}$$

4-22

was developed by Kuo⁶ to estimate the temperature change at the borehole wall, where G can be set as a constant, and $k_{granite}$ is the thermal conductivity of granite. Kuo conservatively estimated the value of G to be 7. Ranade³⁸ did some parametric analyses and found that a value of 6 is more appropriate for G , so this value was used for these calculations.

Equation 4-21 is plotted in Figure 4-3 which shows the results are nearly linear; however, Equation 4-21 produces results within two degrees Celsius of the temperatures

calculated using the iterative Mathcad script, while linear equations deviate by more than ten degrees Celsius over this range.

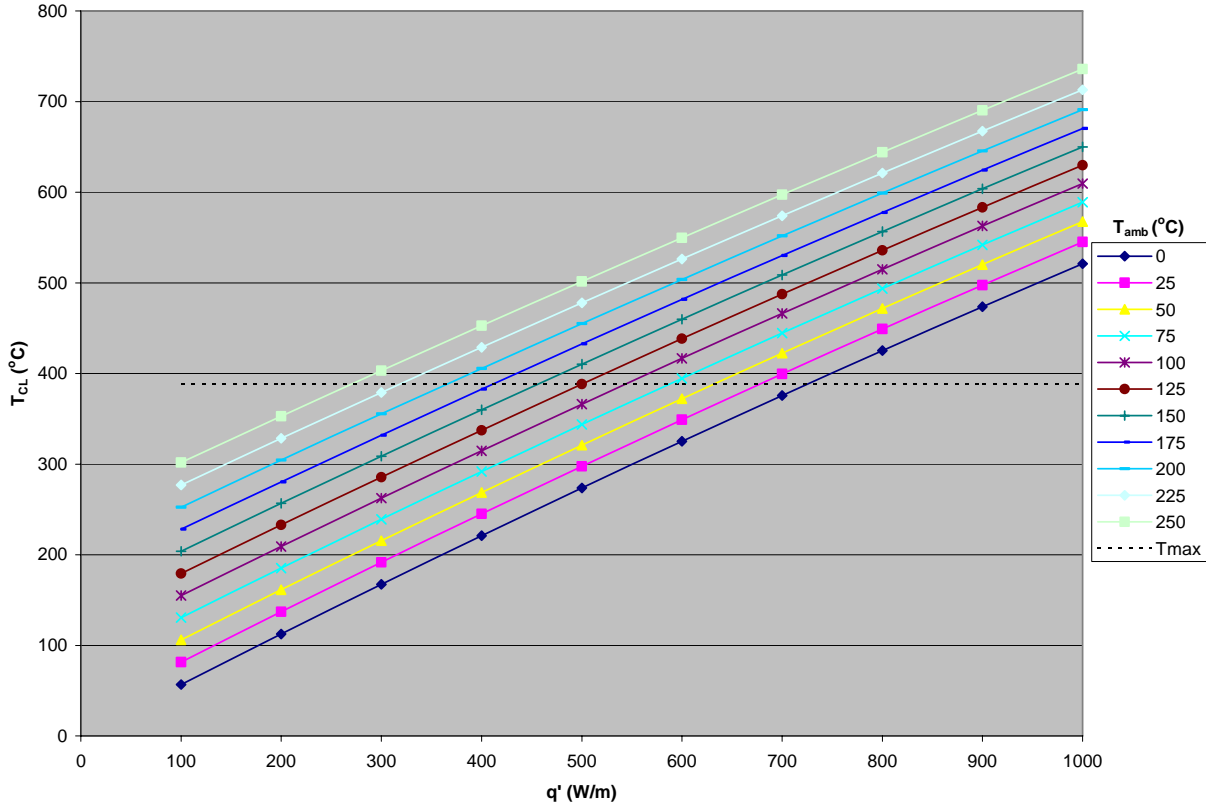


Figure 4-3 Center Line Temperature, T_{CL} , as a function of linear power, q' , and ambient granite temperature, T_{amb}

The temperature difference from ambient granite temperature to peak centerline temperature can be broken up into the peak temperature rise in the granite at the borehole wall, and the temperature difference from the borehole wall to the center of the canister. The peak temperature rise in the granite at the borehole wall is described above in Equation 4-22. The third and fourth term in Equation 4-21 estimate the temperature difference from the borehole wall to the center of the canister (ΔT_{hole}), where temperatures are in $^{\circ}\text{C}$, and q' is in W/m .

$$\Delta T_{\text{hole}} = \left(7 \cdot 10^{-8} \cdot T_{\text{amb}} - 5.25 \cdot 10^{-5} \right) \cdot q'^2 + \left(3.5 \cdot 10^{-9} \cdot T_{\text{amb}}^3 - 1.4 \cdot 10^{-6} \cdot T_{\text{amb}}^2 - 8 \cdot 10^{-5} \cdot T_{\text{amb}} + 0.3742 \right) \cdot q'$$

4-23

Equation 4-23 is graphed in Figure 4-4. The curvature due to linear power, and the difference in slope due to ambient temperature are more apparent here than in Figure 4-3.

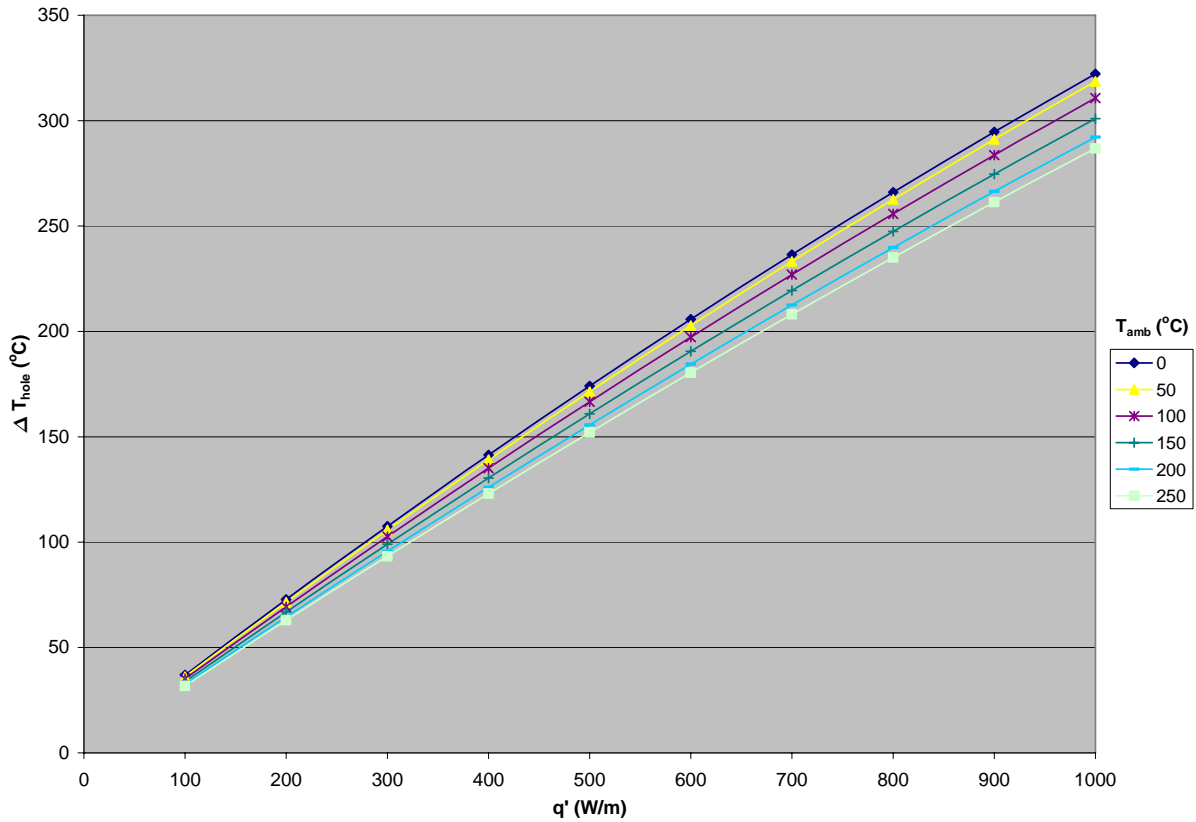


Figure 4-4 Borehole Temperature Difference between Center Line, T_{CL} , and Borehole Wall, T_{rock} as a function of linear power, q' , and ambient granite temperature, T_{amb}

Sensitivity analysis was also performed for the conductivity of the packing material, gap width between the casing and the borehole wall, emissivity of the borehole wall, and emissivity of the casings. The most significant improvement can be made by improving the conductivity of the packing material. As shown in Figure 4-5, the centerline temperature can be decreased by about 80°C by replacing the packing material with an Al-Mg alloy. According

to Hanson, Elliot, and Shunk⁴⁴, an aluminum-magnesium alloy with 35 weight percent magnesium has a melting temperature of 450°C; or with 67.7 weight percent magnesium, a melting temperature of 437°C. Thus the alloy can be poured into the canisters in molten form and allowed to solidify. From the Handbook of Binary Metallic Systems: Structure and Properties⁴⁵, the thermal conductivity of the alloy is found to be about 25 W/m*°C.

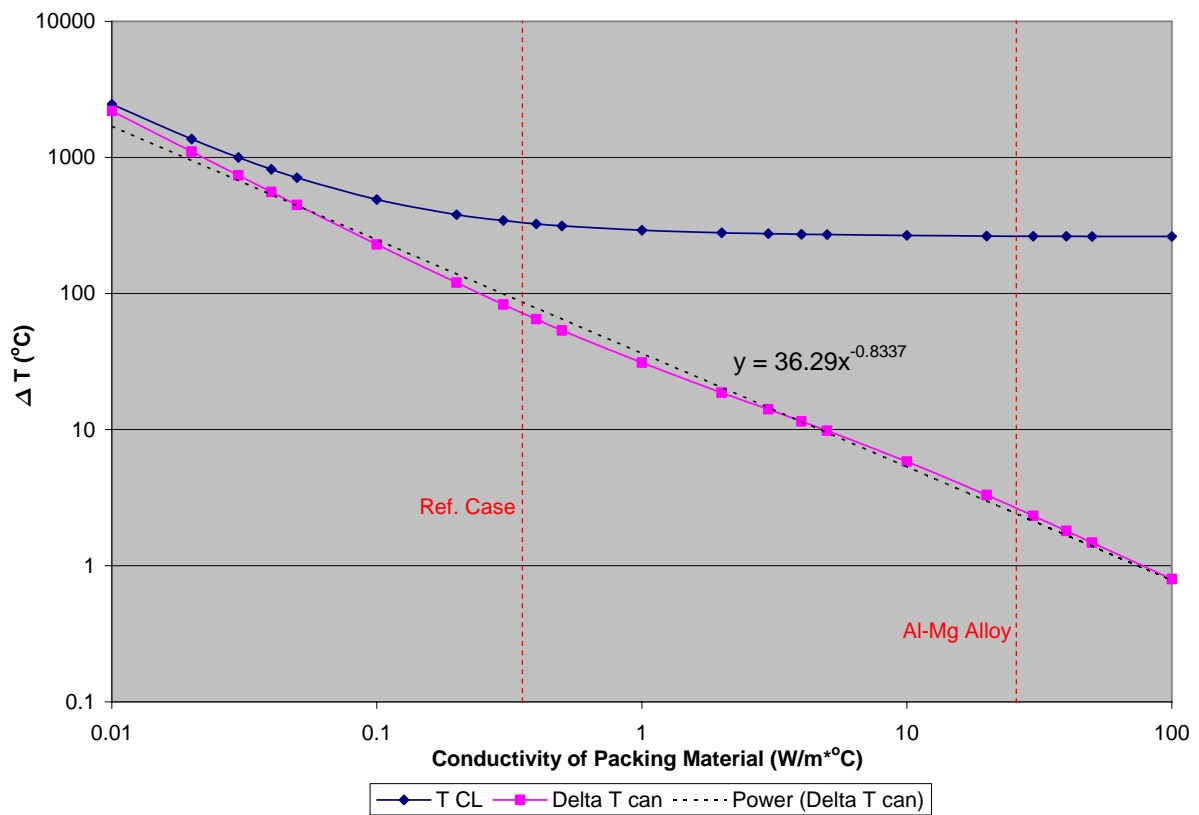


Figure 4-5 Effect of Packing Material Conductivity on Centerline Temperature, T_{CL} , and the "Delta T" of the Canister, ΔT_{can}

The other sensitivity analysis graphs can be found in Appendix C. The thickness of each air gap only affects the temperature difference by a couple of degrees, but it is interesting to note the coincidence that the drill bit commonly used for the liner casing creates an air gap width near the peak of the ΔT curve. By improving the borehole wall emissivity the centerline

temperature can only be decreased by about three degrees Celsius. For the casing emissivity, the reference case assumes rough oxidized steel with an emissivity of 0.8, so there is not much room for improvement. However, if the steel is not oxidized the centerline temperature would be 15 to 20°C higher.

The linear power of the waste, q' , obviously has the greatest effect on temperature. The linear heat rate depends primarily on cooling time. Based on a curve fit to Figure 2-1, an approximation of linear power as a function of cooling time, for 60 GWd/MTU burnup fuel is:

$$q'(t_c) := \frac{2200}{t_c^{0.75}}$$

4-24

Where t_c is the cooling time in years. Thus, the half-life of the linear power is about 15 years, and the centerline temperature would be reduced by about 75°C from the reference case after one half-life.

4.5 Summary

There are many variables affecting the centerline temperature of the borehole system: the various material properties, geometry of the waste, cooling time prior to emplacement, linear power of the waste, and ambient rock temperature. Calculating the centerline temperature from all these variables is an iterative process, due to the radiation equation (Equation 4-15); however, for a chosen design, the centerline temperature can be closely approximated with a single equation (in the form of Equation 4-21) requiring only two input variables: 1) ambient rock temperature prior to emplacement and 2) the linear power of the waste at the time of emplacement.

For the borehole system described in this thesis, at an ambient granite temperature of 180°C (based on a high vertical thermal gradient of 40°C/km), high burnup (60 GWd/MTU) PWR assemblies with a linear power of 300 W/m (less than ten years cooling) will not exceed the maximum storage and shipping temperature of 380°C¹⁰.

5 ECONOMICS

5.1 *Introduction*

For the deep borehole concept for permanent disposal of nuclear waste to be an acceptable solution, it should be economically competitive with shallower mined repositories such as Yucca Mountain. Woodward-Clyde Consultants⁵ performed a thorough cost analysis of the deep borehole drilling for nuclear waste disposal in the early 1980's. This chapter will convert costs based on the Woodward-Clyde analysis to year 2000 dollars. These costs will also be compared to the latest depth-dependent drilling cost index developed by Augustine and Tester.⁴⁶

The Nuclear Waste Policy Act of 1982 established a financing mechanism for disposal of nuclear waste in which utility companies pay 1 mill (0.1 cent) per kilowatt hour of nuclear electricity into the Nuclear Waste Fund. The Nuclear Waste Fund currently contains just over 14 billion dollars, and increases by about 750 million dollars each year.⁴⁷ According to the calculations conducted by the DOE in 2001 of detailed nuclear waste fund cash flows for reference cost estimate using a current forecasted 10-year real treasury note economic assumption, the value of the Nuclear Waste Fund in year 2000 dollars will be about \$45.6 billion by 2042.⁴⁸ The DOE's assessment concludes that the Nuclear Waste Fund Fee will be adequate.

Another thesis worth noting is Siegel's work from 1989 titled: "Economic Ramifications of a Delay in the National High Level Waste Repository Program." In addition to making an argument that solving the nuclear waste problem should not be delayed, he also

estimated overall waste disposal system costs. His estimate is about 23 billion 1989 dollars, but he notes that he could not accurately predict development and engineering costs.

5.2 Daily Rig Costs

Table D-1 in the Woodward-Clyde analysis lists basic rig cost, fully equipped rig cost, and an overhead factor depending on hole depth and bottom hole diameter. At a depth of 15000 feet (4.57 km) the following costs are listed in mid 1980 dollars:

Bottom Diameter	Basic Rig Cost	Fully Equipped Rig Cost	Overhead Factor
17½"	\$11,000 / day	\$25,000 / day	0.20
26"	\$12,000 / day	\$28,000 / day	0.20

Table 5-1 Applicable Rig Costs and Overhead Factors

Interpolating between these points for a 20" bottom diameter hole results in the following numbers: \$11,300 per day for basic rig cost and \$25,900 for the fully equipped rig cost. Assuming a fully equipped rig is required, and applying the overhead factor, the daily rig cost is \$31,080/day.

5.3 Total Drilling Operation Cost for a Single Hole

Table D-2 of the Woodward-Clyde analysis lists approximate drilling rates for various bit diameters. Iterating between points in this table gives a drilling rate of 78ft/day for the emplacement zone, 72ft/day for the surface casing, and 63ft/day for the conductor casing. Table D-3 of the Woodward-Clyde analysis lists cost per foot and cementing time based on casing diameter. Numbers from the Woodward-Clyde tables are used in a cost analog in Table 5-2. A 25% verticality premium is recommended for holes deeper than four kilometers, so it

may not be necessary but is included to be conservative. Mud cost is expected to be 15% of the daily costs for the rig. Mobilization and demobilization costs are expected to be \$300,000.

Table 5-2 Drilling Operations Cost Analog per Hole					
<u>Bit Diameter</u> <u>in (mm)</u>	<u>Casing Diameter</u> <u>in / mm</u>	<u>Depth</u> <u>ft (km)</u>	<u>Drilling</u> <u>ft/day</u>	<u>days</u>	<u>Casing and Cementing</u> <u>Days</u>
36 (914.4)	20 (508.0)	65 (0.020)	63	2	5
26 (660.4)	18 5/8 (473.1)	3,300 (1)	72	45	4
20 (508.0)	16 (406.4)	13,124 (4)	78	126	14
Sub-Totals:				173	23
25% 2-degree verticality premium:				44	
Total rig days:					240
Rig cost:			\$31,080 / day		\$7,459,000
Mud cost (15% of daily cost):					\$1,119,000
<u>Casing and cement:</u>					
	Casing Diameter	Depth	Cost / ft		
	20 (508.0)	65 (0.020)	\$200		\$13,000
	18 5/8 (473.1)	3,300 (1.0)	\$200		\$660,000
Mobilization and demobilization:					\$300,000
TOTAL DRILLING OPERATION COST:					\$9,551,000

5.4 Estimation of Current Costs for Drilling

The Woodward-Clyde report lists costs in “mid-1980’s” dollars; however, the MITDD (Massachusetts Institute of Technology Depth Dependent) Drilling Cost Index shows a steep decline in the cost of drilling in the mid 1980’s. Since the Woodward-Clyde analysis was published in December of 1983, it will be assumed that the associated index value is the 1983 MITDD Drilling Cost Index value (203.6 for a four kilometer deep hole). Since the year 2000, the MITDD Drilling Cost Index has been rapidly increasing. Coincidentally, the index was approximately the same in 2000 as in 1983. When adjusted for inflation, as shown in Augustine’s Figure 9, the index for a four kilometer (13,123 ft.) deep hole is 10 to 20 percent lower in 2000, and the following years, than it was in 1983.

Technology advances and the price of oil have had more of an effect on increasing costs than inflation. Augustine's Figure 6 shows the drilling cost index is closely tied to the cost of crude oil and natural gas. For these reasons, \$10,000,000 is still a conservatively high estimate of the cost of drilling a borehole for disposal of nuclear waste. Comparable holes have recently been drilled for about half this cost. At Soultz, France, the GPK-3 geothermal well cost 6.571 million 2003 dollars, and the GPK-4 well cost 5.14 million 2004 dollars⁴⁶. Both GPK holes reached a depth of five kilometers, and no significant costs were incurred due to trouble.

The DOE report, Analysis of the Total System Life Cycle Cost of the Civilian Radioactive Waste Management Program⁴⁹, suggests a need to dispose of 83,800 MTHM of commercial spent nuclear fuel, about 2,500 MTHM of DOE spent nuclear fuel, and 22,147 canisters of HLW of unspecified size and weight, by the year 2040, according to current licenses for nuclear power plants. If each borehole can hold 200 MTHM, 500 boreholes would be required to dispose of 100,000 MTHM. If each borehole costs ten million dollars to drill, the total drilling cost would be five billion dollars, or one third of the current Nuclear Waste Fund. From another perspective, the drilling operation costs account for \$50 per kilogram, which is only one eighth of the approximately \$400 per kilogram available based on the 1 mill/kW*hr waste fee.

5.5 Comparison to Yucca Mountain Costs

Yucca Mountain is in its final stages of approval at a cost of nearly six billion dollars to date. It is likely that the approval process for a borehole repository system will incur equal costs. Waste Acceptance, Storage and Transportation, Nevada Transportation, Program

Integration, and Institutional costs add up to about 15 billion dollars. The projected cost to complete the monitored geologic repository at Yucca Mountain is another 36 billion dollars. The monitored geologic repository costs are further broken down in Table 5-3.

Phase	Historical (1983-2000)	Future Costs (2001-2119)
Development and Evaluation (1983-2003)	5,780	800
Licensing (2003-2006)	0	1,290
Pre-Emplacement Construction (2006-2010)	0	4,450
Emplacement Operations (2010 – 2041)	0	19,710
Monitoring (2041 – 2110)	0	6,000
Closure and Decommissioning (2110 – 2119)	0	4,040
Total	5,780	36,290

NOTE: Historical costs total \$4.8 Billion in YOE dollars.

Table 5-3 Monitored Geologic Repository Costs by Phase (in Millions of 2000\$)

For a borehole repository system, the drilling costs would replace the Pre-Emplacement Construction costs. For the same cost, only 445 boreholes may be affordable, which would still be capable of holding 89,000 MTHM (19,000 MTHM more than Yucca Mountain is planned to hold). However, if the cost of drilling is as low as the Soultz wells indicate, the drilling cost may be cut in half.

5.6 Summary

The construction cost of a deep borehole repository system is competitive with the construction cost of Yucca Mountain. However; the bulk of the costs are from other requirements which would most likely be the same for a deep borehole repository. So, overall the deep borehole concept is competitive with Yucca Mountain, but the current predictions for the Nuclear Waste Fund can only afford one or the other. If Yucca Mountain is not approved, or if another 80,000 MTHM or more is expected to be generated, the deep borehole repository system should be considered. If Yucca Mountain is approved and the nuclear power industry

does not continue to produce more waste than it is currently licensed for, the deep borehole repository system should still be considered, but the 1 mill per kilowatt hour of nuclear electricity may have to be increased. However, the marginal cost of expanding an already existing Yucca Mountain repository should be considerably less expensive than starting from inception. Fortunately, Sweden's Aspo Hard Rock Laboratory is already conducting experiments at a depth of nearly half a kilometer in granite, as explained in the article: Final Resting Place.²²

A more detailed analysis of costs is clearly needed in future work. Even more important than the analysis of the cost of drilling, is the analysis of all the other costs associated with starting a repository. What lessons from Yucca Mountain can be used without incurring billions of dollars of time and research? What new costs will be incurred? For example: deep boreholes have the advantage of being modular, and need only be constructed as needed, without the large up-front costs of boring tunnels for a mined repository. The single largest cost at Yucca Mountain is expected to be emplacement operations. Woodward-Clyde suggest that their waste emplacement and borehole plugging will cost a mere million dollars per hole, totaling half a billion dollars for a 500 hole repository, creating a savings of up to 23 billion dollars. On the other hand, the site selection process and licensing may be more expensive if the public continues a state of heightened wariness about nuclear waste.

6 CONCLUSIONS

Thanks to continuous improvements in drilling capability, the very deep borehole concept is a highly competitive option for disposal of spent fuel and other high level waste. Holes can be drilled into granite to the depths proposed in this thesis and previous papers. Standard drill casings can be used in the boreholes, and for the construction of the waste canisters. Even with less than ten years cooling, the waste will not reach unreasonable temperatures. Granite shows via natural analogs its capability to prevent the migration of metallic ions, even over millions of years. And there are promising options for plugging the boreholes. The conclusions of this thesis are supportive of the very deep borehole concept, but there are still many questions to be answered.

6.1 *Thesis Summary*

The problem of disposing of nuclear waste is not simple. Approving and building a repository is challenging both politically and scientifically. The permanent repository must prevent hazardous levels of radiation from reaching the biosphere for up to a million years. At the time of emplacement the waste is so hazardous that it must be handled remotely. The waste must be transported in casks capable of surviving catastrophic highway and rail accidents. Special drilling derricks must be constructed to allow positioning of the waste, and remote handling. After emplacement the environment surrounding the waste may change over the required decay time. An originally dry hole may partially or completely flood. Despite the technically complex process of emplacing the waste and the possibility of a changing environment, the best quality of the very deep borehole concept is that it relies on the proven capability of the host granite to maintain stability and prevent migration of nuclides for over a

million years. And, should retrieval be necessary, it is possible, yet difficult enough to make it unlikely that the waste will fall into the hands of those who would use it against society.

6.1.1 Canister Reference Design

The reference design analyzed contains a PWR assembly inside a waste string canister and final casing liner as listed in Table 6-1 Casing Parameters For A 2km Emplacement Zone. Each canister is five meters tall. The space between the borehole wall and the liner, and the space between the liner and the canister is filled with air. Thermal calculations were also performed for these spaces filled with water. Each borehole is four kilometers deep with a two kilometer emplacement zone.

Table 6-1 Casing Parameters For A 2km Emplacement Zone²⁷		
	<u>Final Casing:</u>	<u>Waste String:</u>
Outer Diameter, OD (mm)	406.40	339.70
Inner Diameter, ID (mm)	387.36	315.32
Thickness, t (mm)	9.52	12.19
Nominal weight, NW (kg/m)	96.73	101.20
Steel	H40	T95
Threads	Short round	Buttress
Bit size (mm)	508.00	444.50

Table 6-2 gives the properties of the steel selected for the canisters and liner.

Table 6-2 API Steel Specifications³⁰									
<u>Grade</u>	<u>Heat Treatment</u>	<u>Min. Yield Strength</u>	<u>Min. Tensile Strength</u>	<u>Chemical Analysis Maximum Concentrations</u>					
		<i>N/mm²</i>	<i>N/mm²</i>	<i>C</i>	<i>Si</i>	<i>Mn</i>	<i>P</i>	<i>S</i>	<i>Other</i>
H40		276	414						
T95	Quenched and Tempered	655	725	0.45	0.45	1.9	0.03	0.03	
Emissivity of steel with a rough oxide layer ³¹ :									0.8

The reference waste form is a Westinghouse 17X17 pin PWR fuel assembly with a conservatively high linear power of 300 W/m. Table 3-2 lists other details about the waste.

6.1.2 Stress Analysis

Some key details for the stress analysis are listed in Table 6-3. The table contains a breakdown of the three weight categories in the waste string.

Table 6-3 Summary of Data for Stress Calculations				
	Mass (MT)			
Casing	405		Cross sectional area of casing:	12,542 mm ²
Waste	280		400 PWR assemblies (details in Table 3-2)	
Packing	236		#16 SiC grit density:	2.015 gm/cm ³
TOTAL	921		Tensile Stress at the surface:	720 MPa

Compressive stress at the bottom of the hole after the waste string is released is the same as the tensile stress at the surface prior to releasing the waste string. General buckling is not expected since the casing is confined within the borehole. The limit for localized buckling is 8.46GPa; therefore, buckling is not expected. Thermal stress in the rock is also not expected to cause any problems due to spalling.

6.1.3 Thermal Analysis

Figure 4-3 is repeated here as Figure 6-1 since it best summarizes the results of the thermal analysis. From Manteufel's paper¹⁰, 388°C is assumed to be the limit for the centerline temperature of the canister. It is also important to note that the conductivity of the packing material has a significant effect on the centerline temperature, as shown in Figure 4-5.

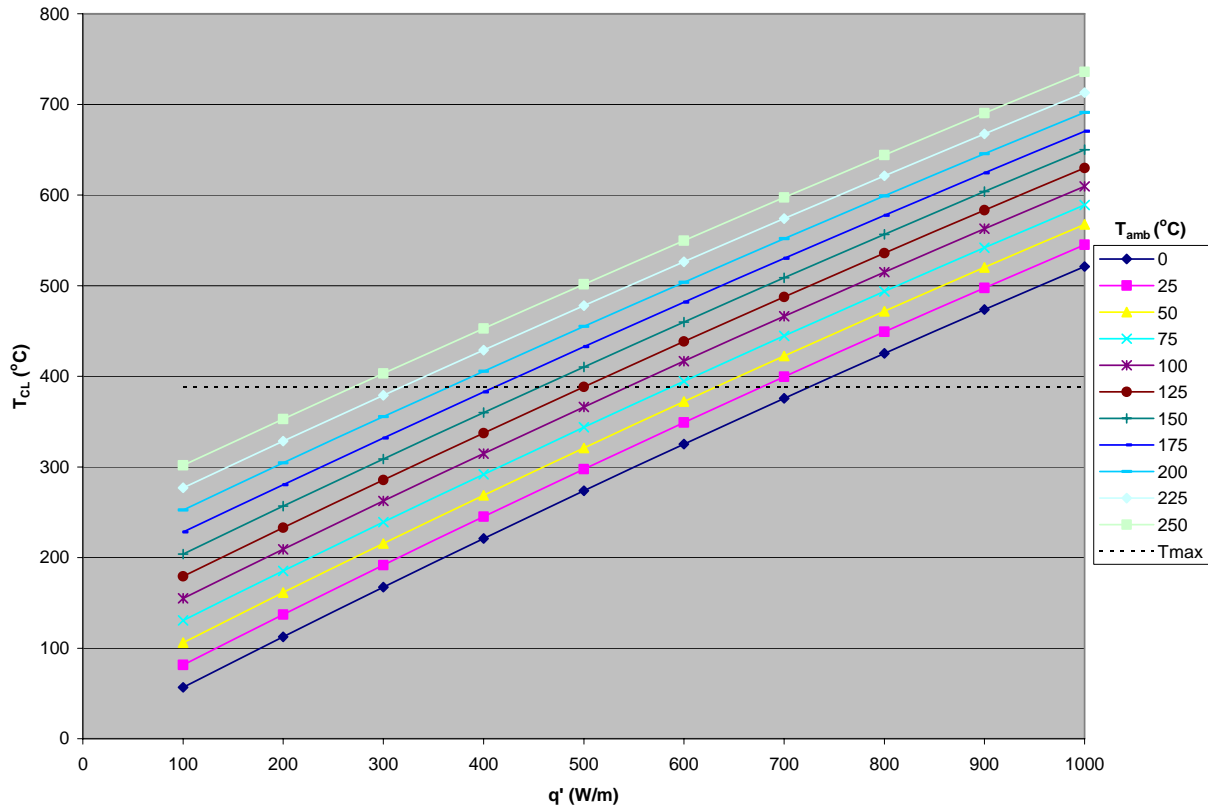


Figure 6-1 Center Line Temperature, T_{CL} , as a function of linear power, q' , and ambient granite temperature, T_{amb}

6.1.4 Economic Analysis

On average, each borehole is expected to cost less than ten million dollars. The total cost to construct a central repository for 100,000 MTHM at this price is about five billion dollars. Although the construction cost is competitive with the construction cost of Yucca Mountain, it is only 10% of the total projected cost of the mined geologic repository at Yucca Mountain. If all costs other than construction are the same, the money expected to accumulate in the Nuclear Waste Fund (based on current licenses) will only be enough to build one repository or the other. It is interesting to note that, “The TSLCC analysis [the basis for the fee adequacy statement] projects costs through the year 2119 for a surrogate, single potential repository, expanded to accommodate all the SNF and HLW projected,”⁴⁸ despite the 70,000 MTHM legislative limit for Yucca Mountain. Although there are difficult decisions facing the United States, the very deep borehole concept is a good option for the rest of the world, since granite can be found in most areas of the earth’s crust.

6.2 Future Work

6.2.1 Thermal Analysis

Two things were not accounted for in the thermal analysis conducted in this thesis. The first omission is the role of axial cooling. The waste is modeled as a line source, which is a conservative approximation. In reality, some heat would travel axially away from each borehole. At first axial cooling would occur in both directions, but due to the vertical thermal gradient, most of the cooling would be toward the surface of the earth.

The second omission was the vertical thermal gradient inside the borehole due to convection. Since the gaps are filled with air, the top end of the borehole may be hotter than the bottom end of the borehole. Luckily, the vertical thermal gradient of the granite is in the opposite direction, which should counteract the accumulation of hot air at the upper end of the borehole. Furthermore, as the air gets hotter, the heat flux to the granite increases, further reducing the effect of the rising air temperature.

Experiments should be conducted to verify the accuracy of the thermal analysis performed in this thesis, and to assess the importance of the two omissions mentioned above. Concurrent with this thesis, Samina Shaikh is performing experiments to measure the conductivity of the packing material options, and the gaps between the canister and borehole wall.

More work also needs to be done on determining the allowable maximum and time-dependent temperature of the spent fuel after emplacement. This should be planned ahead and

calculated for each borehole prior to waste emplacement. In order to minimize the center line temperature throughout the waste string, assemblies with higher linear power should be placed at the top of the emplacement zone where the granite is cooler due to the vertical thermal gradient.

A variation of the analysis in this thesis could also be done to explore the option of not using any packing material, and increasing the thickness of the canister walls to withstand the lithostatic pressure. Kuo⁶ states that there should be little change in the centerline temperature, since radiative heat transfer with air will make up for the lost conductive heat transfer. A detailed materials cost analysis may also show a benefit of not using packing material.

6.2.2 Plugging

After filling a borehole with waste, it will need to be plugged to prevent radionuclides from reaching the atmosphere via the borehole. In May of 1980, a workshop was held in Columbus by the OECD Nuclear Energy Agency and the United States Department of Energy. These proceedings were published in a book titled Borehole and Shaft Plugging⁵⁰. The book addressed plugging of mined geologic repositories and boreholes in basalt and rock salt. Bentonite, cement based sealants, and grout are all addressed as part of the proposed plugging system. A similar analysis should be performed for plugging boreholes in granite.

In addition to the analysis, experiments should be conducted similar to those started at Sweden's Aspo Hard Rock Laboratory outside the town of Oskarshamn²². The current experiments use cast iron canisters coated with copper, and the holes are plugged with bentonite clay. If the granite in the Aspo lab is similar to granite in likely locations in the United State for deep borehole repositories, the US Department of Energy could use the results

from the Aspo experiments, or perhaps use the Aspo lab to conduct their own experiments. Otherwise, a new deep rock lab may have to be built in the United States. Also, the canisters proposed in this thesis are not coated with copper, as those proposed by Sweden and Finland, since the granite and plug are expected to contain the waste, not the canisters.

6.2.3 Corrosion of Steel Canisters

Like Sweden and Finland, Victoria Anderson⁷ also proposed copper for the canister material due to the high corrosion rate that would occur for other candidate metals in the expected aqueous environment in granite. On the scale of a million years, the canisters would fail quickly if they do not have a copper coating; however, as mentioned earlier, the canisters do not need to last if the granite and plugging perform as the primary barrier to prevent the waste and its products from returning to the atmosphere. Also, the boreholes may be dry (with humidity), or partially flooded. An analysis should be performed to assess what will happen as the waste canisters fail in each of these cases. Does the waste need to be cemented or grouted in place to keep it from falling to the bottom of the hole? Dried up cement or grout may not have good enough conductivity to keep the waste at reasonable temperatures.

6.2.4 Site Selection

Although the process of finding a new site for a repository is a politically difficult process, there is geologic data suggesting there are many good locations to choose from. Based on maps in Structural and Tectonic Principles by Peter C. Badgley, published in 1965, there is a stable granite shelf that encompasses the state of North Dakota. In this stable shelf the granite was formed about 2.5 billion years ago and there are no fault lines to worry about. A more detailed study should be performed to identify other suitable locations for a repository.

The political process could also be analyzed, and recommendations made to streamline the site selection and approval process.

6.2.5 Repository Economics

The chapter on economics in this thesis is very rudimentary, and only addresses details of the construction costs. The largest area of cost for the Yucca Mountain repository is expected to be emplacement operations, while the construction is only a tenth of the total cost of the repository. To be highly competitive economically, a repository needs to save money in areas other than construction. A thorough analysis of the Yucca Mountain costs should be performed with a critical eye for savings opportunities.

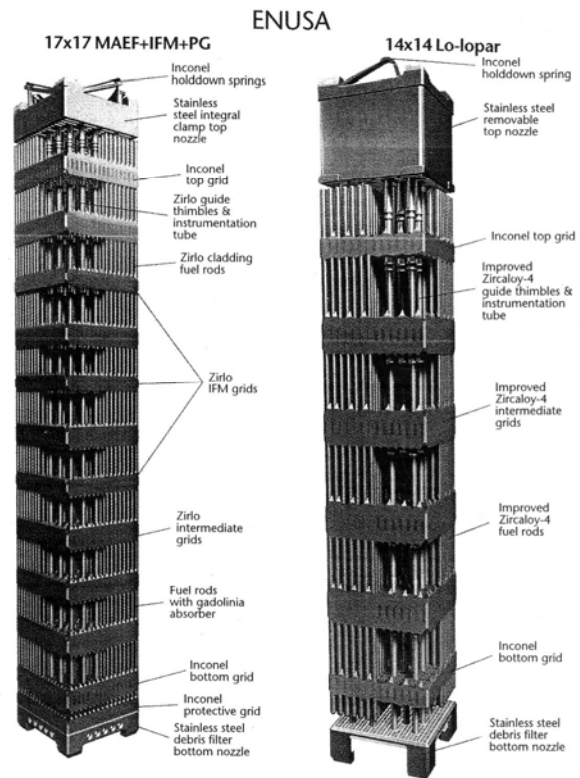
7 APPENDICES

7.1 *Appendix A: Reference Fuel Data*

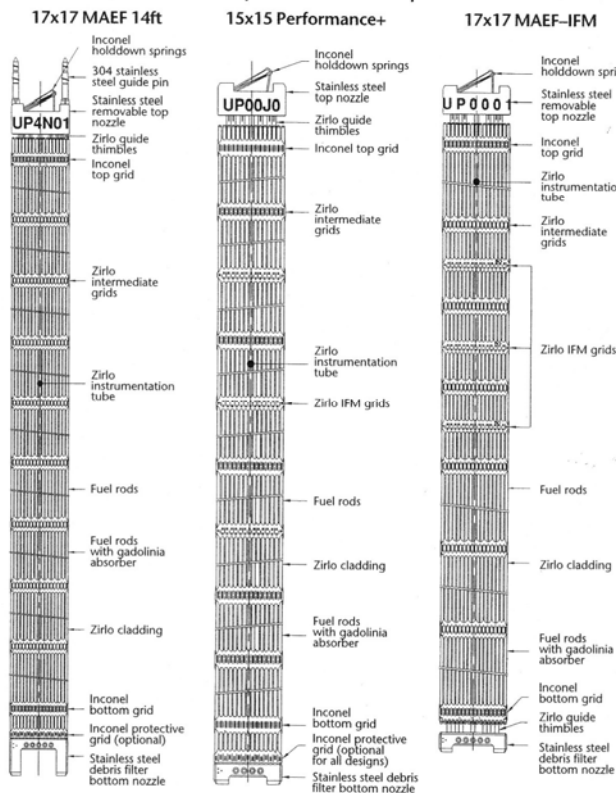
Appendix A contains the latest fuel design data from Nuclear Engineering International²⁵, a table of spent fuel discharges and burnup from Nuclear News²⁶, and the input file for OrigenArp so that the decay power graph in Section 2.2.1 can be recreated. However, this input file was generated using the “Express Form” in OrigenArp with the input values listed in Section 2.2.1.

Fuel design data

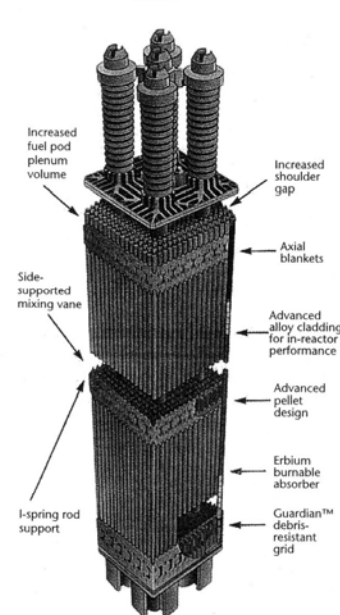
The four main reactor types (PWR, VVER, BWR and heavy water) are represented in the tables. Not all fuel fabricators are included. The illustrations and photographs show representative designs for most of the manufacturers included in the tables.



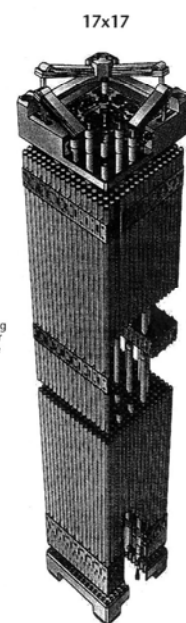
European Fuel Group



Westinghouse CE



Westinghouse Sweden



PWR design data

	Korea Nuclear Fuel (KNFC)						Mitsubishi			
	OFA	ACE7	KSD	Plus7	FORTE	ACE7				
Assembly geometry	14x14	16x16	16x16	16x16	17x17	17x17	14x14 ⁵	15x15 ⁶	17x17 ⁶	17x17 ⁷
No of rods per assembly							179	204	264	264
– Fuelled	179	235	236	236	264	264				
– Unfuelled	17 ¹	21 ²	5 ³	5	25 ⁴	25				
Overall assembly length (mm)	4063	4063	4528	4528	4063	4063	4057	4057	4058	4058
Overall assembly width (mm)	197	197	207	207	214	214	197	214	214	214
Rod length (mm)	3868	3878	4094	4094	3879	3881	3866	3866	3856	3856
Rod outside diameter (mm)	10.16	9.14	9.7	9.5	9.5	9.5	10.72	10.72	9.5	9.5
Pellet length (mm)	10.49	9.4	9.9	9.83	9.83	9.83	12.6	12.6	11.5	11.5
Pellet outside diameter (mm)	8.748	7.84	8.26	8.192	8.192	8.192	9.29	9.29	8.19	8.19
Pellet density (g/cm ³ or TD)	95%	95%	95%	95%	95%	95%	97%	97%	97%	97%
Average linear fuel rating (kW/m)	21.22	17.62	17.245	17.68	17.83	17.85	20.4	20.3	17.1	17.9
Peak linear fuel rating (kW/m)							–	–	–	–
Maximum fuel temperature (°C)							–	–	–	–
Clad material	Zirlo	Zirlo	Zirlo	Zirlo	Zirlo	Zirlo	Imp.Zy4	Imp.Zy4	Imp.Zy4	Imp.Zy4
Clad thickness (mm)	0.617	0.572	0.64	0.572	0.572	0.572	0.62	0.62	0.57	0.57
Average clad temperature (°C)							–	–	–	–
Maximum clad temperature (°C)							–	–	–	–
Grid material	Zirlo or Inc718	Zirlo or Inc718	Zirlo or Inc718	Zirlo or Inc718	Zirlo or Inc718	Zirlo or Inc718	Inc.	Inc.	Inc/Zy-4	Inc/Zy-4
Average discharge burnup (MWd/kgU)	42	55	43	55	48	55				
Maximum assembly burnup (MWd/kgU)	60	75	60	72	60	75	55	55	55	55

PWR design data (continued)

	Framatome ANP							
	Mk-B	Mk-BW17	AFA 3G					
Assembly geometry	15x15	17x17-12'	14x14	15x15	16x16	17x17-12'	17x17-14'	18x18
No of rods per assembly			179	204	236	264	264	300
– Fuelled	208	264						
– Unfuelled	17	25						
Overall assembly length (mm)	4209	4059	2899	4057	4827	4060	4795	4827
Overall assembly width (mm)	217	214	197.2	214	229.5	214	214	229.5
Rod length (mm)	3916	3865	2628.6	3874	4418	3863.4	4497.3	4429
Rod outside diameter (mm)	10.9/10.6 ¹³	9.5	10.72	10.72	10.75	9.5	9.5	9.5
Pellet length (mm)	11.5	10.2	15.25	15.25	11.0	13.46	13.46	9.66
Pellet outside diameter (mm)	9.4/9.8 ¹³	8.19	9.29	9.29	9.11	8.19	8.19	8.06
Pellet density (g/cm ³ or TD)	10.52	10.52	10.4	10.4	10.4	10.4	10.4	10.4
Average linear fuel rating (kW/m)	20.5	17.8	22	23.8 ¹⁷	21.1	20	17.9	16.6
Peak linear fuel rating (kW/m)	60.9	46.9	42 ¹⁶	42 ¹⁶	42 ¹⁶	42 ¹⁶	42 ¹⁶	42 ¹⁶
Maximum fuel temperature (°C)	2800 ¹⁴	2800 ¹⁴	2800 ¹⁴	2800 ¹⁴	2800 ¹⁴	2800 ¹⁴	2800 ¹⁴	2800 ¹⁴
Clad material	MS ¹⁵	MS ¹⁵	Zy4/MS ¹⁵	Zy4/MS ¹⁵	Zy4/MS ¹⁵	Zy4/MS ¹⁵	Zy4/MS ¹⁵	Zy4/MS ¹⁵
Clad thickness (mm)	0.635/0.6 ¹³	0.57	0.62	0.62	0.725	0.57	0.57	0.64
Average clad temperature (°C)	*	*						
Maximum clad temperature (°C)	420	404	400	400	400	400	400	400
Grid material	Zy4/MS ¹⁵ + Inc	Zy4/MS ¹⁵ + Inc	Zy4 + Inc	Zy4 + Inc	Zy4 + Inc	Zy4 + Inc	Zy4 + Inc	Zy4 + Inc
Average discharge burnup (MWd/kgU)	*	*						
Maximum assembly burnup (MWd/kgU)	>58	>67	>60	>60	>60	>60	>60	>60

*Depends on plant requirements. **Depends on plant design. ¹Comprises 16 guide thimbles and one instrumentation rod. ²Comprises 20 outer guides and one centre guide rod. ³Comprises four outer guides and one centre guide rod. ⁴Comprises 24 guide thimbles and one instrumentation rod. ⁵Two-loop. ⁶Three-loop. ⁷Four-loop. ⁸Usually >52 MWd/kgU; peak rod burnup is licensed up to 60MWd/kgU. ⁹Other lattice sizes available. ¹⁰For Westinghouse units. ¹¹For Framatome ANP units. ¹²Fuel incorporating MOX and/or ORP can be supplied to individual requirements. ¹³Wet lattice design option. ¹⁴No melting criteria. ¹⁵Advanced alloy MS is a Framatome ANP trademark. ¹⁶Depends on clad conditioning. ¹⁷Higher reactor power rate. ¹⁸No melting criteria. ¹⁹Different designs available. ²⁰This design is available through ENUSA for Spanish customers. ²¹Peak rod burnup is licensed up to 60 MWd/kgU. ²²ENUSA Industrias Avanzadas designs and manufactures PWR fuel to the Spanish plants.

PWR design data (continued)

Westinghouse CE			Westinghouse ¹²	Westinghouse Sweden & European Fuel Group (EFG – Westinghouse/ENUSA alliance)						ENUSA ²²	
System 80			Robust fuel assembly	RFA900	RFA1300	Performance +				Lo-lopar	17x17 MAEF+IFM+PG
14x14	16x16	16x16	17x17 ⁹	17x17	17x17	15x15	17x17	16x16	18x18	14x14	17x17
176	236	236	264	264	264	204	264	236	300	179	264
				25	25	21	25	20	24	17 ¹	25 ⁴
3994	4491	4528	4058	4058	4795	4058	4053	4827	4827	2854	4063
206	207	207	214	214	214	214	214	229.6	229.6	197	214
3733	4112	4112	3881	3865	4492	3874	3852	4399	4402	2583	3886
11.18	9.70	9.70	9.5	9.5	9.5	10.72	9.5	10.75	9.5	10.72	9.5
11.58	9.91	9.91	9.83	9.83	9.83	11.2	9	10	9	11.13	9.83
9.68	8.26	8.27	8.19	8.19	8.19	9.29	8.19	9.11	8.05	9.29	8.19
10.3-10.58	10.3-10.58	10.3-10.58		10.53	10.53		10.5	10.5	10.5	10.53	10.53
20.44	17.72	17.91		17.9	17.1		17.8	20.7	16.7	16.70	18.93
46.92	42.65	42.98		59.0	59.0					up to 68.9 ¹⁸	up to 68.9 ¹⁸
*	*	*		*	*	*	*	*	*	2800 ¹⁸	2800 ¹⁸
Zr4	Zr4	Zr4	Zirlo™	Zr4	Zr4	Zirlo™	Zr4	Duplex/Zr4	Duplex/Zr4	Improved Zr4	Zirlo
0.660	0.635	0.635	0.57	0.57	0.57	0.62	0.57	0.725	0.64	0.62	0.57
*	*	*		*	*	*	*	*	*		
*	*	*		*	*	*	*	*	*		
Zr4	Zr4	Zr4	Zirlo™	Inc/Zr4	Inc/Zr4	Inc/Zirlo™	Inc/Zr4	Inc/Zr4	Inc/Zr4	Inconel/impr Zr4	Inconel/Zirlo
*8	*	*		*	*	*	*	*	*		
*	*	*		*	*	*	*	*	*	45	57 ²¹

PWR design data (continued)

Framatome ANP					Nuclear Fuel Industries				
HTP									
14x14(16+1)	15x15(20+1)	16x16(20)	17x17(24+1)	18x18(24)	14x14 ⁵	14x14 ⁵	15x15 ⁶	17x17 ^{6,7}	17x17 ^{6,7}
196	225	256	289	324	179	179	204	264	264
179	204	236	264	300					
17	21	20	25	24					
2900	4058	4827	4057 ¹⁹	4827	4057	4057	4057	4058	4055
197.2	214	229.6	214	229.6	197	197	214	214	214
2635	3854	4405	3853 ¹⁹	4405	3856	3866	3856	3852	3862
10.77	10.75	10.75	9.55 ¹⁹	9.5	10.72	10.72	10.72	9.5	9.5
11.0	11.0	11.0	9.37 ¹⁹	9.8					
9.11	9.11	9.11	8.17 ¹⁹	8.05					
10.45	10.45	10.45	10.45 ¹⁹	10.45	95%	97%	95%	95%	97%
**	**	**	**	**	20.4	20.4	20.3	17.1/17.9	17.1/17.9
Up to 46 ¹⁸	Up to 46 ¹⁸	Up to 46 ¹⁸	Up to 46 ¹⁸	Up to 46 ¹⁸	–	–	–	–	–
*	*	*	*	*	–	–	–	–	–
Optimised Zry4/Modified Zry4/Duplex/MS ¹⁵					Imp.Zy-4	NDA	Imp.Zy-4	Imp.Zy-4	NDA
0.725	0.725	0.725	0.61 ¹⁹	0.64	0.66	0.66	0.66	0.57, 0.64	0.57
*	*	*	*	*	–	–	–	–	–
*	*	*	*	*	–	–	–	–	–
Modified Zry4/MS ¹⁵ /HPA-4 + Inconel (bottom grid)					Inc	Inc	Inc	Inc/Zy-4	Inc/Zy-4
Up to 65	Up to 65	Up to 65	Up to 65	Up to 65	–	–	–	–	–
Up to 70	Up to 70	Up to 70	Up to 70	Up to 70	48	55	48	48	55

Spent fuel discharges

U.S. nuclear plants discharged 165 854 fuel assemblies from 1968 through 2002, containing more than 47 023 metric tons of uranium, according to the Department of Energy's Energy Information Administration (EIA). During that time, boiling water reactors had more than 90 000 discharged assemblies stored on site, while pressurized water reactors had almost 70 000.

Annual discharges reached their peak in 1996, when 8226 assemblies were discharged, although that was nearly equaled in 1999, with 8223 discharges, and in 2002, with 8128 discharges. The information, the most current available from the EIA, was posted in October to its Web site, at <www.eia.doe.gov>.

From 1983 through 1995, information was collected annually. Since 1996, it has been collected every three years. The tables at right and below show the total U.S. commercial spent fuel discharges, 1968–2002, and annual discharges and burnup for the same period.

TOTAL U.S. COMMERCIAL SPENT NUCLEAR FUEL DISCHARGES, 1968–2002

Reactor Type	Number of Assemblies		
	Stored at Reactor Sites	Stored at Away-from-Reactor Facilities	Total
Boiling water reactor	90 398	2 957	93 355
Pressurized water reactor	69 800	491	70 291
High-temperature gas-cooled reactor	1 464	744	2 208
Total	161 662	4 192	165 854
Reactor Type	Metric Tons of Uranium (tU)		
	Stored at Reactor Sites	Stored at Away-from-Reactor Facilities	Total
Boiling water reactor	16 153.6	554.0	16 707.6
Pressurized water reactor	30 099.0	192.6	30 291.6
High-temperature gas-cooled reactor	15.4	8.8	24.2
Total	46 268.0	755.4	47 023.4

A number of assemblies discharged prior to 1972, which were reprocessed, are not included in this table (no data is available for assemblies reprocessed before 1972). Totals may not equal sum of components because of independent rounding. (Source: Adapted from the Energy Information Administration, Form RW-859, "Nuclear Fuel Data" [2002].)

ANNUAL SPENT FUEL DISCHARGES AND BURNUP, 1968–2002

Year	Number of Assemblies ^a				Initial Uranium Content (Metric Tons of Uranium)				Average Burnup (GWD/tU)		
	BWR	PWR	HTGR	Total	BWR	PWR	HTGR	Total	All Discharged Assemblies		
1968	5	0	0	5	0.6			0.6	1.7		
1969	97	0	0	97	9.9			9.9	16.6		
1970	29	99	0	128	5.6	39.0		44.6	0.3	18.4	
1971	413	113	0	526	64.7	44.5		109.2	8.3	23.8	
1972	801	282	0	1 083	145.8	99.9		245.7	7.1	22.1	
1973	564	165	0	729	93.5	67.1		160.6	13.2	24.2	
1974	1 290	575	0	1 865	241.6	207.7		449.3	13.1	18.4	
1975	1 223	797	0	2 020	225.9	321.7		547.6	17.1	18.2	
1976	1 666	931	0	2 597	298.1	401.0		699.1	13.6	22.4	
1977	2 047	1 107	0	3 154	383.2	467.0		850.2	17.0	25.2	
1978	2 239	1 665	0	3 904	383.7	698.6		1 082.3	19.8	26.4	
1979	2 131	1 642	246	4 019	399.9	712.0	3.0	1 114.9	22.5	27.2	8.8
1980	3 330	1 457	0	4 787	619.8	618.5		1 238.3	22.5	29.8	
1981	2 467	1 590	240	4 297	458.7	677.8	2.9	1 139.4	24.0	30.3	18.3
1982	1 951	1 491	0	3 442	357.2	640.5		997.7	24.9	29.9	
1983	2 649	1 779	0	4 428	482.2	772.2		1 254.4	27.1	30.2	
1984	2 735	1 933	240	4 908	497.9	839.4	2.7	1 340.0	25.9	29.5	33.2
1985	2 989	2 032	0	5 021	542.8	859.4		1 402.2	23.6	32.0	
1986	2 552	2 254	0	4 806	458.3	978.9		1 437.2	21.4	30.7	
1987	3 316	2 567	0	5 883	596.9	1 097.0		1 693.9	22.6	31.6	
1988	2 956	2 574	0	5 530	535.5	1 093.1		1 628.6	24.6	33.7	
1989	3 803	2 721	1 482	8 006	692.6	1 185.0	15.6	1 893.2	22.6	32.7	38.2
1990	3 487	3 435	0	6 922	632.8	1 481.2		2 114.0	25.2	34.6	
1991	3 191	2 803	0	5 994	576.0	1 218.3		1 794.3	28.4	35.4	
1992	3 932	3 588	0	7 520	713.5	1 547.0		2 260.5	29.2	36.8	
1993	3 759	3 400	0	7 159	677.6	1 477.0		2 154.6	30.6	39.2	
1994	3 777	2 747	0	6 524	676.0	1 176.6		1 852.6	33.4	40.3	
1995	4 425	3 741	0	8 166	787.2	1 629.9		2 417.1	33.1	40.9	
1996	4 690	3 536	0	8 226	832.6	1 514.6		2 347.2	35.4	39.1	
1997	3 849	3 414	0	7 263	673.8	1 510.3		2 184.1	35.8	40.3	
1998	3 867	2 166	0	6 033	674.0	934.8		1 608.8	36.4	44.0	
1999	4 586	3 637		8 223	798.1	1 593.4		2 391.5	35.8	44.1	
2000	4 361	3 177		7 538	758.6	1 393.5		2 152.1	38.2	44.8	
2001	3 904	3 019		6 923	673.4	1 327.1		2 000.5	39.5	45.0	
2002	4 274	3 854		8 128	739.6	1 667.6		2 407.2	40.0	45.7	
Total	93 355	70 291	2 208	165 854	16 707.6	30 291.6	24.2	47 023.4	28.6	36.3	32.2

When utilities reinsert assemblies that had been listed as permanently discharged in previous years, the historical totals change. Totals may not equal sum of components because of independent rounding. BWR = boiling water reactor; PWR = pressurized water reactor; HTGR = high-temperature gas-cooled reactor. GWD/tU = gigawatt-day thermal per metric ton of uranium.

^a Some data for earlier years have been revised.

(Source: Adapted from the Energy Information Administration, Form RW-859, "Nuclear Fuel Data" [2002].)

PlotOPUS input specified for 6 plots.

Number of Isotopes = 4
Input Option = Entering data using form
Input Units = grams

Library: 17x17
Enrichment Factor (Wt%U235) = 4.000000
Moderator Density (g/cc) = 0.729500

Nuclide	ID	Library	Concentration
=====	==	=====	=====
U 234	922340	Actinide	356.000000
U 235	922350	Actinide	40000.000000
U 236	922360	Actinide	184.000000
U 238	922380	Actinide	959460.000000

Neutron Group = 27GrpENDF4
Number of groups = 27

2.0000000e+007	6.4340000e+006	3.0000000e+006	1.8500000e+006	1.4000000e+00
9.0000000e+005	4.0000000e+005	1.0000000e+005	1.7000000e+004	3.0000000e+00
5.5000000e+002	1.0000000e+002	3.0000000e+001	1.0000000e+001	3.0499900e+00
1.7700000e+000	1.2999900e+000	1.1299900e+000	1.0000000e+000	8.0000000e-00
4.0000000e-001	3.2500000e-001	2.2500000e-001	9.9999850e-002	5.0000000e-00
3.0000000e-002	9.9999980e-003	1.0000000e-005		

Gamma Group = 18GrpSCALE
Number of groups = 18

1.0000000e+007	8.0000000e+006	6.5000000e+006	5.0000000e+006	4.0000000e+00
3.0000000e+006	2.5000000e+006	2.0000000e+006	1.6600000e+006	1.3300000e+00
1.0000000e+006	8.0000000e+005	6.0000000e+005	4.0000000e+005	3.0000000e+00
2.0000000e+005	1.0000000e+005	5.0000000e+004	1.0000000e+004	

Number of cases = 5

Case Number #1 -- Irradiation
=====

Title: Cycle 1 -Calvin1
Basis: 1 MTU

Time units= Days

OUTPUT OPTIONS

Tables = Nuclides

Output:

Light Elements
Actinides
Fission Products

Output units = grams
Table cutoff = 0.000010

Power Cumulative Write Results
MW/Basis Time to Dataset

=====	=====	=====
8.5000000e+001	2.3529410e+001	Yes
8.5000000e+001	4.7058820e+001	Yes
8.5000000e+001	7.0588240e+001	Yes
8.5000000e+001	9.4117650e+001	Yes
8.5000000e+001	1.1764710e+002	Yes
8.5000000e+001	1.4117650e+002	Yes
8.5000000e+001	1.6470590e+002	Yes
8.5000000e+001	1.8823530e+002	Yes
8.5000000e+001	2.1176470e+002	Yes
8.5000000e+001	2.3529410e+002	Yes

Case Number #2 -- Irradiation

Title: Cycle 2 -Calvin1
Basis: 1 MTU

Time units= Days

OUTPUT OPTIONS

Tables = Nuclides

Output:

Light Elements
Actinides
Fission Products

Output units = grams
Table cutoff = 0.000010

Power	Cumulative	Write Results
MW/Basis	Time	to Dataset
=====	=====	=====
8.5000000e+001	2.3529412e+001	No
8.5000000e+001	4.7058824e+001	No
8.5000000e+001	7.0588235e+001	No
8.5000000e+001	9.4117647e+001	No
8.5000000e+001	1.1764706e+002	No
8.5000000e+001	1.4117647e+002	No
8.5000000e+001	1.6470588e+002	No
8.5000000e+001	1.8823529e+002	No
8.5000000e+001	2.1176471e+002	No
8.5000000e+001	2.3529412e+002	No

Case Number #3 -- Irradiation

Title: Cycle 3 -Calvin1
Basis: 1 MTU

Time units= Days

OUTPUT OPTIONS

Tables = Nuclides

Output:

Light Elements
Actinides
Fission Products

Output units = grams
Table cutoff = 0.000010

Power MW/Basis =====	Cumulative Time =====	Write Results to Dataset =====
8.5000000e+001	2.3529412e+001	No
8.5000000e+001	4.7058824e+001	No
8.5000000e+001	7.0588235e+001	No
8.5000000e+001	9.4117647e+001	No
8.5000000e+001	1.1764706e+002	No
8.5000000e+001	1.4117647e+002	No
8.5000000e+001	1.6470588e+002	No
8.5000000e+001	1.8823529e+002	No
8.5000000e+001	2.1176471e+002	No
8.5000000e+001	2.3529412e+002	No

Case Number #4 -- Decay
=====

Title: Cycle 3 Down - Calvin1
Basis: 1 MTU

Beginning time = 0.000000
Time units = Years
Neutron source = U02
Bremsstrahlung = U02
Library Type = Total

Output Options:
No output is requested for this case.

Cumulative Time =====	Source Spectra =====	Save Results =====
1.0000000e-002	Yes	Yes
3.0000000e-002	Yes	Yes
1.0000000e-001	Yes	Yes
3.0000000e-001	Yes	Yes
1.0000000e+000	Yes	Yes
3.0000000e+000	Yes	Yes
1.0000000e+001	Yes	Yes
2.0000000e+001	Yes	Yes

Case Number #5 -- Decay
=====

Title: Case 5
Basis: 1 MTU

Beginning time = 20.000000
Time units = Years
Neutron source = U02
Bremsstrahlung = U02
Library Type = Total

Output Options:
No output is requested for this case.

Cumulative Time	Source Spectra	Save Results
-----------------	----------------	--------------

=====	=====	=====
3.0000000e+001	Yes	Yes
1.0000000e+002	Yes	Yes
3.0000000e+002	Yes	Yes
1.0000000e+003	Yes	Yes
3.0000000e+003	Yes	Yes
1.0000000e+004	Yes	Yes
3.0000000e+004	Yes	Yes
1.0000000e+005	Yes	Yes
3.0000000e+005	Yes	Yes
1.0000000e+006	Yes	Yes

7.2 Appendix B: Stress and Thermal Calculations

This appendix contains the sequential calculations used to calculate the temperatures at each radial boundary in the borehole. The design process is iterative, and uses data from early steps throughout the calculations. Thus, the calculations contained in this thesis cover a wide range of topics, but were done on a single template to minimize data entry.

The first section labeled Deep Borehole HLW Disposal Casing and Canister Size Calculations contains the basic inputs of the borehole canister and liner dimensions. Following the size inputs are stress calculations, as discussed in Chapter 3, to ensure the selected size will do the job of lowering the waste into the borehole.

Also included are some calculations for loading calculations for loading the canisters with BWR assemblies instead of PWR assemblies. Since the BWR assemblies are small and have a lower linear power, multiple assemblies can be loaded into a single canister. The stress calculations are also carried out for a configuration of four BWR assemblies loaded into a specially manufactured canister.

If windows are cut out of the final casing, its cross sectional area would be decreased, so stress calculations were also performed to ensure the windows would not weaken the liner too much.

The canister homogenization and heat transfer calculations, as discussed in Chapter 4, are performed in the latter part of the appendix. First the calculations are performed in air, then in water.

7.2.1 Thermal Calculations in Air

Deep Borehole HLW Disposal Casing and Canister Size Calculations

The following is a list of proposed standard casings [24]:

Conductor Casing: - H40 steel, plain end, short round, or long round thread
 - J55 or K55 steel, plain end, short round, long round, or buttress thread

Outer diameter: $OD_c := 508\text{mm}$
Nominal weight: $NW_c := 94 \frac{\text{lb}}{\text{ft}}$ $NW_c = 139.89 \frac{\text{kg}}{\text{m}}$
Wall thickness: $t_{wc} := 11.13\text{mm}$
Inner diameter: $ID_c := OD_c - 2 \cdot t_{wc}$ $ID_c = 485.74\text{mm}$

Surface Casing: - H40 steel, plain end, short round thread
 - J55 or K55 steel, plain end, short round, or buttress thread

Outer diameter: $OD_s := 473.1\text{mm}$
Nominal weight: $NW_s := 87.5 \frac{\text{lb}}{\text{ft}}$ $NW_s = 130.21 \frac{\text{kg}}{\text{m}}$
Wall thickness: $t_{ws} := 11.05\text{mm}$
Inner diameter: $ID_s := OD_s - 2 \cdot t_{ws}$ $ID_s = 451\text{mm}$

Final Casing: - H40 steel, plain end, short round thread
 - J55 or K55, steel, plain end, short round, or buttress thread
 - L80, C95, N80, P110, or Q125 steel, plain end

Outer diameter: $OD_f := 406.4\text{mm}$ $20\text{in} = 508\text{mm}$
Nominal weight: $NW_f := 65 \frac{\text{lb}}{\text{ft}}$ $NW_f = 96.73 \frac{\text{kg}}{\text{m}}$
Wall thickness: $t_{wf} := 9.52\text{mm}$
Inner diameter: $ID_f := OD_f - 2 \cdot t_{wf}$ $ID_f = 387.36\text{mm}$

Waste string: - H40 steel, plain end, short round thread
 - J55, K55, L80, C95, N80, C90, T95, P110, or Q125 steel, plain end, short round, or buttress thread

Outer diameter: $OD_{ws} := 339.7\text{mm}$
Nominal weight: $NW_{ws} := 68 \frac{\text{lb}}{\text{ft}}$ $NW_{ws} = 101.2 \frac{\text{kg}}{\text{m}}$
Wall thickness: $t_{wws} := 12.19\text{mm}$
Inner diameter: $ID_{ws} := OD_{ws} - 2 \cdot t_{wws}$ $ID_{ws} = 315.32\text{mm}$
Length: $L_{ws} := 4\text{km}$
Mass of waste string tubing: $m_{ws} := L_{ws} \cdot NW_{ws}$ $m_{ws} = 404.781 \times 10^3 \text{ kg}$

Waste: Length of storage zone: $d_{sto} := 2\text{km}$

Mass of an assembly[29]: $m_{asm} := 700\text{kg}$

Number of assemblies: $n_{asm} := \frac{d_{sto}}{5\text{m}}$ $n_{asm} = 400$

Mass of assemblies: $M_{asm} := n_{asm} \cdot m_{asm}$ $M_{asm} = 280 \times 10^3 \text{ kg}$

(All assembly data from this point forward is from Nuclear Systems I, [30].)

Volume to be filled with Silicon Carbide or Graphite particle bed:

Canister internal height: $h_{can} := 4.9\text{m}$

BWR # of pins: $n_{Bp} := 4.64$

Pin height: $h_{Bp} := 4.1\text{m}$

Pin diameter: $d_{Bp} := 12.27\text{mm}$

Empty volume:

$$V_B := \pi \cdot h_{Bp} \cdot \left[\left(\frac{ID_{ws}}{2} \right)^2 - n_{Bp} \cdot \left(\frac{d_{Bp}}{2} \right)^2 \right] + \pi \cdot (h_{can} - h_{Bp}) \cdot \left(\frac{ID_{ws}}{2} \right)^2 \quad V_B = 0.26\text{m}^3$$

PWR # of pins: $n_{Pp} := 17.17$

Pin height: $h_{Pp} := 4\text{m}$

Pin diameter: $d_{Pp} := 9.5\text{mm}$

Empty volume:

$$V_P := \pi \cdot h_{Pp} \cdot \left[\left(\frac{ID_{ws}}{2} \right)^2 - n_{Pp} \cdot \left(\frac{d_{Pp}}{2} \right)^2 \right] + \pi \cdot (h_{can} - h_{Bp}) \cdot \left(\frac{ID_{ws}}{2} \right)^2 \quad V_P = 0.29\text{m}^3$$

Density of silicon carbide: $\rho_{pack} := 3.1 \frac{\text{gm}}{\text{cm}^3}$

Packing factor of pebble bed: $PF := 0.65$

Mass of conductive material per assembly:

$$m_{Gpebbles} := V_P \cdot \rho_{pack} \cdot PF \quad m_{Gpebbles} = 590.17\text{kg}$$

Total mass of conductive material inside waste string:

$$M_{Gpebbles} := n_{asm} \cdot m_{Gpebbles} \quad M_{Gpebbles} = 236.07 \times 10^3 \text{ kg}$$

Total weight of waste string: $M_T := M_{Gpebbles} + M_{asm} + m_{ws}$ $M_T = 920.85 \times 10^3 \text{ kg}$

$$W_T := M_T \cdot g \quad W_T = 9030\text{kN}$$

Stress:

Cross section area:
$$A_{ws} := \pi \cdot \left(\frac{OD_{ws}}{2} \right)^2 - \pi \cdot \left(\frac{OD_{ws}}{2} - t_{wws} \right)^2$$

$$A_{ws} = 12542.33 \text{ mm}^2$$

Tensile stress:
$$\sigma_{ws} := \frac{M_T \cdot g}{A_{ws}}$$

$$\sigma_{ws} = 719.998 \times 10^6 \text{ Pa}$$

Minimum tensile strengths[46]:

$$\sigma_{H40} := 6000 \text{ psi}$$

$$\sigma_{H40} = 413.685 \times 10^6 \text{ Pa}$$

$$\sigma_{J55} := 7500 \text{ psi}$$

$$\sigma_{J55} = 517.107 \times 10^6 \text{ Pa}$$

$$\sigma_{K55} := 9500 \text{ psi}$$

$$\sigma_{K55} = 655.002 \times 10^6 \text{ Pa}$$

$$\sigma_{L80} := 9500 \text{ psi}$$

$$\sigma_{L80} = 655.002 \times 10^6 \text{ Pa}$$

$$\sigma_{N80} := 10000 \text{ psi}$$

$$\sigma_{N80} = 689.476 \times 10^6 \text{ Pa}$$

$$\sigma_{C90} := 10000 \text{ psi}$$

$$\sigma_{C90} = 689.476 \times 10^6 \text{ Pa}$$

$$\sigma_{T95} := 10500 \text{ psi}$$

$$\sigma_{T95} = 723.95 \times 10^6 \text{ Pa}$$

$$\sigma_{C95} := 10500 \text{ psi}$$

$$\sigma_{C95} = 723.95 \times 10^6 \text{ Pa}$$

$$\sigma_{P110} := 12500 \text{ psi}$$

$$\sigma_{P110} = 861.845 \times 10^6 \text{ Pa}$$

$$\sigma_{Q125} := 13500 \text{ psi}$$

$$\sigma_{Q125} = 930.792 \times 10^6 \text{ Pa}$$

Buckling:

Young's Modulus for steel: $E := 19000 \text{ MPa}$

Poisson Ratio for steel: $\nu := 0.26$

Mean radius of the waste string casing:
$$R_{ws} := \frac{OD_{ws} + ID_{ws}}{4}$$

$$R_{ws} = 163.75 \text{ mm}$$

Critical stress at which localized buckling occurs [34]:

$$s' := \frac{E}{\sqrt{3} \cdot \sqrt{1 - \nu^2}} \cdot \frac{t_{wws}}{R_{ws}}$$

$$s' = 8.46 \times 10^9 \text{ Pa}$$

Required diameter:

PWR assembly outer dimension: $od_{PWR} := 214\text{mm}$

Diameter required: $dr_{PWR} := \sqrt{2 \cdot od_{PWR}^2}$ $dr_{PWR} = 302.64\text{mm}$

BWR assembly outer dimension (without channel):

Width of a BWR assembly: $od_{BWR} := 16.2\text{mm}$ $od_{BWR} = 129.6\text{mm}$

Diameter required for 4 BWR assemblies: $dr_{4BWR} := \sqrt{2 \cdot (2 \cdot od_{BWR})^2}$ $dr_{4BWR} = 366.56\text{mm}$

Diameter required for 3 BWR assemblies: $dr_{3BWR} := 2od_{BWR} \cdot \sqrt{1 + \left(\frac{13}{16}\right)^2}$ $dr_{3BWR} = 333.97\text{mm}$

Diameter required for 2 BWR assemblies: $dr_{2BWR} := \sqrt{od_{BWR}^2 + \left(\frac{1}{2} \cdot od_{BWR}\right)^2}$ $dr_{2BWR} = 144.9\text{mm}$

Waste string inner diameter: $ID_{ws} = 315.32\text{mm}$

A canister containing 4 BWR assemblies (with channels) needs a special casing with the following dimensions:

$OD_{4BWRws} := 386\text{mm}$ $ID_{4BWRws} := 368\text{mm}$

$t_{4BWRws} := \frac{OD_{4BWRws} - ID_{4BWRws}}{2}$ $t_{4BWRws} = 9\text{mm}$

If the special casing is only used for the waste section then the stress calculation at the top of the waste section is:

$L_{4BWR} := 2\text{m}$ $\rho_{steel} := 7.85 \frac{\text{gm}}{\text{cm}^3}$

$NW_{4BWRws} := \rho_{steel} \cdot \left[\pi \cdot \left(\frac{OD_{4BWRws}}{2} \right)^2 - \pi \cdot \left(\frac{OD_{4BWRws}}{2} - t_{4BWRws} \right)^2 \right]$ $NW_{4BWRws} = 56.23 \frac{\text{lb}}{\text{ft}}$

Mass of waste string tubing: $m_{4BWRws} := L_{4BWR} \cdot NW_{4BWRws}$

$$m_{4BWRws} = 167.353 \times 10^3 \text{ kg}$$

Mass of BWR assemblies: $m_{BWRasm} := 273 \text{ kg}$

Total mass of BWR assemblies: $M_{BWRasm} := 4 \cdot n_{asm} \cdot m_{BWRasm}$

Total mass of the special waste string (from 2km depth down to 4 km depth):

$$M_{4BWRws} := m_{4BWRws} + M_{Gpebbles} + M_{asm} \quad M_{4BWRws} = 683.422 \times 10^3 \text{ kg}$$

Total mass of the special string (from the surface to the bottom):

$$M_{4BWR} := M_{4BWRws} + NW_{ws} \cdot 2 \text{ km} \quad M_{4BWR} = 885.813 \times 10^3 \text{ kg}$$

Tensile Stress:

Cross section area for the special casing:

$$A_{4BWRws} := \pi \cdot \left(\frac{OD_{4BWRws}}{2} \right)^2 - \pi \cdot \left(\frac{OD_{4BWRws}}{2} - t_{4BWRws} \right)^2 \quad A_{4BWRws} = 0.01 \text{ m}^2$$

Cross section area for the top part of the string:

$$A_{4BWR} := \pi \cdot \left(\frac{OD_{ws}}{2} \right)^2 - \pi \cdot \left(\frac{OD_{ws}}{2} - t_{ws} \right)^2 \quad A_{4BWR} = 0.01 \text{ m}^2$$

Tensile stress at 2km: $\sigma_{4BWRws} := \frac{M_{4BWRws} \cdot g}{A_{4BWRws}}$

$$\sigma_{4BWRws} = 628.747 \times 10^6 \text{ Pa}$$

Minimum tensile strengths[46]: $\sigma_{K55} := 75000 \text{ psi}$

$$\sigma_{K55} = 655.002 \times 10^6 \text{ Pa}$$

Tensile stress at surface: $\sigma_{4BWR} := \frac{M_{4BWR} \cdot g}{A_{4BWRws}}$

$$\sigma_{4BWR} = 814.946 \times 10^6 \text{ Pa}$$

$$\sigma_{P110} = 861.845 \times 10^6 \text{ Pa}$$

$$\sigma_{C95} = 723.95 \times 10^6 \text{ Pa}$$

Final Casing with Window Holes

$$MT := 1000 \text{ kg}$$

Mass of lower half without holes:

$$m_{2km} := NW_f \cdot 2km$$

$$m_{2km} = 193.46 \text{ MT}$$

Cross section area:

$$A_f := \pi \cdot \left(\frac{OD_f}{2} \right)^2 - \pi \cdot \left(\frac{OD_f}{2} - t_{wf} \right)^2$$

$$A_f = 11870 \text{ mm}^2$$

Circumference of waste string:

$$c_{wf} := OD_f \cdot \pi$$

$$c_{wf} = 1.28 \text{ m}$$

Window diameter:

$$d_w := 20 \text{ mm}$$

Window interval:

$$i_w := 30 \text{ mm}$$

Based on distance between final casing and waste string. If debris falls through a window, it will fall to the bottom of the hole.

Number of windows per interval:

$$n_w := 36$$

The angles are easy (10 degrees).

Voided circumference:

$$d_{ww} := n_w \cdot d_w$$

$$d_{ww} = 0.72 \text{ m}$$

Reduced cross section area:

$$A_{fr} := A_f - t_{wf} \cdot d_{ww}$$

$$A_{fr} = 5015.5 \text{ mm}^2$$

Reduced mass (with window holes):

$$m_{2kmr} := m_{2km} - \rho_{\text{steel}} \cdot t_{wf} \cdot \pi \cdot \left(\frac{d_w}{2} \right)^2 \cdot \frac{d_{ww}}{d_w} \cdot \frac{2km}{i_w}$$

Average static tensile stress:

$$\sigma_f := \frac{m_{2kmr} \cdot g}{A_{fr}}$$

$$\sigma_f = 268.098 \times 10^6 \text{ Pa}$$

Minimum tensile strength[46]:

$$\sigma_{H40} := 60000 \text{ psi}$$

$$\sigma_{H40} = 413.685 \times 10^6 \text{ Pa}$$

Homogenization of a Spent Fuel Assembly in a Silicon Carbide Particle Bed

Thermal conductivity values:

$$k_{\text{SiC.bed}} := 0.19 \frac{\text{BTU}}{\text{hr} \cdot \text{ft} \cdot \text{R}} \quad k_{\text{SiC.bed}} = 0.33 \frac{\text{W}}{\text{m} \cdot \text{K}} \quad [3]$$

$$k_{\text{UO}_2} := 2 \frac{\text{W}}{\text{m} \cdot \text{K}} \quad k_{\text{clad}} := 13 \frac{\text{W}}{\text{m} \cdot \text{K}} \quad [30]$$

The conductivity of the uranium oxide is an estimate for cracked fuel, based on example problems.

From http://www.engineeringtoolbox.com/air-properties-d_156.html[47]: $k_{\text{air}} := 0.0262 \frac{\text{W}}{\text{m} \cdot \text{K}}$

Number of rods: $\text{rods} := 17^2$ Pitch (between rod center-lines): $p := 12.6 \text{ mm}$

Rod diameter: $d := 9.5 \text{ mm}$ Fuel pellet diameter: $d_{\text{fuel_pellet}} := 8.2 \text{ mm}$

Cladding thickness: $t_{\text{clad}} := 0.57 \text{ mm}$

Area calculations for each material:

$$A_{\text{interior}} := \text{rods} \cdot p^2 \quad A_{\text{interior}} = 0.05 \text{ m}^2$$

$$A_{\text{fuel}} := \text{rods} \cdot \pi \cdot \left(\frac{d_{\text{fuel_pellet}}}{2} \right)^2 \quad A_{\text{fuel}} = 0.02 \text{ m}^2$$

$$A_{\text{clad}} := \text{rods} \cdot \left[\pi \cdot \left(\frac{d}{2} \right)^2 - \pi \cdot \left(\frac{d - t_{\text{clad}}}{2} \right)^2 \right] \quad A_{\text{clad}} = 0 \text{ m}^2$$

$$A_{\text{air}} := \text{rods} \cdot \pi \cdot \left(\frac{d}{2} \right)^2 - A_{\text{clad}} - A_{\text{fuel}} \quad A_{\text{air}} = 0 \text{ m}^2$$

$$A_{\text{SiC}} := A_{\text{interior}} - A_{\text{fuel}} - A_{\text{clad}} \quad A_{\text{SiC}} = 0.03 \text{ m}^2$$

Effective fuel pin conductivity:

$$\Delta T = q' \cdot \left(\frac{1}{4 \cdot \pi k_f} + \frac{1}{2 \cdot \pi \cdot R_{g1} \cdot h_g} + \frac{1}{2 \cdot \pi \cdot k_c} \cdot \ln \left(\frac{R_{co}}{R_{ci}} \right) \right) \quad [30]$$

$$R_{g1} := \frac{d - 2 \cdot t_{clad} + d_{fuel_pellet}}{4} \quad R_{g1} = 4.14 \text{ mm}$$

$$R_{co} := \frac{d}{2} \quad R_{ci} := R_{co} - t_{clad} \quad h_{g1} := 31000 \frac{\text{W}}{\text{m}^2 \cdot \text{K}}$$

$$\text{Let: } \frac{1}{4 \cdot \pi k_{eff}} = \frac{1}{4 \cdot \pi k_f} + \frac{1}{2 \cdot \pi \cdot R_{g1} \cdot h_g} + \frac{1}{2 \cdot \pi \cdot k_c} \cdot \ln \left(\frac{R_{co}}{R_{ci}} \right)$$

$$\text{Then: } k_{eff} := \frac{k_{UO2} \cdot R_{g1} \cdot h_{g1} \cdot k_{clad}}{R_{g1} \cdot h_{g1} \cdot k_{clad} + 2 k_{UO2} \cdot k_{clad} + 2 \ln \left(\frac{R_{co}}{R_{ci}} \right) \cdot k_{UO2} \cdot R_{g1} \cdot h_{g1}} \quad k_{eff} = 1.87 \frac{\text{W}}{\text{m} \cdot \text{K}}$$

Cell homogenization: using Selengut's relation:

$$k_{hom} = \frac{(1 + n \cdot v) \cdot k_0 + n(1 - v) \cdot k_1}{(1 - v) \cdot k_0 + (n + v) \cdot k_1} \cdot k_1 \quad (n = 0, 1, 2) \text{ for: } (\text{number_of_dimensions} = 1, 2, 3)$$

$v = \text{volume_fraction}$

$$n := 1 \quad v := \frac{\pi \cdot d^2}{4p} \quad v = 0.45 \quad [35]$$

$$k_{hom} := \frac{(1 + n \cdot v) \cdot k_{eff} + n(1 - v) \cdot k_{SiC.bed}}{(1 - v) \cdot k_{eff} + (n + v) \cdot k_{SiC.bed}} \cdot k_{SiC.bed} \quad k_{hom} = 0.63 \frac{\text{W}}{\text{m} \cdot \text{K}}$$

Diameter of homogenized interior region:

$$d_{int} := 2 \sqrt{\frac{A_{interior}}{\pi}} \quad d_{int} = 241.7 \text{ mm}$$

Heat Transfer between Rock and Fuel

From Manteufel paper[11], transportation and storage center-line limit:

$$T_{CLmax} = 653K$$

Conservative (high) estimate of linear power:

$$q' := 300 \frac{W}{m}$$

Gap 1 (between rock and liner)

Using a temperature gradient of 20 degrees Celsius per kilometer, and the 60 degrees Celsius peak temperature change at borehole wall, as calculated by Ranade[4], the maximum wall temperature will be 160 degrees Celsius. T_2 is the borehole wall temperature. T_1 is the temperature at the outer diameter of the liner or final casing. T_1 was found using an iterative process.

$$T_{rock} := (240 + 273) \cdot K \quad \text{Let: } T_1 := 524.2K \quad T_{avg} := \frac{T_1 + T_{rock}}{2} \quad T_{avg} = 518.6K$$

Convection & Conduction: A very general correlation for convection is found in Fundamentals of Heat Transfer by M. Mikheyev[36]. This correlation is backed up with data which shows that the correlation includes conduction. The quadratic equation for specific heat is an approximation based on data between 100 and 300 degrees Celsius. The data is from:

http://www.efunda.com/Materials/common_matl/show_gas.cfm?MatlName=Air0C [38].

"L" is the height of the emplacement zone, and delta is the distance between the two surfaces.

The worst case scenario is at atmospheric pressure. A table in "Modern Petroleum" [24] lists the bit sizes commonly used with each casing size.

$$\text{Bit size:} \quad BS_{ws} := 17.5in \quad BS_{ws} = 444.5mm$$

$$\text{Gap width:} \quad \delta_1 := \frac{BS_{ws} - OD_{ws}}{2} \quad \delta_1 = 52.4mm$$

$$P := 1atm \quad L := 2km$$

$$k_{air} = 0.03 \frac{W}{m \cdot K} \quad m_{air} := 28.8 \frac{gm}{mol} \quad R_g := 8.3144 \frac{J}{mol \cdot K}$$

$$\text{Density:} \quad \rho := \frac{P \cdot m_{air}}{R_g \cdot T_{avg}} \quad \rho = 0.68 \frac{kg}{m^3}$$

Dynamic viscosity: by solving for the constants in the Sutherland Equation for gases.

$$\mu := \frac{1.464 \times 10^{-6} \cdot T_{avg}^{1.5}}{T_{avg} + 113.29K} \cdot \frac{Pa \cdot s}{\sqrt{K}} \quad \mu = 2.74 \times 10^{-5} Pa \cdot s$$

$$\text{Kinematic viscosity:} \quad \nu := \frac{\mu}{\rho} \quad \nu = 4.04 \times 10^{-5} \frac{m^2}{s}$$

$$\text{Specific heat:} \quad C_p := \left[0.0005 \left(\frac{T_{avg}}{K} - 273 \right)^2 - 0.3 \left(\frac{T_{avg}}{K} - 273 \right) + 1010 \right] \frac{kJ}{kg \cdot K}$$

$$C_p = 966.48 \frac{kJ}{kg \cdot K}$$

Grashof number: $G_{fb} := \frac{g \cdot (T_1 - T_{rock}) \cdot \delta_1^3}{T_{avg} \cdot \nu^2}$ $G_{fb} = 18642.62$

Prandtl number: $Pr := \frac{C_p \cdot \nu \cdot \rho}{k_{air}}$ $Pr = 1009.33$

Rayleigh number: $Ra := G_{fb} \cdot Pr$ $Ra = 18816578.33$

Correlation ($Ra > 10^3$): $k_{eq1} := k_{air} \cdot 0.18 Ra^{0.25}$ $k_{eq1} = 0.31 \frac{W}{m \cdot K}$

Convection ratio: $\epsilon_c := \frac{k_{eq1}}{k_{air}}$ $\epsilon_c = 11.86$

Accounting for the annular shape:

$h_{eq1} := \frac{k_{eq1}}{\frac{OD_f}{2} \cdot \ln \left(\frac{OD_{ws} + 2 \cdot \delta_1}{OD_{ws}} \right)}$ $h_{eq1} = 5.68 \frac{W}{m^2 \cdot K}$

Radiation: The following equation for the heat-transfer coefficient due to radiation and conduction between parallel slabs is found in Nuclear Systems 1, by Todreas & Kazimi, p. 333 [30].

$h = \frac{k}{\delta} + \frac{\sigma}{\frac{1}{\epsilon_1} + \frac{1}{\epsilon_2} - 1} \cdot \left(\frac{T_1^4 - T_2^4}{T_1 - T_2} \right)$ sigma: Stephan-Boltzmann constant
delta: gap thickness
epsilon: emissivity

$\sigma := 5.67 \cdot 10^{-12} \frac{W}{cm^2 \cdot K^4}$

For rough steel with a thick oxide layer (Schaum's Heat Transfer): $\epsilon_1 := 0.8$

Emissivity of granite (from internet search): $\epsilon_2 := 0.45$

Accounting for the annular shape (according to Eqn. 12-53 in of the text Basic Heat Transfer, by M. Necati Ozisik [39]) and eliminating the conduction term, since it is accounted for in the convection correlation:

$h_{rad1} := \frac{\sigma}{\frac{1}{\epsilon_1} + \left(\frac{OD_f}{OD_f + 2 \cdot \delta_1} \right) \cdot \left(\frac{1}{\epsilon_2} - 1 \right)} \cdot \left(\frac{T_1^4 - T_{rock}^4}{T_1 - T_{rock}} \right)$ $h_{rad1} = 14.24 \frac{W}{m^2 \cdot K}$

$k_{rad1} := h_{rad1} \cdot \frac{OD_f}{2} \cdot \ln \left(\frac{OD_f + 2 \cdot \delta_1}{OD_f} \right)$ $k_{rad1} = 0.66 \frac{W}{m \cdot K}$

The liner outer wall temperature (T1) is calculated below, and the iterative process was performed updating T1 until T1new was within 0.1 degrees of T1.

$$k_{g1} := k_{eq1} + k_{rad1} \quad T_{1new} := T_{rock} + q' \cdot \frac{\ln\left(\frac{OD_f + 2 \cdot \delta_1}{OD_f}\right)}{2\pi \cdot k_{g1}} \quad T_1 = 524.2 \text{ K} \quad T_{1new} = 524.24 \text{ K}$$

The following numbers are provided for comparison:

$$h_{cond1} := \frac{k_{air}}{\frac{OD_f}{2} \cdot \ln\left(\frac{OD_f + 2 \cdot \delta_1}{OD_f}\right)} \quad h_{conv1} := h_{eq1} - h_{cond1}$$

$$h_{rad1} = 14.24 \frac{\text{W}}{\text{m}^2 \cdot \text{K}}$$

$$h_{cond1} = 0.56 \frac{\text{W}}{\text{m}^2 \cdot \text{K}}$$

$$h_{conv1} = 5.12 \frac{\text{W}}{\text{m}^2 \cdot \text{K}}$$

Liner:

Outer diameter: $OD_f = 406.4 \text{ mm}$

Wall thickness: $t_{wf} = 9.52 \text{ mm}$

Inner diameter: $ID_f = 387.36 \text{ mm}$

$$T_{OD.f} := T_1 \quad T_{OD.f} = 524.2 \text{ K}$$

$$k_{steel} := 50.2 \frac{\text{W}}{\text{m} \cdot \text{K}}$$

$$T_{ID.f} := T_{OD.f} + \frac{q' \cdot \ln\left(\frac{OD_f}{ID_f}\right)}{2 \cdot \pi \cdot k_{steel}} \quad T_{ID.f} = 524.25 \text{ K}$$

Gap 2 (between liner and canister)

Let: $T_2 := 533.7 \text{ K}$ $T_{avg} := \frac{T_2 + T_{ID.f}}{2}$ $T_{avg} = 528.97 \text{ K}$ $\delta_2 := 33 \text{ mm}$

Convection & Conduction:

Density: $\rho_{ww} := \frac{P \cdot m_{air}}{R_g \cdot T_{avg}}$ $\rho = 0.66 \frac{\text{kg}}{\text{m}^3}$

Dynamic viscosity: $\mu_{ww} := \frac{1.464 \times 10^{-6} \cdot \left(\frac{T_{avg}}{\text{K}}\right)^{1.5}}{\frac{T_{avg}}{\text{K}} + 113.299} \cdot \text{Pa} \cdot \text{s}$ $\mu = 0 \text{ Pa} \cdot \text{s}$

Kinematic viscosity: $\nu_{ww} := \frac{\mu}{\rho}$ $\nu = 0 \frac{\text{m}^2}{\text{s}}$

Specific heat: $C_p := \left[0.0005 \left(\frac{T_{avg}}{K} - 273 \right)^2 + -0.3 \left(\frac{T_{avg}}{K} - 273 \right) + 1010 \right] \frac{kJ}{kg \cdot K}$

$C_p = 966 \frac{kJ}{kg \cdot K}$

Grashof number: $Gr := \frac{g \cdot (T_2 - T_{ID.f}) \cdot \delta_2^3}{T_{avg} \cdot \nu^2}$

$Gr = 3605.84$

Prandtl number: $Pr := \frac{C_p \cdot \nu \cdot \rho}{k_{air}}$

$Pr = 1022.43$

Rayleigh number: $Ra := Gr \cdot Pr$

$Ra = 3686725.09$

Correlation ($Ra > 10^3$): $k_{eq2} := k_{air} \cdot 0.18 Ra^{0.25}$

$k_{eq2} = 0.21 \frac{W}{m \cdot K}$

Convection ratio: $\varepsilon_c := \frac{k_{eq2}}{k_{air}}$

$\varepsilon_c = 7.89$

$h_{eq2} := \frac{k_{eq2}}{\frac{OD_f}{2} \cdot \ln \left(\frac{OD_{ws} + 2 \cdot \delta_2}{OD_{ws}} \right)}$

$h_{eq2} = 5.73 \frac{W}{m^2 \cdot K}$

Radiation:

For rough steel with a thick oxide layer (Schaum's Heat Transfer):

$\varepsilon_1 = 0.8 \quad \varepsilon_{2b} := \varepsilon_1$

$h_{rad2} := \frac{\sigma}{\frac{1}{\varepsilon_1} + \left(\frac{OD_{ws}}{OD_{ws} + 2 \cdot \delta_2} \right) \cdot \left(\frac{1}{\varepsilon_{2b}} - 1 \right)} \cdot \left(\frac{T_2^4 - T_{ID.f}^4}{T_2 - T_{ID.f}} \right)$

$h_{rad2} = 23.01 \frac{W}{m^2 \cdot K}$

$k_{rad2} := h_{rad2} \cdot \frac{OD_{ws}}{2} \cdot \ln \left(\frac{OD_{ws} + 2 \cdot \delta_2}{OD_{ws}} \right)$

$k_{rad2} = 0.69 \frac{W}{m \cdot K}$

The liner outer wall temperature (T2) is calculated below, and the iterative process was performed by updating T2 until T2new was within 0.1 degrees of T2.

$k_{g2} := k_{rad2} + k_{eq2}$

$T_{2new} := T_{ID.f} + q' \cdot \frac{\ln \left(\frac{OD_{ws} + 2 \cdot \delta_2}{OD_{ws}} \right)}{2\pi \cdot k_{g2}}$

$T_2 = 533.7 K$

$T_{2new} = 533.66 K$

The following numbers are provided for comparison:

$$h_{\text{cond2}} := \frac{k_{\text{air}}}{\frac{\text{OD}_f}{2} \cdot \ln\left(\frac{\text{OD}_f + 2 \cdot \delta_2}{\text{OD}_f}\right)} \quad h_{\text{conv2}} := h_{\text{eq2}} - h_{\text{cond2}}$$

$$h_{\text{rad2}} = 23.01 \frac{\text{W}}{\text{m}^2 \cdot \text{K}}$$

$$h_{\text{cond2}} = 0.86 \frac{\text{W}}{\text{m}^2 \cdot \text{K}}$$

$$h_{\text{conv2}} = 4.87 \frac{\text{W}}{\text{m}^2 \cdot \text{K}}$$

Canister:

Outer diameter: $\text{OD}_{\text{ws}} = 339.7 \text{ mm}$

Wall thickness: $t_{\text{wvs}} = 12.19 \text{ mm}$

Inner diameter: $\text{ID}_{\text{ws}} = 315.32 \text{ mm}$

$$T_{\text{OD.ws}} := T_2$$

$$T_{\text{OD.ws}} = 533.7 \text{ K}$$

$$k_{\text{steel}} := 50.2 \frac{\text{W}}{\text{m} \cdot \text{K}}$$

$$T_{\text{ID.ws}} := T_{\text{OD.ws}} + \frac{q' \cdot \ln\left(\frac{\text{OD}_{\text{ws}}}{\text{ID}_{\text{ws}}}\right)}{2 \cdot \pi \cdot k_{\text{steel}}}$$

$$T_{\text{ID.ws}} = 533.77 \text{ K}$$

The contents of the canister are divided into two sections: the Interior and the Edge regions. The Interior region consists of the homogenized fuel assembly in a silicon carbide particle bed. The Edge region consists only of the silicon carbide particle bed. These regions are separated by an imaginary line at the effective diameter of the Interior region.

Effective Interior region diameter:

$$d_{\text{int}} = 241.7 \text{ mm}$$

Conductivity of No.16 silicon carbide grit [3]:

$$k_{\text{SiC.bed}} = 0.33 \frac{\text{W}}{\text{m} \cdot \text{K}}$$

Temperature at the Edge region boundary:

$$T_e := T_{\text{ID.ws}} + \frac{q' \cdot \ln\left(\frac{\text{ID}_{\text{ws}}}{d_{\text{int}}}\right)}{2 \cdot \pi \cdot k_{\text{SiC.bed}}}$$

$$T_e = 572.38 \text{ K}$$

From homogenized cylindrical fuel assembly:

$$k_{\text{hom}} = 0.63 \frac{\text{W}}{\text{m} \cdot \text{K}}$$

Center-line temperature: $T_{\text{CL}} := T_e + \frac{q'}{4 \cdot \pi \cdot k_{\text{hom}}}$

$$T_{\text{CL}} = 610.38 \text{ K}$$

For comparison: $\Delta T_{\text{hole}} := T_{\text{CL}} - T_{\text{rock}}$

$$\Delta T_{\text{hole}} = 97.38 \text{ K}$$

$$T_{\text{CLmax}} = 653 \text{ K}$$

Effective k for the borehole: $k_{\text{HOLE}} := \frac{q'}{4 \cdot \pi \cdot (\Delta T_{\text{hole}})}$

$$k_{\text{HOLE}} = 0.25 \frac{\text{W}}{\text{m} \cdot \text{K}}$$

7.2.2 Thermal Calculations in Water

Heat Transfer from Rock to Fuel

From Manteufel paper, transportation and storage center-line limit:

$$T_{CLmax} := 653K$$

Conservative (high) estimate of linear power:

$$q' := 300 \frac{W}{m}$$

Gap 1 (between rock and liner)

Using a temperature gradient of 40 degrees Celsius, and the 60 degrees Celsius peak temperature change at borehole wall, as calculated by Ranade [4], the maximum wall temperature will be 240 degrees Celsius. T2 is the borehole wall temperature. T1 is the temperature at the outer diameter of the liner or final casing. T1 was found using an iterative process.

$$T_{rock} := (240 + 273) \cdot K \quad \text{Let: } T_1 := 513.7K \quad T_{avg} := \frac{T_1 + T_{rock}}{2} \quad T_{avg} = 513.35K$$

Convection & Conduction: A very general correlation for convection is found in Fundamentals of Heat Transfer by M. Mikheyev [36]. This correlation is backed up with data which shows that the correlation includes conduction. The data used to calculate the coefficients in Andrade's Equation is for distilled water and is found online at:

http://www.efunda.com/materials/common_matl/show_liquid.cfm?MatlName=WaterDistilled4C [48]. "L" is the height of the emplacement zone, and delta is the distance between the two surfaces. Pressure is assumed to be hydrostatic pressure at a depth of 4km.

$$P := 386 \text{ atm} \quad L := 2 \text{ km} \quad \delta_1 := 20 \text{ mm} \quad k_{H_2O} := 0.606 \frac{W}{m \cdot K}$$

$$\text{Density:} \quad \rho := 1 \frac{gm}{cm^3} \quad \rho = 1 \times 10^3 \frac{kg}{m^3}$$

Dynamic viscosity: by solving for the constants in Andrade's Equation for liquids.

$$D := 1.81 \cdot 10^{-6} \quad B := 1.884 \times 10^3 K$$

$$\mu := D \cdot e^{\frac{B}{T_{avg}}} \cdot Pa \cdot s \quad \mu = 7.105 \times 10^{-5} Pa \cdot s$$

$$\text{Kinematic viscosity:} \quad \nu := \frac{\mu}{\rho} \quad \nu = 7.105 \times 10^{-8} \frac{m^2}{s}$$

$$\text{Specific heat:} \quad C_p := 4.186 \frac{kJ}{kg \cdot K}$$

$$\text{Grashof number: } Gr_b := \frac{g \cdot (T_1 - T_{\text{rock}}) \cdot \delta_1^3}{T_{\text{avg}} \cdot \nu^2} \quad Gr_b = 2.119 \times 10^7$$

$$\text{Prandtl number: } Pr := \frac{C_p \cdot \nu \cdot \rho}{k_{\text{H2O}}} \quad Pr = 0.491$$

$$\text{Rayleigh number: } Ra := Gr_b \cdot Pr \quad Ra = 1.04 \times 10^7$$

$$\text{Correlation (Ra > 10^3): } k_{eq1} := k_{\text{H2O}} \cdot 0.18 Ra^{0.25} \quad k_{eq1} = 6.195 \frac{\text{W}}{\text{m} \cdot \text{K}}$$

$$\text{Convection ratio: } \varepsilon_c := \frac{k_{eq1}}{k_{\text{H2O}}} \quad \varepsilon_c = 10.222$$

Accounting for the annular shape:

$$h_{eq1} := \frac{k_{eq1}}{\frac{OD_f}{2} \cdot \ln \left(\frac{OD_{ws} + 2 \cdot \delta_1}{OD_{ws}} \right)} \quad h_{eq1} = 273.857 \frac{\text{W}}{\text{m}^2 \cdot \text{K}}$$

Radiation: It is safe to assume that thermal radiation is negligible through water.

$$k_{rad1} := 0 \frac{\text{W}}{\text{m} \cdot \text{K}} \quad h_{rad1} := 0 \frac{\text{W}}{\text{m}^2 \cdot \text{K}}$$

The liner outer wall temperature (T1) is calculated below, and the iterative process was performed by updating T1 until T1new was within 0.1 degrees of T1.

$$k_{g1} := k_{rad1} + k_{eq1} \quad T_{1\text{new}} := T_{\text{rock}} + q' \cdot \frac{\ln \left(\frac{OD_f + 2 \cdot \delta_1}{OD_f} \right)}{2\pi \cdot k_{g1}} \quad T_1 = 513.7 \text{ K} \quad T_{1\text{new}} = 513.72 \text{ K}$$

The following numbers are provided for comparison:

$$h_{cond1} := \frac{k_{\text{H2O}}}{\frac{OD_f}{2} \cdot \ln \left(\frac{OD_f + 2 \cdot \delta_1}{OD_f} \right)} \quad h_{conv1} := h_{eq1} - h_{cond1}$$

$$h_{rad1} = 0 \frac{\text{W}}{\text{m}^2 \cdot \text{K}}$$

$$h_{cond1} = 31.768 \frac{\text{W}}{\text{m}^2 \cdot \text{K}}$$

$$h_{conv1} = 242.089 \frac{\text{W}}{\text{m}^2 \cdot \text{K}}$$

Liner:

Outer diameter: $OD_f = 406.4 \text{ mm}$

Wall thickness: $t_{wf} = 9.52 \text{ mm}$

Inner diameter: $ID_f = 387.36 \text{ mm}$

$$T_{OD.f} := T_1$$

$$T_{OD.f} = 513.7 \text{ K}$$

$$k_{\text{steel}} := 50.2 \frac{\text{W}}{\text{m} \cdot \text{K}}$$

$$T_{ID.f} := T_{OD.f} + \frac{q' \cdot \ln\left(\frac{OD_f}{ID_f}\right)}{2 \cdot \pi \cdot k_{\text{steel}}}$$

$$T_{ID.f} = 513.75 \text{ K}$$

Gap 2 (between liner and canister)

Let: $T_2 := 515.1 \text{ K}$

$$T_{\text{avg}} := \frac{T_2 + T_{ID.f}}{2}$$

$$T_{\text{avg}} = 514.423 \text{ K}$$

$$\delta_2 := 33 \text{ mm}$$

Convection & Conduction:

$$\mu := D \cdot e^{\frac{B}{T_{\text{avg}}}} \cdot \text{Pa} \cdot \text{s}$$

$$\mu = 7.051 \times 10^{-5} \text{ Pa} \cdot \text{s}$$

Kinematic viscosity:

$$\nu := \frac{\mu}{\rho}$$

$$\nu = 7.051 \times 10^{-8} \frac{\text{m}^2}{\text{s}}$$

Specific heat:

$$C_p := 4.186 \frac{\text{kJ}}{\text{kg} \cdot \text{K}}$$

Grashof number:

$$Gr := \frac{g \cdot (T_2 - T_{ID.f}) \cdot \delta_2^3}{T_{\text{avg}} \cdot \nu^2}$$

$$Gr = 1.867 \times 10^8$$

Prandtl number:

$$Pr := \frac{C_p \cdot \nu \cdot \rho}{k_{H_2O}}$$

$$Pr = 0.487$$

Rayleigh number:

$$Ra := Gr \cdot Pr$$

$$Ra = 9.09 \times 10^7$$

Correlation ($Ra > 10^3$):

$$k_{eq2} := k_{H_2O} \cdot 0.18 Ra^{0.25}$$

$$k_{eq2} = 10.651 \frac{\text{W}}{\text{m} \cdot \text{K}}$$

Convection ratio:

$$\varepsilon_c := \frac{k_{eq2}}{k_{H_2O}}$$

$$\varepsilon_c = 17.576$$

$$h_{eq2} := \frac{k_{eq2}}{\frac{OD_f}{2} \cdot \ln\left(\frac{OD_{ws} + 2 \cdot \delta_2}{OD_{ws}}\right)}$$

$$h_{eq2} = 295.219 \frac{\text{W}}{\text{m}^2 \cdot \text{K}}$$

Radiation: It is safe to assume that thermal radiation is negligible through water.

$$k_{\text{rad}2} := 0 \frac{\text{W}}{\text{m} \cdot \text{K}} \quad h_{\text{rad}2} := 0 \frac{\text{W}}{\text{m}^2 \cdot \text{K}}$$

The liner outer wall temperature (T2) is calculated below, and the iterative process was performed by updating T2 until T1new was within 0.1 degrees of T2.

$$k_{g2} := k_{\text{rad}2} + k_{\text{eq}2} \quad T_{2\text{new}} := T_{\text{ID},f} + q' \cdot \frac{\ln\left(\frac{\text{OD}_{\text{ws}} + 2 \cdot \delta_2}{\text{OD}_{\text{ws}}}\right)}{2\pi \cdot k_{g1}} \quad T_2 = 515.1 \text{ K} \quad T_{2\text{new}} = 515.1 \text{ K}$$

The following numbers are provided for comparison:

$$h_{\text{cond}2} := \frac{k_{\text{air}}}{\frac{\text{OD}_f}{2} \cdot \ln\left(\frac{\text{OD}_f + 2 \cdot \delta_2}{\text{OD}_f}\right)} \quad h_{\text{conv}2} := h_{\text{eq}2} - h_{\text{cond}2}$$

$$h_{\text{rad}2} = 0 \frac{\text{W}}{\text{m}^2 \cdot \text{K}}$$

$$h_{\text{cond}2} = 0.857 \frac{\text{W}}{\text{m}^2 \cdot \text{K}}$$

$$h_{\text{conv}2} = 294.362 \frac{\text{W}}{\text{m}^2 \cdot \text{K}}$$

Canister:

Outer diameter: $\text{OD}_{\text{ws}} = 339.7 \text{ mm}$

Wall thickness: $t_{\text{wws}} = 12.19 \text{ mm}$

Inner diameter: $\text{ID}_{\text{ws}} = 315.32 \text{ mm}$

$$T_{\text{OD},\text{ws}} := T_2$$

$$T_{\text{OD},\text{ws}} = 515.1 \text{ K}$$

$$k_{\text{steel}} := 50.2 \frac{\text{W}}{\text{m} \cdot \text{K}}$$

$$T_{\text{ID},\text{ws}} := T_{\text{OD},\text{ws}} + \frac{q' \cdot \ln\left(\frac{\text{OD}_{\text{ws}}}{\text{ID}_{\text{ws}}}\right)}{2 \cdot \pi \cdot k_{\text{steel}}}$$

$$T_{\text{ID},\text{ws}} = 515.17 \text{ K}$$

The contents of the canister are divided into two sections: the Interior and the Edge regions. The Interior region consists of the homogenized fuel assembly in a silicon carbide particle bed. The Edge region consists only of the silicon carbide particle bed. These regions are separated by an imaginary line at the effective diameter of the Interior region.

Effective Interior region diameter:

$$d_{\text{int}} = 0.242 \text{ m}$$

Conductivity of No.16 silicon carbide grit [3]:

$$k_{\text{SiC.bed}} = 0.329 \frac{\text{W}}{\text{m}\cdot\text{K}}$$

Temperature at the Edge region boundary:

$$T_e := T_{\text{ID.ws}} + \frac{q' \cdot \ln\left(\frac{\text{ID}_{\text{ws}}}{d_{\text{int}}}\right)}{2 \cdot \pi \cdot k_{\text{SiC.bed}}}$$

$$T_e = 553.78 \text{ K}$$

From homogenized cylindrical fuel assembly:

$$k_f := k_{\text{hom}}$$

$$k_f = 0.628 \frac{\text{W}}{\text{m}\cdot\text{K}}$$

Center-line temperature:

$$T_{\text{CL}} := T_e + \frac{q'}{4 \cdot \pi \cdot k_f}$$

$$T_{\text{CL}} = 591.78 \text{ K}$$

For comparison:

$$\Delta T := T_{\text{CL}} - T_{\text{rock}}$$

$$\Delta T = 78.778 \text{ K}$$

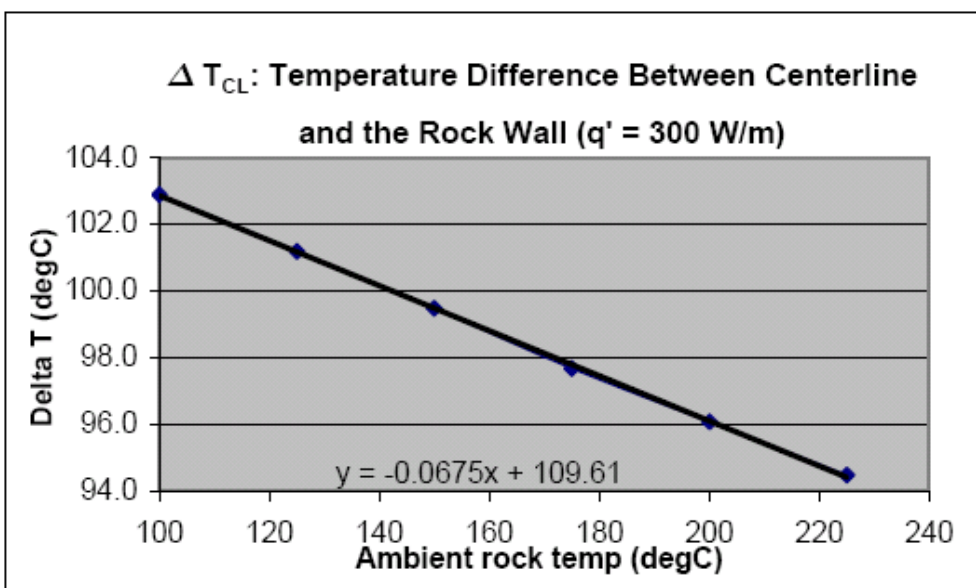
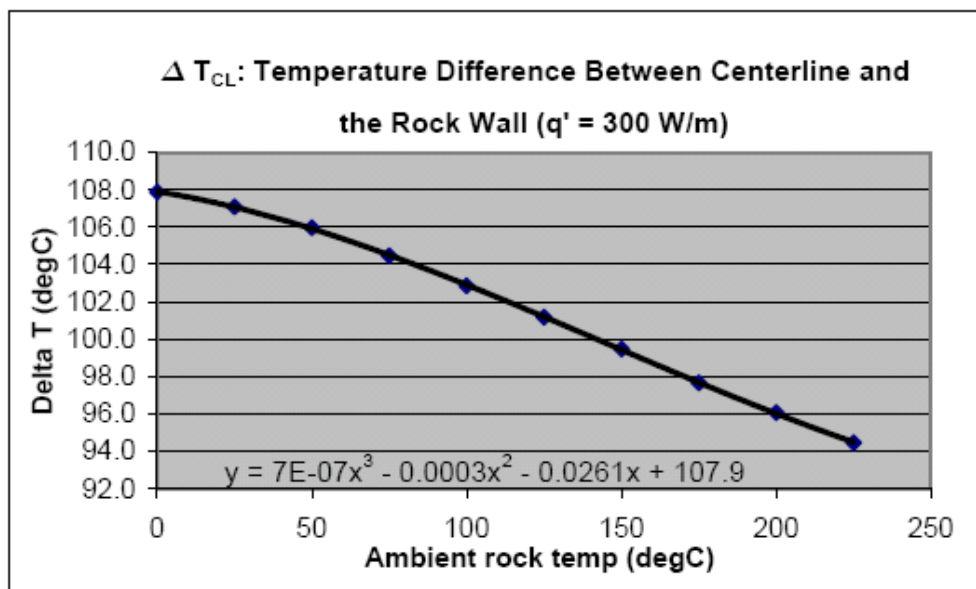
$$T_{\text{CLmax}} = 653 \text{ K}$$

7.3 Appendix C: Sensitivity Analysis of Thermal Calculations

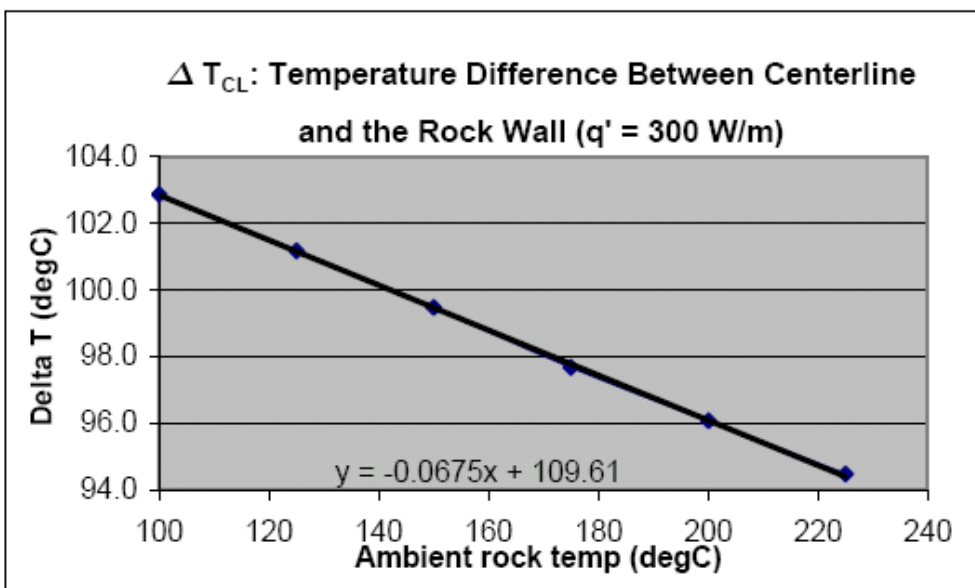
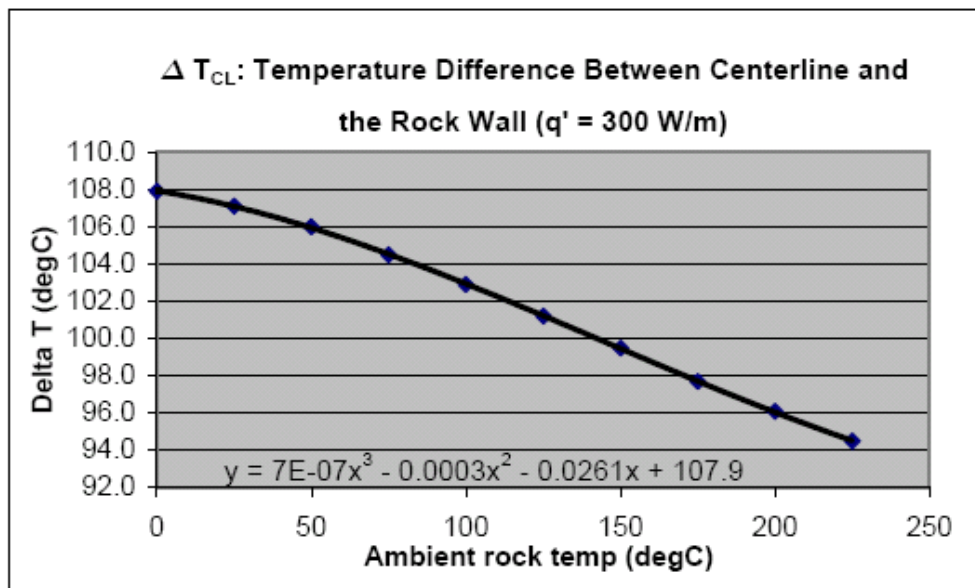
Appendix C contains the tables and figures of the sensitivity analysis discussed in Section 4.4. T_{amb} is the temperature of the granite prior to waste emplacement. T_{rock} is the peak temperature of the borehole wall after emplacement. Δ_{T1} is the temperature difference between the outer surface of the liner (final casing) and T_{rock} . Δ_{T1b} is the temperature difference between the inner surface of the liner and T_{rock} . Δ_{T2} is the temperature difference between the outer surface of the canister and T_{rock} . Δ_{T2b} is the temperature difference between the inner surface of the canister casing and T_{rock} . Δ_{Thole} is the temperature difference between T_{CL} (the centerline temperature), and T_{rock} . On the second page, $k_{granite}$ is the thermal conductivity of granite. G is a factor for calculating the peak temperature change in the granite at the borehole wall, as explained in Section 4.4.

\

q' (W/m)	T_{amb}	T_{rock}	ΔT_1	ΔT_{1b}	ΔT_2	ΔT_{2b}	ΔT_{hole}	
300	0	59.7	15.8	15.9	31.2	31.3	107.9	All temperatures are in °C.
300	25	84.7	15.6	15.7	30.4	30.5	107.1	
300	50	109.7	15.2	15.3	29.3	29.4	106.0	
300	75	134.7	14.6	15.7	27.8	27.9	104.5	
300	100	159.7	13.9	14.0	26.2	26.3	102.9	
300	125	184.7	13.1	13.2	24.5	24.6	101.2	
300	150	209.7	12.3	12.4	22.8	22.9	99.5	
300	175	234.7	11.4	11.5	21.0	21.1	97.7	
300	200	259.7	10.6	10.7	19.4	19.5	96.1	
300	225	284.7	9.7	9.8	17.8	17.9	94.5	



q' (W/m)	T_{amb}	T_{rock}	ΔT_1	ΔT_{1b}	ΔT_2	ΔT_{2b}	ΔT_{hole}	
300	0	59.7	15.8	15.9	31.2	31.3	107.9	All temperatures are in °C.
300	25	84.7	15.6	15.7	30.4	30.5	107.1	
300	50	109.7	15.2	15.3	29.3	29.4	106.0	
300	75	134.7	14.6	15.7	27.8	27.9	104.5	
300	100	159.7	13.9	14.0	26.2	26.3	102.9	
300	125	184.7	13.1	13.2	24.5	24.6	101.2	
300	150	209.7	12.3	12.4	22.8	22.9	99.5	
300	175	234.7	11.4	11.5	21.0	21.1	97.7	
300	200	259.7	10.6	10.7	19.4	19.5	96.1	
300	225	284.7	9.7	9.8	17.8	17.9	94.5	



q' (W/m)	T _{amb}	T _{rock}	ΔT _{hole}	T _{CL}
100	0	19.9	38.2	58.1
200	0	39.8	73.6	113.4
300	0	59.7	107.9	167.6
400	0	79.6	141.2	220.8
500	0	99.5	173.7	273.1
600	0	119.4	205.1	324.4
700	0	139.3	235.5	374.8
800	0	159.2	265.1	424.2
900	0	179.0	293.9	473.0
1000	0	198.9	322.0	520.9
100	50	69.9	37.8	107.7
200	50	89.8	72.4	162.2
300	50	109.7	106.0	215.7
400	50	129.6	138.2	267.8
500	50	149.5	169.6	319.1
600	50	169.4	199.9	369.2
700	50	189.3	229.4	418.7
800	50	209.2	258.0	467.1
900	50	229.0	286.1	515.2
1000	50	248.9	313.6	562.5
100	100	119.9	36.7	156.6
200	100	139.8	70.5	210.3
300	100	159.7	102.9	262.6
400	100	179.6	134.2	313.8
500	100	199.5	164.6	364.1
600	100	219.4	194.1	413.4
700	100	239.3	222.8	462.1
800	100	259.2	251.0	510.1
900	100	279.0	278.5	557.6
1000	100	298.9	305.6	604.5
100	150	169.9	35.2	205.1
200	150	189.8	68.0	257.8
300	150	209.7	99.5	309.2
400	150	229.6	129.8	359.4
500	150	249.5	159.5	409.0
600	150	269.4	188.4	457.7
700	150	289.3	216.6	505.9
800	150	309.2	244.2	553.3
900	150	329.0	271.5	600.6
1000	150	348.9	298.2	647.1
100	200	219.9	33.8	253.7
200	200	239.8	65.5	305.3
300	200	259.7	96.1	355.8
400	200	279.6	125.7	405.3
500	200	299.5	154.8	454.3
600	200	319.4	183.1	502.4
700	200	339.3	210.9	550.2
800	200	359.2	238.3	597.4
900	200	379.0	267.0	646.1
1000	200	398.9	291.9	690.8

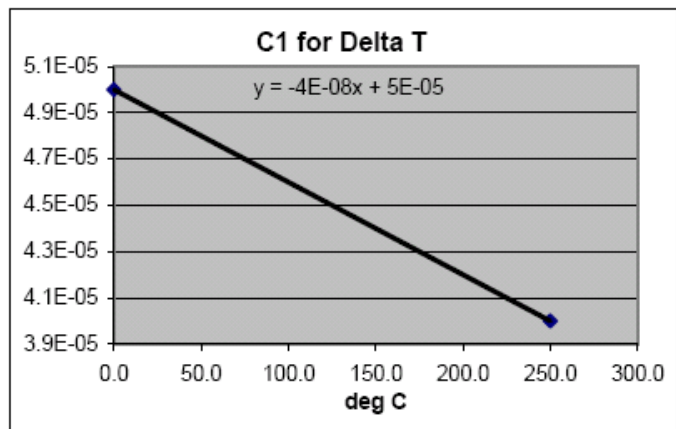
$$k_{\text{granite}} = 2.4 \text{ W/m}^2\text{K}$$

$$G = 6$$

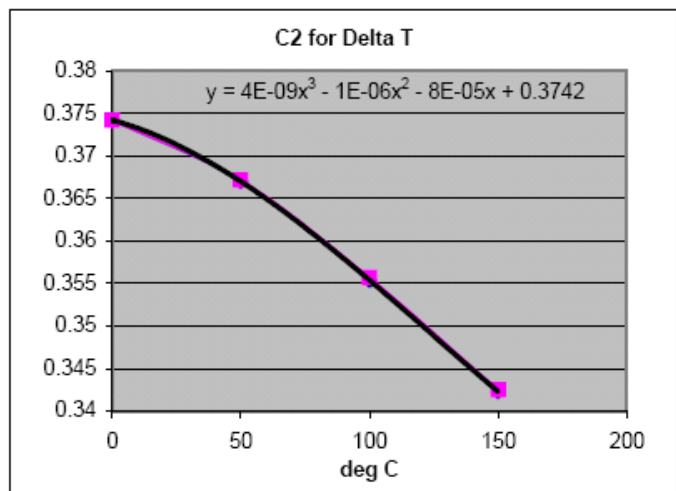
See chart labeled "Delta T: CL to Rock Wall." Equations on the right are of the form: $y = C1 \cdot x^2 + C2 \cdot x$. The charts below are used to find C1 and C2; however the coefficients in the trendline equations only have one significant digit, therefore some trial error and error was needed to find the second significant digit in each equation.

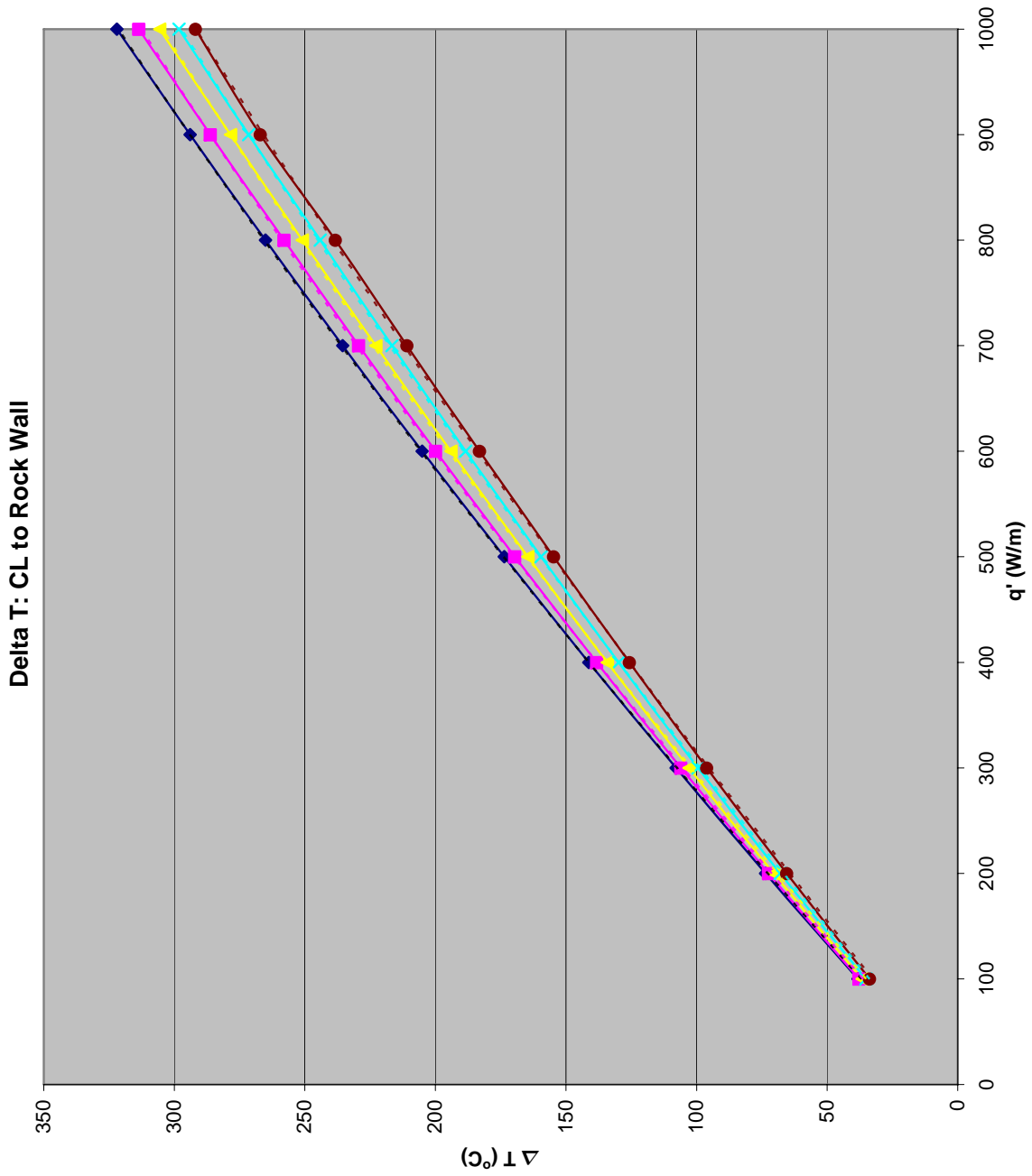
$$0.0 \quad 5.0\text{E-}05$$

$$250.0 \quad 4.0\text{E-}05$$



0	0.3742	0.3742
50	0.367	0.36714
100	0.3554	0.3557
150	0.3423	0.34251





The following tables are calculated using the trendline equations derived from the data above.

Center line temperature, T_{CL} , based on T_{amb} (across the top of the table), and q' (left column of the table).

	0	25	50	75	100	125	150	175	200	225	250
100	56.8	81.5	106.1	130.6	155.0	179.4	203.7	228.1	252.5	277.1	301.7
200	112.5	137.1	161.3	185.3	209.1	232.9	256.6	280.4	304.3	328.4	352.7
300	167.3	191.6	215.5	239.0	262.3	285.5	308.7	331.9	355.3	379.0	403.0
400	220.9	245.1	268.7	291.8	314.7	337.3	359.9	382.7	405.6	428.9	452.6
500	273.6	297.6	320.9	343.7	366.1	388.2	410.4	432.6	455.1	478.0	501.5
600	325.2	349.1	372.2	394.6	416.6	438.3	459.9	481.7	503.8	526.4	549.8
700	375.7	399.6	422.5	444.6	466.2	487.5	508.7	530.0	551.8	574.1	597.3
800	425.2	449.1	471.8	493.7	514.9	535.8	556.6	577.6	599.0	621.1	644.2
900	473.7	497.6	520.2	541.8	562.7	583.3	603.7	624.3	645.4	667.4	690.4
1000	521.1	545.1	567.6	589.0	609.6	629.9	650.0	670.3	691.1	712.9	735.8

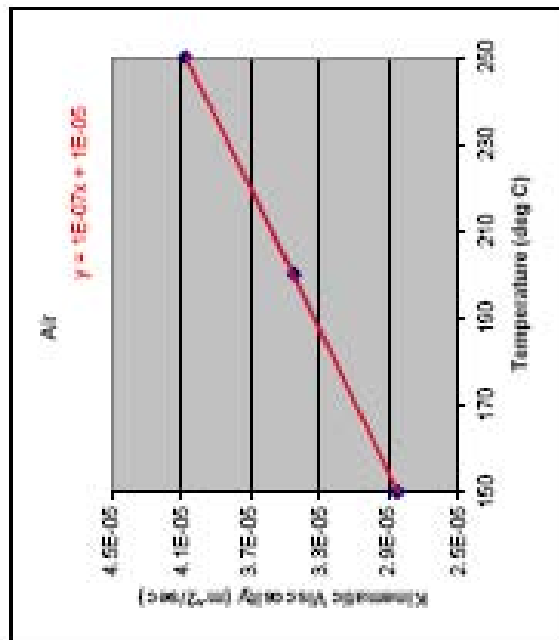
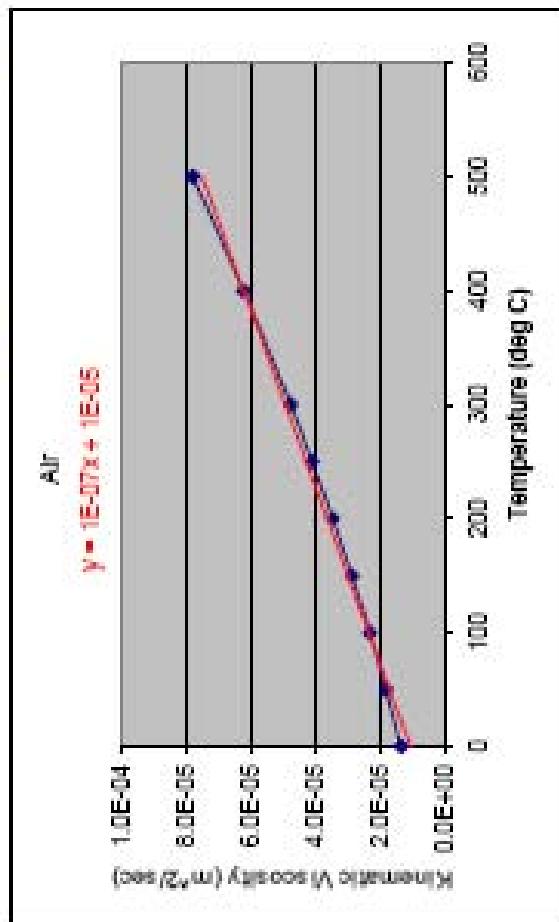
ΔT from centerline to borehole wall, based on T_{amb} (across the top of the table), and q' (left column of table).

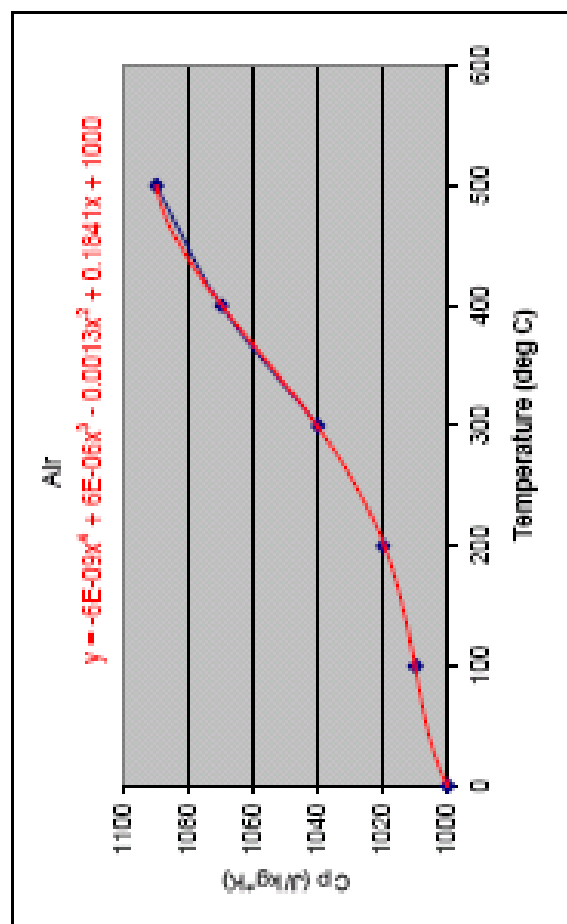
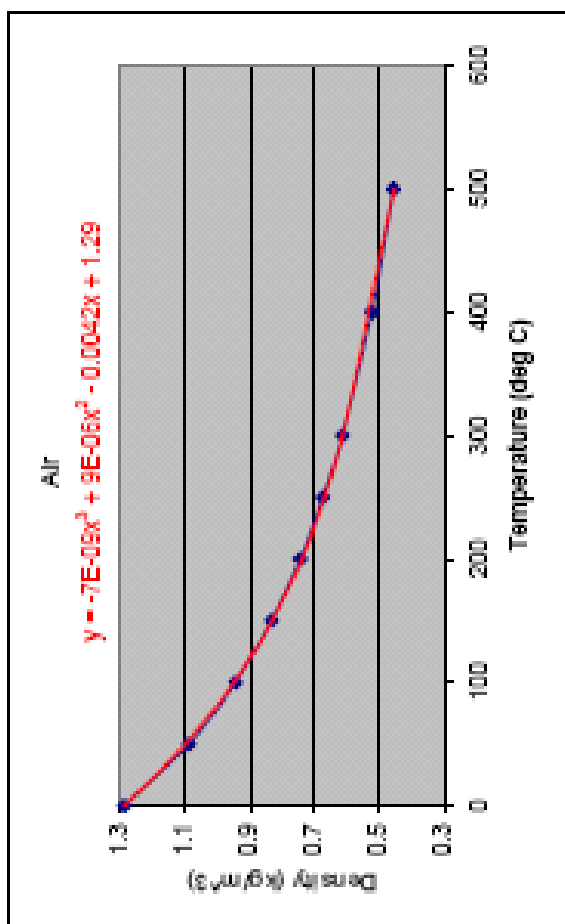
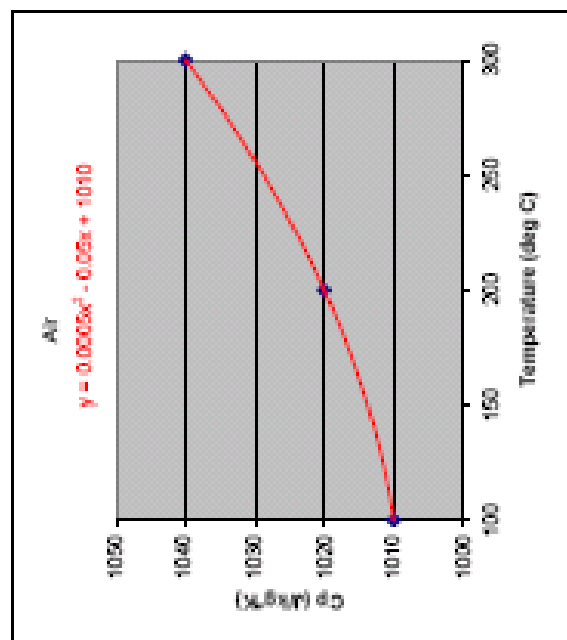
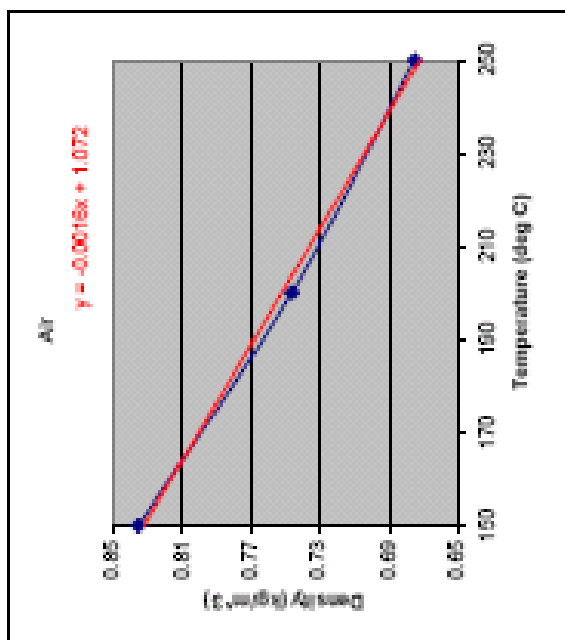
	0	25	50	75	100	125	150	175	200	225	250
100	36.9	36.6	36.2	35.7	35.1	34.5	33.8	33.2	32.6	32.2	31.8
200	72.8	72.3	71.5	70.5	69.3	68.1	66.8	65.6	64.5	63.6	62.9
300	107.6	106.9	105.8	104.3	102.7	100.9	99.0	97.2	95.6	94.3	93.3
400	141.4	140.5	139.1	137.2	135.1	132.7	130.4	128.1	126.0	124.3	123.0
500	174.1	173.1	171.4	169.2	166.6	163.8	160.9	158.1	155.6	153.5	152.1
600	205.8	204.7	202.8	200.3	197.2	193.9	190.6	187.3	184.4	182.1	180.4
700	236.5	235.3	233.2	230.4	226.9	223.2	219.4	215.8	212.5	209.9	208.1
800	266.1	264.9	262.7	259.5	255.8	251.6	247.5	243.4	239.8	237.0	235.0
900	294.7	293.5	291.1	287.8	283.7	279.2	274.6	270.3	266.4	263.3	261.3
1000	322.2	321.1	318.6	315.1	310.7	305.9	301.0	296.3	292.2	288.9	286.9

7.4 Appendix D: Properties of Air⁴²

Appendix D contains a table of properties of air at temperatures ranging from 0°C to 500°C. The properties listed are density, viscosity, kinematic viscosity, constant pressure specific heat, constant volume specific heat, and specific heat ratio. Kinematic viscosity, density, and constant pressure specific heat were plotted and a trendline was fit to the data. A trendline was also fit to the data for a limited temperature range of 150°C to 250°C (the expected temperature range of the air gaps in the borehole) and a new trendline was fit to the limited range of data. However, only the specific heat trendline equation was used in the thermal analysis calculations. Although the trendline for kinematic viscosity was not used, the data for dynamic viscosity was used to calculate the constants in the Sutherland equation.

Temp. (°C)	Density (kg/m ³)	Viscosity (Pa-s)	Kinematic Viscosity (m ² /s)	Gas Constant (J/kg-K)	Constant Pressure Specific Heat (J/kg-K)	Constant Volume Specific Heat (J/kg-K)	Specific Heat Ratio
0	1.29	1.71E-05	1.33E-05	287	1000	716	1.4
50	1.09	1.95E-05	1.79E-05	287	-	-	-
100	0.946	2.17E-05	2.30E-05	287	1010	723	1.4
150	0.835	2.38E-05	2.86E-05	287	-	-	-
200	0.746	2.57E-05	3.45E-05	287	1020	737	1.39
250	0.675	2.75E-05	4.08E-05	287	-	-	-
300	0.616	2.93E-05	4.75E-05	287	1040	758	1.38
400	0.525	3.25E-05	6.20E-05	287	1070	781	1.37
500	0.457	3.55E-05	7.77E-05	287	1090	805	1.36





REFERENCES

¹ Driscoll, M. J., "Boredom, The Weekly Newsletter on Deep Boreholes," vol. 1, no. 6, April 24, 2002.

Foley, M. G., and Ballou, L. M. G., eds, *Deep Injection Disposal of Liquid Radioactive Water in Russia*, Battelle Press, 1998.

² Lester, R. K., Massachusetts Institute of Technology, Class 22.77: Nuclear Waste Management, Lecture 19: Economics and Finance, 2005.

³ Pearce, Fred, "Underground Power Hots Up," New Scientist, Vol. 182, No. 2441, Pg. 23, April, 2003.

⁴ Badgley, P. C., *Structural and Tectonic Principles*, Harper & Row, Publishers, New York, 1965.

⁵ Woodward-Clyde Consultants, "Very Deep Hole Systems Engineering Studies," BMI/ONWI-226, prepared for ONWI, Battelle Memorial Institute, December, 1983.

⁶ Kuo, W. S., "Evaluation of Deep Drillholes For High Level Nuclear Waste Disposal," Massachusetts Institute of Technology, 1981.

⁷ Anderson, V. K., "An Evaluation of the Feasibility of Disposal of Nuclear Waste in Very Deep Boreholes," Massachusetts Institute of Technology, 2004.

⁸ Gibb, F., and Chapman, N., "A Truly Final Waste Management Solution," *Radwaste Solutions*, July/August 2003.

⁹ http://www.ag.ohio-state.edu/~rer/rerhtml/rer_27.html, 2005.

¹⁰ Manteufel, R. D., and Todreas, N. E., "Effective Thermal Conductivity and Edge Conductance Model for a Spent-Fuel Assembly," *Nuclear Technology*, Vol. 105, 1994.

¹¹ Hiruo, Elaine, "DOE plan for 'clean' repository shifts canister loading onus to utilities," *Nucleonics Week*, Volume 46, Number 43, October, 2005.

¹² http://ej.iop.org/links/q28/H2mTnjZkXEU+zW1yX+6BLg/d4_24_007.pdf, Asghari Maqsood, Kashif Kamran and Iftikhar Hussain Gul, "Prediction of thermal conductivity of granite rocks from porosity and density data at normal temperature and pressure: *in situ* thermal conductivity measurements," *Journal Of Physics D: Applied Physics*, Institute Of Physics Publishing, 2004.

-
- ¹³ http://www.marine.usm.edu/mar151/MAR_151_Chap_2.html, Pinet, Paul, “The Planet Oceanus”, 2005.
- ¹⁴ http://en.wikipedia.org/wiki/Specific_heat, 2006.
- ¹⁵ <http://rubble.phys.ualberta.ca/~doug/G221/ThermalLec/thermal.html>, 2006.
- ¹⁶ Gueguen, Yves, and Palciauskas, Victor, *Introduction to the Physics of Rocks*, Princeton University Press, 1994, p. 84.
- ¹⁷ Ibid. p. 103
- ¹⁸ Ibid. p. 121
- ¹⁹ Olhoeft, Gary R., “Electrical properties of granite with implications for the lower crust,” *Journal of Geophysical Research*, Volume 86, Issue B2, p. 931-936, February 1981.
- ²⁰ <http://www.omega.com/literature/transactions/volume1/emissivityb.html>, 2005.
- ²¹ Krauskopf, K. B., *Radioactive Waste Disposal Geology*, Topics in the Earth Sciences Volume 1, University Press, Cambridge, 1988.
- ²² Nielsen, Rolf H., “Final Resting Place,” *NewScientist*, March 2006, p. 41.
- ²³ <http://www.ustransportcouncil.org/documents/USTCSummitIII/USTCSummitIII-NEI-Kraft.pdf>, 2005.
- ²⁴ Roxburgh, I. S., “Geology of High-Level Nuclear Waste Disposal – An Introduction,” Chapman and Hall Ltd., New York, NY, 1987.
- ²⁵ “Fuel Design Data,” *Nuclear Engineering International*, Williams Press, Berkshire, UK, Sep. 2005.
- ²⁶ “Spent fuel discharges,” *Nuclear News*, December, 2004.
- ²⁷ Berger, B. D., and Anderson, K. E., “Modern Petroleum – A Basic Primer of the Industry,” PennWell Publishing Company, Tulsa, OK, 1992.
- ²⁸ http://www.tps-technitube.de/Catalogues/Files/OCTG_GESAMT.pdf, TPS Technitube Röhrenwerke GmbH.
- ²⁹ “Fuel Design Data,” *Nuclear Engineering International*, Williams Press, Berkshire, UK, Sep. 2005.

-
- ³⁰ http://www.tps-technitube.de/Catalogues/Files/OCTG_E_D.pdf, TPS Technitube Röhrenwerke GmbH.
- ³¹ Pitts, Donald R., and Sissom, Leighton E., "Schaum's Outline of Theory and Problems of Heat Transfer," McGraw Hill, p. 319.
- ³² Goluoglu, Sedat, and Davis, J. Wesley, "Shippingport PWR Fuel, Criticality Analyses For Viability Evaluation Of Codisposal In A Geologic Repository," Oak Ridge National Lab, 2000.
- ³³ Todreas, Neil E. and Kazimi, Mujid S., Nuclear Systems I, Thermal Hydraulic Fundamentals, Hemisphere Publishing Corporation, 1990.
- ³⁴ <http://www.azom.com/details.asp?ArticleID=1630>, 2006.
- ³⁵ <http://www.azom.com/details.asp?ArticleID=2254>, 2006.
- ³⁶ <http://www.phy.mtu.edu/~jaszczak/graphprop.html>, 2006.
- ³⁷ Roark, Raymond J, Formulas for Stress and Strain, McGraw-Hill Book Company, 1943, pg. 239.
- ³⁸ Ranade, R., "Thermal Simulation of a Deep-Borehole Storage Facility for Nuclear Waste," Massachusetts Institute of Technology, August, 2005.
- ³⁹ Han, J.-C., Driscoll, M. J., and Todreas, N. E., "The Effective Thermal Conductivity of Prismatic MHTGR Fuel," MIT Energy Laboratory and Department of Nuclear Engineering, September, 1989.
- ⁴⁰ Mikheyev, M., Fundamentals of Heat Transfer, Peace Publishers, Moscow
- ⁴¹ Munson, B. R., Young, D. F., and Okiishi, T. H., Fundamentals of Fluid Mechanics, Third Edition Update, John Wiley & Sons, Inc., 1998, pg. 19.
- ⁴² http://www.efunda.com/Materials/common_matl/show_gas.cfm?MatlName=Air0C.
- ⁴³ Ozisik, M. N., Basic Heat Transfer, McGraw-Hill Book Company, 1977.
- ⁴⁴ Hansen, M., Elliot, R., and Shunk, F., *Constitution of Binary Alloys*, McGraw Hill, New York, 1958.
- ⁴⁵ Ageev, N. V., *Handbook of Binary Metallic Systems; Structure And Properties*, Jerusalem, Israel, 1966.
- ⁴⁶ Augustine, C., Tester, J., and Anderson, B., "A Comparison of Geothermal with Oil And Gas Well Drilling Costs," Chemical Engineering Department, Massachusetts Institute of Technology, 2006

⁴⁷ <http://www.nei.org/index.asp?catnum=2&catid=95>, “Summary of Nuclear Waste Fund Payments by State”

⁴⁸ “Nuclear Waste Fund Fee Adequacy: An Assessment,” U.S. Department of Energy, May, 2001

⁴⁹ <http://www.ocrwm.doe.gov/pm/pdf/tslccr1.pdf>, DOE 2001, *Analysis of the Total System Life Cycle Cost for the Civilian Radioactive Waste Program*, DOE/RW-0533, Office of Civilian Radioactive Waste Management

⁵⁰ Various authors, *Borehole and Shaft Plugging Proceedings*, OECD, 1980.